RESTRICTED REPORT 204R

Division of
EXPLORATION GEOSCIENCE

Institute of Minerals, Energy and Construction

MAGNETIC PROPERTIES AND MAGNETIC MINERALOGY OF SOME AUSTRALIAN KIMBERLITES AND LAMPROITES

D.A. CLARK

P.O. Box 136
North Ryde
NSW 2113

March 1991

RESTRICTED REPORT 204R Copy 6 of 9 copies

Report to Stockdale Prospecting Ltd

DISTRIBUTION LIST	Copy
Stockdale Prospecting Ltd	1-4
CSIRO Division of Exploration Geoscience	
D.A. Clark	5
P.W. Schmidt	6
B.J.J. Embleton	7
A.A. Green	8
D.H. French	9

CSIRO
AUSTRALIA

Division of Exploration Geoscience
Underwood Avenue, Floreat Park, WA. Postal Address: CSIRO Private Bag, Wembley WA 6014
Telephone: (09) 387 4233. Telex: AA92178. Fax: (09) 387 6046

Chief: Dr B.J.J. Embleton

POLICY ON RESTRICTED REPORTS

Restricted Reports issued by this Division deal with projects where CSIRO has been granted privileged access to research material. Initially, circulation of Restricted Reports is strictly controlled, and we treat them as confidential documents at this stage. They should not be quoted publicly, but may be referred to as a "personal communication" from the author(s) if my approval is sought and given beforehand.

The results embodied in a Restricted Report may eventually form part of a more widely circulated CSIRO publication. Agreements with sponsors or companies generally specify that drafts will be first submitted for their approval, to ensure that proprietary information of a confidential nature is not inadvertently included.

After a certain period of time, the confidentiality of particular Restricted Reports will no longer be an important issue. It may then be appropriate for CSIRO to announce the titles of such reports, and to allow inspection and copying by other persons. This procedure would disseminate information about CSIRO research more widely to Industry. However, it will not be applicable to all Restricted Reports. Proprietary interests of various kinds may require an extended period of confidentiality. Premature release of Restricted Reports arising from continuing collaborative projects (especially AMIRA projects) may also be undesirable, and a separate policy exists in such cases.

You are invited to express an opinion about the security status of the enclosed Restricted Report. Unless I hear to the contrary, I will assume that in eighteen months time I have your permission to place this Restricted Report on open file, when it will be generally available to interested persons for reading, making notes, or photocopying, as desired.

B J J EMBLETON
Chief of Division

North Ryde
Location: Delhi Road, North Ryde
Postal Address: PO Box 136, North Ryde NSW 2113
Telephone (02) 887 8666
Telex AA25817
Fax (02) 887 8909

Lindfield
Location: Bradfield Road, Lindfield
Postal Address: PO Box 218, Lindfield NSW 2070
Telephone: (02) 467 6733
Telex: AA26296
Fax: (02) 467 1902

TABLE OF CONTENTS

LIST OF TABLES

LIST OF FIGURES

SUMMARY

The bulk magnetic properties of a suite of Australian kimberlite and lamproite samples were measured and their magnetic mineralogy was characterised by rock magnetic techniques, including thermomagnetic analysis and AF and thermal demagnetisation of natural and artificial remanences. The magnetisation of the Group I kimberlites is associated with fine-grained (small MD to SD) spinels with a wide range of Curie points. The susceptibility of the kimberlites usually increases after heating. The ferromagnetic grains are interpreted as zoned spinels with thin magnetite-rich rims.

The Group I kimberlites are moderately to strongly magnetic, with susceptibilities comparable to those of Southern African Group I kimberlites, whereas the lamproites have generally lower susceptibilities, similar to those of Group II kimberlites. The magnetisations of kimberlites and lamproites tend to be dominated by remanence, implying that modelling assuming magnetisation by induction can produce erroneous results. The NRM of the mid-Jurassic Eyre Peninsula kimberlites is subvertical, slightly steeper than the present field. Kimberlites of slightly different age in this province could have remanence of either polarity and therefore could be associated with either positive or negative anomalies. The mid-Jurassic palaeofield direction has been calculated for use in modelling Eyre Peninsula kimberlites. The NRMs of the Miocene Ellendale lamproites can also be of either polarity and anomalies of both signs are known to be associated with these bodies. The lamproites are detectable by aeromagnetic surveys only because of the magnetically quiet environment (non-magnetic Canning Basin sediments.

All the lamproite samples were found to contain small to trace amounts of ferromagnetic spinels, ranging up to pure or nearly pure magnetite in composition, in spite of the reported absence of highly evolved spinels in these rocks. The magnetisation of these rocks is predominantly carried by spinels, although haematite and goethite, which are both probably weathering products, are present in some samples. These spinels are in the small multidomain to pseudosingle domain size range and presumably represent thin magnetite-rich rims on early-crystallising spinel grains. The lamproite samples exhibit a broad range of Curie temperatures, similar to that of the kimberlites, but the susceptibility tends to decrease after heating, rather than increase as for the kimberlites. This difference may reflect the different evolutionary trends for Group I kimberlites and lamproites, which produce moderately evolved ferromagnetic spinels with differing compositions in the two cases.

1. INTRODUCTION

A suite of kimberlite drill core samples and surface samples collected from a number of exposed Ellendale lamproites was submitted by F. Arnott for characterisation of magnetic properties and magnetic mineralogy. Table 1 lists the samples included in this study. Cores of 25 mm diameter were drilled out of the samples and sliced into standard cylindrical specimens with a height of 22 mm. Remanent magnetisations were measured using a CTF Cryogenic (SQUID) Magnetometer and susceptibilities and k-T curves were determined on the CSIRO balanced transformer bridge. The magnetic mineralogy was characterised using a number of palaeomagnetic cleaning techniques as described in an earlier report (Clark and French, 1990).

2. BASIC MAGNETIC PROPERTIES OF THE KIMBERLITE SAMPLES

Table 2 gives the susceptibilities, remanent intensities, NRM inclinations and Koenigsberger ratios of the kimberlite samples. The three kimberlite bodies from the Eyre Peninsula (V8875-77 dyke and pipes S8173/MH1 and MH2) have moderate to strong susceptibilities. Their magnetisations are dominated by remanence ($Q > 1$) and the NRMs are generally directed steeply upwards. The declinations of the NRMs could not be determined because the samples were azimuthally unoriented. Nevertheless, the steepness of the inclinations implies that the NRM directions can be defined to within ~30°. These Group I kimberlite samples are moderately to strongly magnetic overall and have similar bulk magnetic properties to the Group I kimberlites from Southern Africa studied by Clark and French (1990).

Mean remanence vectors for each pipe cannot be calculated exactly, because the declinations are unknown, but bulk properties for each of the Eyre Peninsula bodies are roughly estimated as:

V8875-77: $k = 580\ \mu G/Oe$; $J = 730\ \mu G$; $I = -75°$; $Q = 2.1$

MH1: $k = 1160\ \mu G/Oe$; $J = 3500\ \mu G$; $I = -75°$; $Q = 5.0$

MH2/56J: $k = 85\ \mu G/Oe$; $J \approx 330\ \mu G$; $I \approx -40°$; $Q = 6.5$

MH2/56C,L: $k = 1130\ \mu G/Oe$; $J = 3800\ \mu G$; $I = -75°$; $Q = 5.6$

The results from DDH MH2/56J have been averaged separately because this hole evidently intersected a much more weakly magnetic zone of MH2, which may be a multiple pipe, and because of the anomalously shallow remanence inclination. Logging of

the complete core showed that susceptibilities in hole MH2/56C were consistently much higher than in MH2/56J, which was 80 m distant within the same anomaly.

Fig.1 presents AF demagnetisation data for the NRMs of samples from MH1 and MH2. The diagrams include Zijderveld plots (orthogonal projections of successive vector end-points), stereograms, demagnetisation curves and coercivity spectra. The plots indicate that the NRMs of most of the samples are substantially monocomponent, with minor palaeomagnetic noise components superimposed. After removal of the noise components by 100-150 Oe AF, successive remanence vector end-points trend directly towards the origin. The stereograms confirm the stability of remanence directions during cleaning. The NRMs are generally quite hard, with median destructive fields ranging from ~90 Oe to ~400 Oe and with substantial signal remaining after 600-800 Oe AF. The overall shape of the demagnetisation curves suggests the the NRM carriers are predominantly PSD grains. The samples exhibiting simple demagnetisation behaviour are interpreted to have NRMs dominated by a primary component, directed steeply upwards.

Two samples from MH2, high susceptibility sample 56C-78m and low susceptibility sample 56J-109m, are exceptional. The sample mean NRM directions of these samples are anomalous, NRM directions of individual specimens within each sample are scattered (see Fig.1) and AF demagnetisation reveals complex, multicomponent magnetisations. The two specimens from MH2/56C-78m have opposite polarities. The Zijderveld plot for AF demagnetisation of specimen 56C78A shows removal of a steep up component up to 300 Oe AF, revealing a hard component that is approximately antiparallel to the soft component. The soft, normal polarity component is absent from the adjacent specimen 56C-78B, which has a steep down NRM. At the highest fields there is a hint that a small, very hard, residual component of normal polarity may be present.

The scattered NRM directions and the anomalously shallow inclination of the vector mean NRM for sample 56J-109m reflects the presence of normal and reversed components within this sample. AF cleaning does not completely resolve these components, indicating that they have overlapped coercivity spectra. In fact the Zijderveld plots suggest that in some specimens both components have very broad, perhaps bimodal coercivity spectra, such that preferential demagnetisation of the components proceeds alternately. For example, in specimen 56J-109E a very soft component, possibly noise, is removed by 25 Oe AF, after which reversed then normal components are removed, finally leaving a reversed component.

Comparison of different specimens from this sample shows that in general a shallow component with variable azimuth is removed initially, after which the remanence directions head initially towards a steep up direction, then backtrack via shallow directions to finally attain, in most cases, a steep

down direction. Specimen 56J109B is exceptional, in that the general trajectory of remanence directions is opposite to that of the other specimens. For this specimen a steep down component is removed up to 500 Oe, revealing a normal component that becomes steeper and then shallower. The softest components from individual specimens are scattered and may represent palaeomagnetic noise acquired, for instance, by testing of the core with a pencil magnet. Contamination of the remanence by IRM may also account for the exceptionally high Koenigsberger ratio (Q = 31) of this sample. Thus the NRM of this sample is probably unrepresentative of the *in situ* properties. However the complex multicomponent character of the harder fraction of the remanence that remains after AF demagnetisation to > 100 Oe is interpreted to reflect geological effects, rather than post-collection contamination.

The presence of multiple components in the stable portion of the remanence in two samples from MH2 suggests thermochemical overprinting due to multiple intrusion. The presence of high and low susceptibility zones within this pipe is also consistent with distinct intrusive phases. The evidence suggests two or more intrusions occurred within the pipe, separated by at least one geomagnetic reversal, to account for the dual polarity of the remanence components. Generation of new magnetic material within one kimberlite phase due to intrusion by another magmatic pulse could account for the highly overlapped stability spectra of the remanence components, whereas simple thermal overprinting would probably have produced more discrete stability ranges for the primary and secondary components. Chemical overprinting is also dependent on the composition and mineralogy of the affected zone and is therefore inherently more variable in its properties and distribution than purely thermal overprinting. Thus thermochemical overprinting is more consistent with the heterogeneous development of normal and reversed components within a single core sample than thermal overprinting.

The Q values indicate that the magnetisation of these kimberlites is enhanced by factors of ~3-6 with respect to the contribution of susceptibility alone. Thus the anomalies caused by pipes of given size should be several times larger than would be estimated from susceptibility measurements, if remanence is neglected. Conversely, targets may be substantially smaller than indicated by models that assume magnetisation by induction, using typical susceptibility values for these kimberlites. The simplest approach to allow for the effects of remanence is to augment the model susceptibility by a factor of (1+Q). This is strictly valid only if the remanence is parallel to the geomagnetic field, but should provide a reasonable approximation in this instance, where the steep up remanence is subparallel to the present field.

An alternative, and preferable, approach to modelling is to estimate the true remanence direction for these pipes by using information about their age and the Australian Apparent

Polar Wander Path. The Eyre Peninsula kimberlites are Jurassic. In particular, a kimberlite from Cleve has been precisely dated at 183 ± 3 Ma, which is Middle Jurassic. The Middle Jurassic (190-170 Ma) palaeomagnetic pole position for Australia is well-defined and lies south of New Zealand (lat = 48°S, long = 180°E). This position is an average of eight palaeomagnetic poles and has a 95% cone of confidence equal to 5°. The corresponding palaeofield direction at Cleve is:

Middle Jurassic Palaeofield Direction

dec = 307°, inc = -71° (normal polarity)

dec = 127°, inc = +71° (reversed polarity)

The calculated palaeofield inclination is similar to the majority of the observed remanence inclinations, which are distinctly steeper than the present field. This suggests that the NRM is dominated by an ancient component which is probably primary, given the stable tectonic environment since emplacement of the kimberlites and the hardness and directional stability during palaeomagnetic cleaning. Southern African kimberlites are generally good palaeomagnetic recorders, suggesting that remanence directions can be inferred with reasonable confidence from the palaeofield direction corresponding to the age of the kimberlites. It should be noted that geomagnetic reversals were relatively frequent during the Jurassic, although normal polarities predominate. Thus some Jurassic kimberlites may have reversed polarity remanent magnetisations, in which case they would be associated with negative anomalies, assuming Q values greater than unity. Multiple pipes may have more complex magnetic signatures, if the different kimberlite phases have very different magnetic mineralogies or magnetic mineral abundances, or if both remanence polarities are present. This appears to apply to pipe MH2.

The remanent magnetisation of kimberlites is probably acquired very rapidly, recording a "snapshot" of the palaeofield direction which is affected by short-term deviations from an axial geocentric dipole field. The palaeofield direction given above corresponds to a time-averaged palaeopole position, i.e. secular variation is believed to have been removed by averaging VGPs spanning about a million years or more. Thus the remanence direction of individual penecontemporaneous kimberlites may depart from the calculated palaeofield direction by up to ~ 20° (two standard deviations) due to secular variation.

The two country rock samples that are not from the contact zone (gneiss sample MH2/55Z-100m and schist sample MH2/56P-68m) are weakly magnetic. The baked gneiss sample in contact with kimberlite (MH1/55Z-93m), on the other hand, is strongly magnetic and has a relatively intense remanence (Q ≈ 7) with

similar inclination to that of the kimberlite. The properties of the kimberlite and gneiss within this core sample could only be measured approximately, because of the irregular shape of the kimberlite and gneiss subsamples cut from the core. The large contrast between the properties of the baked gneiss and its unbaked equivalent seven metres distant suggests that reaction with the kimberlite has produced magnetic minerals in the baked gneiss, which acquired thermochemical remanence parallel to the remanence of the kimberlite.

The single sample from a different province, BF1986, has high susceptibility and a moderately intense remanence of reversed polarity. If this sample is representative of the bulk properties of the pipe, the associated anomaly amplitude should be only ~40% of the magnitude predicted from the measured susceptibility, because the induced magnetisation is opposed by an approximately antiparallel remanence with $Q \approx 0.6$. The calculated value of the Koenigsberger ratio for this sample assumes an ambient field of 0.6 Oe (60,000 nT) and should be recalculated for the true field intensity at the locality.

3. BASIC MAGNETIC PROPERTIES OF THE LAMPROITE SAMPLES

Table 3 gives the susceptibilities, remanent intensities and Koenigsberger ratios of the lamproite samples. Most of the samples are quite weakly magnetic and are only detectable by high resolution aeromagnetic surveys because the background field is very smooth and flat due to the absence of magnetic material in the surrounding Canning Basin sediments. Several of the samples have moderate susceptibilities and in most cases the magnetisation is dominated by remanence. There are insufficient data to make any generalisations about relative magnetisations of different petrographic types or magmatic versus pyroclastic lamproites. It should be noted, however, that the moderately magnetic samples include hypabyssal olivine and leucite lamproites and lamproitic tuffs. Some samples have exceptionally high Q values that are attributed to nearby lightning strikes and are thought not to be representative of bulk properties. These lamproites are Late Tertiary in age, a period of frequent geomagnetic reversals, and pipes of both remanence polarities are known. This accounts for the occurrence of negative anomalies associated with some of the lamproites.

The ranges in susceptibility and remanent intensity of the Ellendale lamproites are comparable to those of Group II kimberlites from Southern Africa (Clark and French, 1990). It is evident that the magnetisations, and accordingly the magnetic anomalies, of lamproites are quite sensitive to variations in magma composition and emplacement conditions. This will be discussed further in the section on magnetic mineralogy. Omitting the lightning affected samples from consideration, most of the remaining samples have $Q \gtrsim 1$, and some have $Q >> 1$, indicating that remanence is an important,

often dominant, contributor to the total magnetisation of the Fitzroy lamproites. Palaeomagnetic studies have shown that the NRMs of most Fitzroy lamproites are dominated by primary TRM (normal or reversed) that is generally slightly steeper than the present field. The pipes can be modelled, in a first approximation, as magnetised by induction, either with the effective susceptibility enhanced by remanence of normal polarity or reduced by reversed remanence. In the latter case, the effective susceptibility is negative when, as is usual, the Q value is greater than unity.

4. MAGNETIC MINERALOGY OF THE KIMBERLITE SAMPLES

4.1 Rock Magnetic Techniques

A number of rock magnetic techniques, including susceptibility-temperature curves and AF demagnetisation of NRM and saturation remanence, were used to characterise the composition and domain state of the magnetic minerals in these samples. These techniques are described by Clark and French (1990). The unblocking temperature spectra of the magnetic carriers were investigated using a method recently proposed by Lowrie (1990). This method involves imparting a saturation remanence (SIRM) in a very strong field, H_1, along one axis of a specimen, followed by application of a substantially lower field, H_2, along an orthogonal direction and, finally, application of a still lower field, H_3, along the remaining Cartesian axis. This imparts a three-component remanence to the specimen. The coercivity spectra of the components are discrete: the component along the first axis carried by grains with coercivities between H_2 and H_1, the component along the second axis corresponding to grains with coercivities between H_3 and H_2 and the component along the third axis corresponding to grains with coercivities less than H_3.

Thermal demagnetisation of this three-component remanence allows simultaneous determination of the unblocking temperature spectra of the highest, intermediate and lowest coercivity fractions, providing much more information about composition and microstructure than can be obtained from thermal demagnetisation of a monocomponent remanence, particularly when the magnetic mineralogy is complex. Lowrie (1990) imparted IRMs along each of the specimen axes. For this study, the specimen was first saturated in a field of ~10,000 Oe along the z-axis, then an anhysteretic remanence (ARM) was imparted in a peak alternating field of 1000 Oe with a DC biassing field of ~1 Oe along the x-axis. A second ARM in a peak AF of 200 Oe was then imparted along the y-axis. ARMs were used instead of IRMs for the intermediate and low coercivity components because a field of ~ 50 Oe between the pole pieces, that remained even when the electromagnet was switched off, tended to reorient the magnetisation of the softest grains as the specimen was removed from the electromagnet.

Low-field thermomagnetic (k-T) curves for the kimberlites are shown in Fig.2. Fig.3 shows AF demagnetisation curves of SIRM and corresponding coercivity spectra for selected kimberlite samples and Fig.4 displays thermal demagnetisation curves for three-component (SIRM + ARM1 +ARM2) remanence. The compositions and domain structures of the magnetic grains in the kimberlite samples identified by the rock magnetic experiments are summarised in Table 4.

The variability in thermomagnetic behaviour and the absence of closely similar curves from any of the Southern African kimberlites examined by Clark and French (1990) illustrates the complexity and variability of the magnetic mineralogy of kimberlites. It is notable, however, that within each kimberlite pipe there is less variability and that, taken together, the Eyre Peninsula kimberlites resemble each other more closely than they resemble Southern African kimberlites. This suggests that the magnetic mineralogy of kimberlites may show some common features within provinces that are not shared between provinces.

4.2 Samples V8875, V8876 and V8877

The thermomagnetic curves for samples V8875-8877 are all very similar, indicating homogeneous magnetic mineralogy in the sampled section of this kimberlite. The form of the curves is a very broad hump, with the susceptibility increasing steadily from -200°C to ~100°C and then gradually decreasing to zero between 520°C and 580°C. The curve is essentially reversible up to at least 550°C, but some new magnetic material has been created after heating to 700°C.

The thermomagnetic behaviour indicates the presence of a broad range of magnetic compositions with Curie points ranging from ~100°C to 580°C. This range in Curie temperatures corresponds to titanomagnetite compositions ranging from about 70 mole% ulvospinel to pure magnetite. However, quenched intermediate to ulvospinel-rich titanomagnetites are metastable and exsolve readily on heating to several hundred degrees, producing highly irreversible k-T curves. Thus the low T_C phases in these samples cannot be simple titanomagnetites. Magnesium content cannot explain the low Curie temperatures either, because magnesioferrite-magnetite solid solutions have T_C between ~400°C and 580°C. The most likely candidates for the low T_C phases are relatively chromite-rich spinels (up to ~60 mole% (Mg-Al-Ti) chromite in solid solution with magnetite), which should be less prone to unmixing and oxidation than titaniferous magnetites.

Sample V8876 exhibits a broad, continuous distribution of Curie points with no hint of a compositional gap, whereas sample V8875 does show an inflection in the k-T curve at ~320°C, indicating a somewhat lower abundance of phases with T_C between about 300°C and 400°C. Sample V8877 (not shown)

exhibits behaviour intermediate between the other two samples from this kimberlite. After heating to 700°C all samples exhibit a discrete Curie temperature at 580°C, indicating the creation of a small amount of end-member magnetite, presumably by exsolution. Apart from the contribution of this magnetite to the susceptibility of sample V8876 during subsequent cooling, the cooling curve would almost exactly retrace the heating curve. This implies that chemical change in the dominant magnetic phases during heating of this sample is minor. The cooling curve for sample V8875 shows a smooth, broad, symmetrical hump, suggesting that the compositional gap has been closed by homogenisation of phases that originally straddled the gap. Homogenisation requires intimate contact between the phases, implying that the different compositions occur within single grains, either as intergrown lamellae or, more typically, as zoned crystals.

AF demagnetisation of SIRM carried by V8875-8877 (Fig.3) shows that the magnetic grains in these samples have a broad range of coercivities, with the coercivity spectra peaking between 50 and 75 Oe AF and 1-5% of the remanence remaining after 500 Oe AF. Median destructive fields are ~100 Oe. These data indicate that the magnetic carriers are predominantly multidomain (MD), tens of microns in size or larger, but a minor portion of harder pseudosingle domain (PSD) grains in the 1-20 μm size range is also present. Thermal demagnetisation of three-component remanence (Fig.4) shows that the softest (Y) component, carried by grains with coercivities less than 200 Oe, is 50% unblocked at relatively low temperatures: below 180°C for V8876, between 180°C and 270°C for V8875 and between 325°C and 385°C for V8877. By contrast, the hardest component (coercivities greater than 1000 Oe) unblocks predominantly at much higher temperatures. Thus the softest multidomain grains correspond predominantly to the relatively magnetite-poor (low T_C) compositions and the very hard small PSD and SD grains are substantially richer in magnetite.

4.3 Samples S8173 and MH1/55

Thermomagnetic curves for two samples from pipe MH1 seem rather different at first sight, but closer examination reveals several similarities. The susceptibility of sample S8173 exhibits a prominent peak at ~100°C, followed by a fairly rapid descent signifying a range of Curie points from ~100°C to ~280°C. The curve is slightly irreversible on cooling from 280°C, indicating some chemical change has taken place at relatively low temperatures. The susceptibility is then almost constant up to ~400°C, after which there is a gradual drop, corresponding to Curie points from ~400°C to ~580°C, with a discernable discrete Curie point at ~500°C. The slight tail on the k-T curve up to 620°C reflects a temperature gradient through the sample, rather than traces of magnetic material with T_C > 580°C. On cooling from 700°C, the compositional gap corresponding to 200°C < 400°C has been closed and the peak associated with low T_C phases has been modified. This suggests

partial homogenisation of originally discrete magnetite-poor and relatively magnetite-rich compositions, which presumably occur within single grains. Thermal demagnetisation of three-component remanence (Fig.4) shows that the phase with $T_C \approx 100^\circ C$ is magnetically soft (coercivity < 200 Oe), whereas the higher T_C compositions are almost entirely hard PSD or SD grains.

The k-T curve for sample MH1/55Z-83m exhibits a similar range of Curie points above 400°C, but the compositional gap between the low and high T_C phases that is so evident for S8173 is partially closed. The range of T_C for this sample extends from ~200°C to 580°C, with an inflection, corresponding to a discrete Curie point, at ~400°C. Chemical change is evident in the heating curve by 300°C. After heating to 700°C, this inflection point has shifted to a lower temperature, ~260°C, suggesting exsolution of a phase poorer in magnetite (~ 45 mole% magnetite) from a phase that initially had intermediate magnetite content (~70 mole % for $T_C \approx 400^\circ C$). The limited irreversibility of the curves suggests that cations other than titanium comprise a substantial proportion of the substitutions for iron in the spinels.

Thermal demagnetisation of three-component remanence carried by S8173D shows that the low coercivity grains predominantly unblock by 180°C and totally unblock by 450°C, whereas remanence carried by intermediate and high coercivity grains persists up to 580°C. There is also evidence in the demagnetisation curves of the intermediate and high coercivity components for a discrete Curie point close to 500°C, corresponding to the inflection point in the k-T curve. The demagnetisation curves show that the low T_C phase in this sample corresponds to relatively large MD grains, whereas the effective grain size of the grains with $400^\circ C < T_C < 580^\circ C$ is smaller, in the PSD and SD range. Partial homogenisation of the magnetic phases after heating to 700°C that is indicated by the cooling k-T curve suggests that the higher T_C phases are fine magnetite-rich lamellae within larger magnetite-poor spinel grains or thin magnetite-rich rims on such grains.

AF demagnetisation of the NRMs of samples from MH1 (Figs.1,3) show bimodal coercivity spectra, with peaks below 100 Oe and secondary peaks between 200 Oe and 300 Oe, with an extended tail towards higher fields. These peaks correspond to the MD, low T_C grains and the PSD/SD fraction with higher T_C. Thermal demagnetisation of SIRM of specimens 55A-58A and 55Z-83D shows prominent unblocking between 160°C and 230°C, with subsidiary unblocking peaks close to the magnetite Curie point (Fig.4). Specimen 55Z-83D shows in addition pronounced unblocking between 360°C and 420°C, suggesting a discrete Curie point around 400°C. This corresponds well with the inflection at this temperature in the k-T curve. Specimen 55A-58A has a less prominent compositional gap, judging by the more gradual demag-netisation and correspondingly broader spread of unblocking temperatures.

4.4 Samples from MH2

Thermomagnetic curves for two samples from the magnetic zone of MH2 both exhibit broad distributions of Curie temperature. For sample MH2/56L-56m T_C ranges from ~250°C to 570°C and for sample MH2/56C-78m T_C extends from ~350°C to 570°C. Thus in both samples a variety of ferromagnetic spinels is present, with compositions ranging from ~50 mole% magnetite (MH2/56L-56m) or ~65 mole% magnetite (MH2/56C-78m) to nearly pure magnetite. Inflections in the k-T curves, representing discrete Curie points, occur at ~450°C, ~500°C and 570°C in both cases, whilst MH2/56L-56m also has a minor inflection at ~400°C. In both cases the susceptibility increases on cooling from high temperature, but the increase is much more pronounced for MH2/56C-78m. The distinct inflections, apart from the magnetite Curie point, are less evident in the cooling curves, indicating homogenisation of spinel grains.

The lower limit of the Curie temperature range has shifted down to ~250°C in sample MH2/56C-78m after the heating, indicating formation of of more magnetite-deficient spinel, either by exsolution from the compositions with intermediate magnetite contents or by homogenisation with originally paramagnetic chromian spinel. This complex series of chemical changes may occur within single zoned grains, with zones of intermediate composition reacting along their inner boundaries with early-formed chromian spinel cores; reacting along their outer boundaries with later crystallising magnetite-rich rims; and possibly undergoing spinodal decomposition in the central portion of the zone. The overall effect would be to create more magnetic material, with a greater range of Curie temperatures, as observed.

The thermomagnetic behaviour of sample MH2/56J-141m, from the relatively weakly magnetic zone of the kimberlite, is very similar to that of MH2/56C-78m, once allowance is made for the much greater relative contribution of paramagnetic minerals to the total susceptibility of the less magnetic sample. Thus the ferromagnetic mineralogy of the weakly magnetic and strongly magnetic kimberlite phases in MH2 appear to be similar. The difference in magnetisation simply reflects the relative abundance of this ferromagnetic assemblage. Thermal demagnetisation of SIRM (Fig.4), which does not reflect paramagnetic phases, confirms that the unblocking temperature spectra for specimens from the low and high susceptibility zones are qualitatively similar. Broad unblocking temperature spectra reflect a wide range of compositions, with the most pronounced unblocking occurring in the approximate ranges 400-500°C and 530-560°C. The relative prominence of these two peaks varies from sample to sample. Subsidiary peaks in the unblocking temperature spectra commonly occur at lower temperatures. Peaks in the spectra correlate well with the steeply descending portions of the k-T curves. The thermal demagnetisation data show that the bulk of the SIRM is carried by impure magnetites

with Curie temperatures from ~400°C up to 500-570°C. These phases also dominate the susceptibility.

Coercivity spectra derived from AF demagnetisation of NRMs of MH2 samples are quite variable. This is largely due to the presence of relatively intense, but very soft, IRM noise components in some specimens. After removal of these components by 100 Oe AF, the coercivity spectra are all broad, reflecting remanence carriers with a wide range of grain sizes. PSD and SD grains are important contributors to the NRMs of these samples. This confirms the ability of the kimberlite to retain stable ancient remanence.

5. MAGNETIC MINERALOGY OF THE LAMPROITE SAMPLES

5.1 Characteristics of Lamproites

Mitchell (1985, 1988) has reviewed the mineralogy of lamproites and has drawn the distinction between less evolved phlogopite lamproites (e.g. wyomingite, orendite, fitzroyite) containing phenocrystal phlogopite and more evolved madupitic lamproites (e.g. madupite, wolgidite), which have poikilitic groundmass phlogopite. According to Mitchell, spinels are common only in olivine lamproites from the West Kimberley region and in madupitic lamproites from the Leucite Hills and some other localities. Primary spinels are supposedly absent from other lamproites and from madupitic lamproites (wolgidites) of the West Kimberleys, although the present study demonstrates the presence of trace amounts of fine-grained ferromagnetic spinels in the Ellendale olivine and leucite lamproites. The compositions inferred from the Curie temperatures suggest that these spinels predominantly contain substantial amounts of end-members other than magnetite, suggestive of moderately evolved primary spinels rather than alteration products.

Spinels in lamproites can be classified into four broad compositional groups (Mitchell, 1985):

Group 1 - Ti-poor (< 1 wt% TiO_2) aluminous (> 10 wt% Al_2O_3) magnesiochromites

Group 2 - titanian (1-5% TiO_2) aluminous (1-10% Al_2O_3) magnesiochromites

Group 3 - Al-poor (< 1% Al_2O_3) titanian (> 5% TiO_2) magnesian (< 5% MgO) ferrichromites

Group 4- magnesian (< 5% MgO) titaniferous magnetites.

Goup 1 and 2 spinels have paramagnetic compositions, whereas Group 3 and 4 spinels are ferromagnetic. Typically Group 3 spinels contain 40-50 mole% magnetite, ~20 mole% chromite, ~20 mole% ulvospinel and ~15 mole% magnesian ulvospinel, when

recalculated to end members. Based on the compositions, the corresponding Curie temperatures are estimated to be ~250-300°C. Group 4 spinels typically contain 65-80 mole% magnetite in solid solution with 15-20 mole% ulvospinel and 5-10 mole % magnesian ulvospinel. The estimated Curie temperatures are ~360-460°C.

The interpreted evolutionary trend of lamproite spinels proceeds from Group 1 compositions through to Group 4. Thus more evolved lamproites should have ferromagnetic Group 3 and 4 spinels and have relatively high susceptibility, whilst less evolved lamproites are expected to be paramagnetic. The lamproite spinel trend is identical to the characteristic trend for micaceous (Group II) kimberlites (magmatic trend 2). As crystallisation proceeds Ti, total iron and Fe^{3+} increase at the expense of Al, Cr and Mg. Group 2-4 lamproite spinels are relatively poor in Al and Mg, and rich in total iron and Fe^{3+}, compared to spinels of magmatic trend 1, which characterises, and is unique to, phlogopite-poor monticellite-serpentine-calcite (Group I) kimberlites. This difference may reflect removal of Mg and Al from the melt by extensive phlogopite precipitation, prior to crystallisation of spinel. The lamproite/micaceous kimberlite spinel trend is also a Cr-rich variant of the lamprophyre trend. Kimberlite trends 1 and 2 and the lamprophyre trend converge on the titanomagnetite apex of the spinel prism, culminating in crystallisation of end-member magnetite. By analogy, pure magnetite probably represents the last-crystallising spinel in fully-evolved lamproites also. Almost pure magnetite is also a possible alteration product of olivine, micas and amphiboles in these rocks.

Complete spinel trends frequently do not occur within individual lamproites. Ilmenites are rare in lamproites and reported compositions are all paramagnetic. The variable susceptibilities of these rocks should therefore predominantly reflect the degree of magmatic evolution, which determines the occurrence and abundance of late-crystallising ferromagnetic spinels relative to early-crystallising paramagnetic spinels. Spinels in West Kimberley olivine lamproites reportedly belong predominantly to Groups 1 and 2 and rarely to Group 3. Madupitic wolgidites from the West Kimberleys are reported to contain priderite, which has an antipathetic relationship to spinels, as the only primary oxide mineral. Alteration producing secondary magnetic minerals is a possible complicating factor, although secondary magnetite or other ferromagnetic phases do not appear to have been described from these rocks.

Carmichael *et al.* (1974, pp.252-255) indicate that titanomagnetite is a ubiqitous accessory in madupites from the Leucite Hills, Wyoming, whereas the phlogopite-phyric types, wyomingite and orendite, contain only occasional chrome-spinel microphenocrysts as the only Fe-Ti-bearing oxides. This observation is consistent with Mitchell's (1985) interpretation.

Magmatic redox conditions are also important. Spinels from the Argyle lamproite, for example, exhibit a crystallisation trend with negligible enrichment in Fe^{3+} and Ti as Cr/Al and Fe^{2+}/Mg increase (Jaques *et al.*, 1988). The lack of an enrichment trend towards Ti-magnetite (i.e. constant Fe^{3+} over a wide Fe-Mg range) in the Argyle lamproites is interpreted to represent crystallisation under reduced conditions, with oxygen fugacity remaining close to the magnetite-wustite buffer. The low oxygen fugacity probably reflects the reduced nature of the source region.

The magnetic properties, however, show that ferromagnetic spinels, with compositions suggesting primary phases, are present in all the lamproite samples, at least in trace amounts. The Curie points suggest compositions for these phases corresponding to Group 3 and 4 spinels, usually extending to minor amounts of pure or nearly pure magnetite. This conflict with the published mineralogical data can plausibly be explained by the very small amounts of these spinels (maximum ~0.2 vol%, frequently much less) and the generally small grain size indicated by the coercivity spectra. The ferromagnetic spinel grains range from small MD (at most a few tens of microns) to submicron SD, and probably represent thin outer zones and rims on rare paramagnetic spinels. Thus these phases could easily escape attention during petrographic examination.

5.2 Thermomagnetic Curves and Demagnetisation Experiments

The k-T curves of the more magnetic (k > 100 μG/Oe) lamproite samples are shown in Fig.5, Fig.6 presents AF demagnetisation curves and corresponding coercivity spectra for selected specimens and Fig.7 shows thermal demagnetisation of three-component remanence. The thermomagnetic curves are quite similar overall to the kimberlite k-T curves, suggesting spinel populations with comparable ranges in magnetite content are present in the lamproites, albeit at lower concentration. The main range of Curie points generally lies between 300-450°C and the magnetite Curie temperature. The tail in the curves above 600°C is due to the use of large samples, in an effort to boost the signal/noise ratio, leading to a thermal gradient through the heated samples. Sample V8879 also has a phase with a very low Curie point, around room temperature, V8882 has a phase with a slightly lower T_C and there is a hint of a similar feature in the curve for sample V8885. These low T_C phases probably represent spinels containing about 20 mole% magnetite in solid solution with paramagnetic end members. They have disappeared as distinct compositions with discrete Curie points after heating to 700°C.

One distinction between the thermomagnetic behaviour of the lamproites and kimberlites in this collection is that magnetic material is generally created by heating of the kimberlites, but tends to be destroyed for the lamproites. This suggests there is a fundamental difference (either in

composition or microstructure) between the spinels of the two rock types. The spinels of these Group I kimberlites are expected to follow magmatic trend 1, whereas the lamproite spinels should correspond to compositions along magmatic trend 2. Therefore the low to moderate T_C spinels of the kimberlite samples should be Mg-Ti-rich magnetites, whilst the spinels with similar Curie temperatures in the lamproites should be Mg-poor, Cr-rich titanomagnetites. In both cases the spinel grains are likely to be mantled by titanomagnetite ranging to pure magnetite in evolved representatives.

AF demagnetisation of SIRM indicates predominantly PSD characteristics (Fig.6). Thermal demagnetisation of three-component remanence is particularly diagnostic of magnetic mineralogy for the weakly magnetic samples, for which thermomagnetic analysis is hampered by a low signal/noise ratio. The demagnetisation curves (Fig.7) show a major inflection at the magnetite Curie point for at least the softer components, except for sample V8883, which appears to have no magnetite-rich spinels. The presence of haematite in some of the samples (V8878, V8881, V8883, V8889) is clearly revealed by the form of the curve for the hardest (Z) component, which corresponds to coercivities greater than 1000 Oe. For these samples the z-component does not unblock completely until well above the magnetite Curie point, but finally vanishes close to the haematite Curie temperature of 670°C. Haematite is difficult to detect using k-T curves, unless it is very abundant, and thermal demagnetisation is a much more sensitive technique for identification of traces of weakly ferromagnetic phases.

Comparison of the form of the demagnetisation curves for the soft, intermediate and hard components indicates that lower coercivity grains correspond generally to lower T_C compositions. For example, the softest component carried by specimen V8879C vanishes by 510°C, whereas the intermediate and high coercivity components persist up to 580°C. However the coercivity range of the composition with $T_C \approx 500$°C does extend above 1000 Oe, implying a wide range of grain sizes for this composition alone. Compositions with $T_C \approx 500$°C, 550°C and 580°C are successively harder. Some samples contain ultrafine SD grains with lower T_C, corresponding to relatively magnetite-poor compositions. For example, specimen V8880B contains hard SD grains with $T_C \approx 325$°C, plus SD-PSD grains with $T_C \approx 450$°C, plus MD grains with $485°C \leq T_C \leq 570°C$, plus SD-PSD grains with compositions very close to magnetite. Specimen V8888E contains MD grains which all have $T_C \leq 270$°C, plus SD-PSD grains with $T_C \approx 325$°C, plus PSD grains with Curie points between 385°C and 510°C, plus SD grains with $T_C = 510$°C. Specimen V8883B contains only weakly ferromagnetic high coercivity grains. The substantial unblocking by 180°C suggests that this sample contains goethite, which is very hard but has T = 120°C. Minute amounts of ultrafine spinels, unblocking between 180°C and 385°C, may also be present, but the bulk of the remanence above 180°C is carried by haematite. This remanence unblocks by

640°C, which is well below the Curie point of 670°C, implying that the haematite grains must be small SD, close to the superparamagnetic threshold size of ~ 0.03 μm.

The composition and domain structure of the magnetic grains in the lamproite samples inferred from the rock magnetic experiments are summarised in Table 5. Haematite and goethite, which are present in several samples, are probably produced by weathering. The ferromagnetic spinel compositions within individual samples range from sp20-80 (typically ~sp40) up to magnetite or slightly impure magnetite (sp0-10). The absolute amounts vary widely, producing the range of susceptibilities in Table 3 (14-600 μG/Oe). Small MD to PSD/SD grains predominate, corresponding to effective grain sizes from ~20 μm down to the submicron range. These phases are probably not present as discrete grains, but occur within zoned spinels.

6. CONCLUSIONS

(i) The magnetisation of the Group I kimberlites is associated with fine-grained (small MD to SD) spinels with a wide range of Curie points, a feature characteristic of kimberlites generally. Inferred compositions within individual samples range from sp30-75 up to sp0-7. Smaller, high coercivity grains tend to be more magnetite-rich. Magnetite-poor and magnetite-rich compositions are in intimate contact and tend to homogenise on heating. The susceptibility of the kimberlites ususally increases after heating. The ferromagnetic grains are interpreted as zoned spinels with thin magnetite-rich rims.

(ii) The kimberlites have moderate to high susceptibilities (~600-4700 μG/Oe), except for the relatively weakly magnetic zone of MH2 intersected by hole MH2/56J (k = 85 μG/Oe). This zone has similar magnetic mineralogy to the more magnetic kimberlites, but substantially lower concentrations of ferromagnetic minerals. The occurrence of dual polarity remanence components in MH2 also indicates that this pipe is a multiple intrusion.

(iii) The Q values indicate that the magnetisation of the kimberlites is enhanced by factors of ~3-6 with respect to the contribution of susceptibility alone. Thus the anomalies caused by pipes of given size should be several times larger than would be estimated from susceptibility measurements, if remanence is neglected. Conversely, targets may be substantially smaller than indicated by models that assume magnetisation by induction, using typical susceptibility values for these kimberlites.

(iv) The simplest approach to allow for the effects of remanence on the anomalies due to the South Australian kimberlites is to augment the model susceptibility by a factor of (1+Q). This is strictly valid only if the remanence is parallel to the geomagnetic field, but should provide a reasonable approximation in this instance, where the steep up

remanence is subparallel to the present field. A more rigorous approach is to incorporate remanence into modelling using intensities consistent with measured values and assuming that the remanence direction corresponds to the Mid-Jurassic palaeofield. The normal polarity palaeofield direction is (dec = 307°, inc = -71°) and the reversed polarity direction is (dec = 127°, inc = +71°). The assumption that the *in situ* NRM is essentially primary is supported by palaeomagnetic cleaning and by analogy with other kimberlites.

(v) The estimated bulk magnetic properties of the Eyre Peninsula kimberlites are:

V8875-77: k = 580 μG/Oe; J = 730 μG; I = -75°; Q = 2.1

MH1: k = 1160 μG/Oe; J = 3500 μG; I = -75°; Q = 5.0

MH2/56J: k = 85 μG/Oe; J ≈ 330 μG; I ≈ -40°; Q = 6.5

MH2/56C,L: k = 1130 μG/Oe; J = 3800 μG; I = -75°; Q = 5.6

Although the less magnetic zone of MH2 intersected by hole MH2/56J has low susceptibility, it is still sufficiently magnetic to produce a detectable anomaly, because of the moderately intense remanence.

(vi) The Ellendale lamproites have low to moderate susceptibilities (14-600 μG/Oe). Taking remanence into account, the magnetisation of most lamproites is sufficient to produce a small anomaly, detectable from the air only because of the very quiet magnetic environment. The data are insufficient to draw any conclusions about differences between mineralogical types or magmatic versus pyroclastic facies. Koenigsberger ratios are generally greater than unity and pipes may have remanence of either polarity, as expected for Miocene rocks. The remanence of the lamproites is somewhat steeper than the present field, reflecting the more southerly position of Australia during the Miocene. Thus either negative or positive anomalies may be associated with West Kimberley lamproites.

(vii) The Ellendale lamproites all contain at least trace amounts of ferromagnetic spinels with a range of compositions extending to pure or nearly pure magnetite, although the dominant magnetic phases contain substantial proportions of other end members. This contradicts the reported absence of evolved spinels from these rocks. The supposed absence of magnetite-rich spinels probably reflects the very small quantities and small effective grain size of the most evolved spinel phases, which probably occur mainly as thin rims on earlier-formed paramagnetic spinel grains. Ferromagnetic spinel compositions within individual lamproites range from sp20-80 (typically ~sp40) up to sp0-7. Haematite is present in several samples, some of which also contain goethite. The goethite, and probably also the haematite, are produced by weathering.

(viii) Although the k-T curves of the moderately magnetic lamproites broadly resemble those of the kimberlite samples, there seems to be a different response of the ferromagnetic assemblages to heating. Rehomogenisation of spinels after heating to > 600°C occurs for both rock types, but extra ferromagnetic material is usually created in kimberlite samples, whereas some ferromagnetic material is destroyed by heating of the lamproites. This may reflect differing compositions of moderately evolved spinels for Group I kimberlites, characterised by magmatic trend 1, and lamproites, which follow magmatic trend 2. The intermediate composition spinels of Group I kimberlites are magnesian ulvospinel-ulvospinel-magnetite solid solutions, evolving to Mg-Ti-magnetites, whereas the comparably evolved lamproite spinels are probably ferrichromites to Cr-Ti-magnetites.

(ix) The most magnetic lamproites are expected to be relatively highly evolved madupitic lamproites characterised by poikilitic groundmass phlogopite, rather than less evolved phlogopite-phyric lamproites. This conclusion is contingent on redox conditions in the magma becoming sufficiently oxidising to allow enrichment of Fe^{3+} in late-crystallising spinels. The bulk composition, particularly the relative proportions of iron and alkalis, should also influence the crystallisation of titanomagnetites, which can only form when the amount of ferric iron that can be accomodated in potassium aluminium silicates, alkali amphiboles and sodic pyroxenes is exceeded. In lamproites, such as those at Argyle, which have crystallised under highly reducing conditions, possibly reflecting a reduced source region, the late-crystallising spinels remain para-magnetic and the magnetisation is accordingly weak.

7. REFERENCES

Carmichael, I.S.E., Turner, F.J. and Verhoogen, J., 1974. *Igneous Petrology*, McGraw Hill, New York, 739 pp.

Clark, D.A. and French, D.H., 1990. Rock magnetism and magnetic petrology of kimberlites. CSIRO Restricted Report 118R.

Jaques, A.L., Haggerty, S.E., Lucas, H. and Boxer, G.L., 1988. Mineralogy and petrology of the Argyle (AK1) lamproite pipe, Western Australia, *in* Kimberlites and Related Rocks (Proceedings of the Fourth International Kimberlite Conference, Perth 1986), GSA Special Publication No. 14, pp.153-169.

Lowrie, W., 1990. Identification of ferromagnetic minerals in a rock by coercivity and unblocking temperature properties. Geophys. Res. Lett., 17, 159-162.

Mitchell, R.H., 1985. A review of the mineralogy of lamproites. Trans. geol. Soc. S. Afr., 88, 411-437.

Mitchell, R.H., 1988. Aspects of the petrology of kimberlites and lamproites: some definitions and distinctions, *in* Kimberlites and Related Rocks (Proceedings of the Fourth International Kimberlite Conference, Perth 1986), GSA Special Publication No. 14, pp.7-45.

Table 1. DESCRIPTION OF SAMPLES

Sample	Rock type	Locality
BF1986	kimberlite	-
MH1/55*	kimberlite	Eyre Peninsula
MH2/56*	kimberlite	Eyre Peninsula
S8173	kimberlite	Eyre Peninsula
V8875	kimberlite	Eyre Peninsula
V8876	kimberlite	Eyre Peninsula
V8877	kimberlite	Eyre Peninsula
V8878	lamproite lapilli tuff	Mt North (Ellendale)
V8879	Ol-di-richt-phlog-leuc-lamproite	" "
V8880	coarse phlogopite-leucite lamproite	81 Mile Vent (Ellendale)
V8881	basal surge tuff	" "
V8882	phlogopite-olivine lamproite	Ellendale 9
V8883	olivine lamproite	Ellendale 9
V8884	coarse richt-phlog-leuc-lamproite	81 Mile Vent (Ellendale)
V8885	bedded tuff, lapilli tuff	" "
V8886	coarse tuff breccia	" "
V8887	diopside-leucite lamproite	Hills Cone (Ellendale)
V8888	olivine lamproite lapilli tuff (weathered)	Ellendale 9
V8889	weathered lamproite tuff	Walgidee Hill (Ellendale)
V8890	fine olivine-leucite lamproite	" "

V8875-77 are from one pipe, as are MH1 and S8173.
The kimberlites are all Group I.

Table 2. MAGNETIC PROPERTIES OF KIMBERLITE SAMPLES

Sample	k(μG/Oe)	J(μG)	Inc	Q
BF1986	4720	1610	+71°	0.6
V8875	550	430	-78°	1.3
V8876	470	1020	-71°	3.6
V8877	710	730	±71°	1.7
S8173	810	1080	-78°	2.2
MH1/55A-51m	670	2610	-74°	6.5
MH1/55A-58m	840	2890	-83°	5.7
MH1/55Z-83m	1440	3450	-72°	4.0
MH1/55Z-93m (Kimberlite)	~2050	~7450	~-61°	~6.1
MH1/55Z-93m (Gneiss)	~530	~2190	~-72°	~6.9
MH1/55Z-100m (Gneiss)	22	0.7	±82°*	0.05
MH2/56C-78m	880	1050	+84°	2.0
MH2/56J-79m	59	156	-72°	4.4
MH2/56J-109m	65	1110	-13°	31.4
MH2/56J-141m	138	303	-73°	3.7
MH2/56J-156m	77	240	-74°	5.2
MH2/56L-56m	1380	6930	-75°	7.7
MH2/56P-68m (Schist)	95	39	-69°	0.68

k = cgs (emu) susceptibility x 10^6

J = NRM intensity in microgauss (10 μG = 1 γ)

Inc = NRM inclination (assuming vertical drill hole), positive downwards

Q = Koenigsberger ratio = J/kF, where F = 0.6 Oe

* Up-hole direction not marked on sample

Table 3. MAGNETIC PROPERTIES OF ELLENDALE LAMPROITE SAMPLES

Sample	k(μG/Oe)	J(μG)	Q
V8878	23	17	1.5
V8879	102	61	1.2
V8880	45	1.6	0.07
V8881	14	115*	16*
V8882	250	55	0.4
V8883	14	2	0.6
V8884	28	610*	44*
V8885	570	890	3.1
V8886	270	500	3.7
V8887	600	11,330*	38*
V8888	48	155	6.5
V8889	50	320*	13*
V8890	25	10	0.8

* sample probably affected by lightning: J and Q unrepresentative

k = cgs (emu) susceptibility x 10^6

J = NRM intensity in microgauss (10 μG = 1 γ)

Inc = NRM inclination (assuming vertical drill hole), positive downwards

Q = Koenigsberger ratio = J/kF, where F = 0.5 Oe

Table 4. MAGNETIC MINERALS IN KIMBERLITE SAMPLES

Sample	Curie Points (°C)	Composition	Domain structure	Rank
V8875	100	sp70	MD-PSD	3
	325	sp40	SD	2
	325-535	sp40-sp7	MD-SD	1
	555	sp4	MD-PSD	4
	580	mt	SD	5
V8876	100	sp70	MD-PSD	3
	180-485	sp60-sp15	MD-PSD	1
	450	sp20	SD-PSD	2
	450-535	sp20-sp7	SD-PSD	4
	555	sp4	SD	5
V8877	100-485	sp70-sp15	MD-SD	2
	385	sp30	MD-PSD	4
	485	sp15	SD-MD	1
	535	sp7	SD-MD	3
S8173	80-220	sp75-sp55	MD-PSD	2
	385-485	sp30-sp15	MD-SD	1
	485	sp15	SD-MD	3
	555	sp4	SD-PSD	4
	580	mt	SD-PSD	5
MH1/55A58	160-530	sp60-sp8	MD?	2
	230	sp55	MD-PSD?	3
	500	sp13	MD-PSD?	4
	580	mt	PSD-SD?	1
MH1/55Z83	200-400	sp55-sp30	MD-SD?	3
	420	sp25	MD-PSD	2
	450-580	sp20-sp0	PSD-SD?	1
	580	mt	SD?	4
MH2/56C78	360-500	sp35-sp13	MD-SD	1
	420	sp25	MD-SD	3
	500	sp13	MD-SD	2
	580	mt	SD?	4

(continued)

Table 4 (continued)

MH2/56J79	300-560	sp45-sp3	PSD?	1
	360	sp35	PSD-MD	3
	560	sp3	PSD-SD	2
	580	mt	SD?	4
MH2/56J109	300-560	sp45-sp3	MD-PSD	1
	360	sp35	MD-PSD	4
	500	sp13	MD-SD	3
	570	sp1	PSD?	2
MH2/56J141	400-580	sp30-sp0	MD-SD	1
	500	sp13	MD-SD?	3
	560	sp3	PSD-SD?	2
MH2/56J156	360-580	sp35-sp0	PSD	1
	500	sp13	PSD?	4
	560	sp3	PSD?	2
MH2/56L56	250-360	sp50-sp35	MD-SD	2
	500	sp13	PSD-SD?	1
	560	sp3	PSD-SD?	3

Here, sp10 means magnetite containing ~ 10 mole % of other spinel end members; mt = magnetite = sp0; hm = haematite; goe = goethite; MD = multidomain; SD = single domain; PSD = pseudosingle domain; SPM = superparamagnetic. Where more than one domain structure type is given, the dominant domain structure is given first. The rank indicates the estimated relative contributions to the magnetisation of the different phases, with 1 signifying the largest contribution.

Table 5. MAGNETIC MINERALS IN LAMPROITE SAMPLES

Sample	Curie Points (°C)	Composition	Domain structure	Rank
V8878	325	sp40	MD-SD	4
	450	sp20	MD-PSD	5
	485-535	sp15-sp7	MD-SD	3
	580	mt	MD-SD	1
	640	hm	SD-SPM	2
V8879	10	sp80	para	5
	385	sp30	SD-MD	2
	510	sp10	MD-SD	1
	550	sp5	PSD-SD	3
	580	mt	SD-PSD	4
V8880	325	sp40	SD-PSD	1
	450	sp20	SD-PSD	2
	510	sp10	SD-MD	4
	580	mt	SD-MD	3
V8881	385	sp30	PSD-MD	4
	510	sp10	MD-SD	2
	555	sp4	PSD	5
	580	mt	SD-PSD	3
	670	hm	SD	1
V8882	0	sp80	para	5
	~300	sp45	MD-PSD	3
	480	sp15	MD-PSD	2
	540	sp6	MD-PSD	1
	580	mt	PSD?	4
V8883	<180	goe	SD	3
	385	sp30	SD	1
	640	hm	SD-SPM	2
V8884	450	sp20	SD-PSD	2
	535	sp7	MD-SD	1
V8885	450	sp20	SD	3
	485-555	sp15-sp4	SD-MD	1
	570	sp1	SD	2

(continued)

Table 5 (continued)

V8886	450	sp20	MD	4
	535	sp7	MD	3
	485-570	sp15-sp1	SD-MD	1
	580	mt	PSD-SD	2
V8887	400-580	sp30-sp0	MD-SD	
V8888	270	sp45	MD	3
	325	sp40	SD-PSD	1
	385-510	sp30-sp10	PSD	4
	510	sp10	SD	2
V8889	<180	sp60+	MD-PSD	4
	180-270	sp60-sp45	SD	3
	580	mt	SD-PSD	2
	670	hm	SD	1
V8890	385	sp30	SD	1
	555	sp4	SD	3
	640	hm	SD-SPM	2

Here, sp10 means magnetite containing ~ 10 mole % of other spinel end members; mt = magnetite = sp0; hm = haematite; goe = goethite; MD = multidomain; SD = single domain; PSD = pseudosingle domain; SPM = superparamagnetic. Where more than one domain structure type is given, the dominant domain structure is given first. The rank indicates the estimated relative contributions to the magnetisation of the different phases, with 1 signifying the largest contribution.

Fig.1 AF demagnetisation data for MH1 and MH2 kimberlite samples

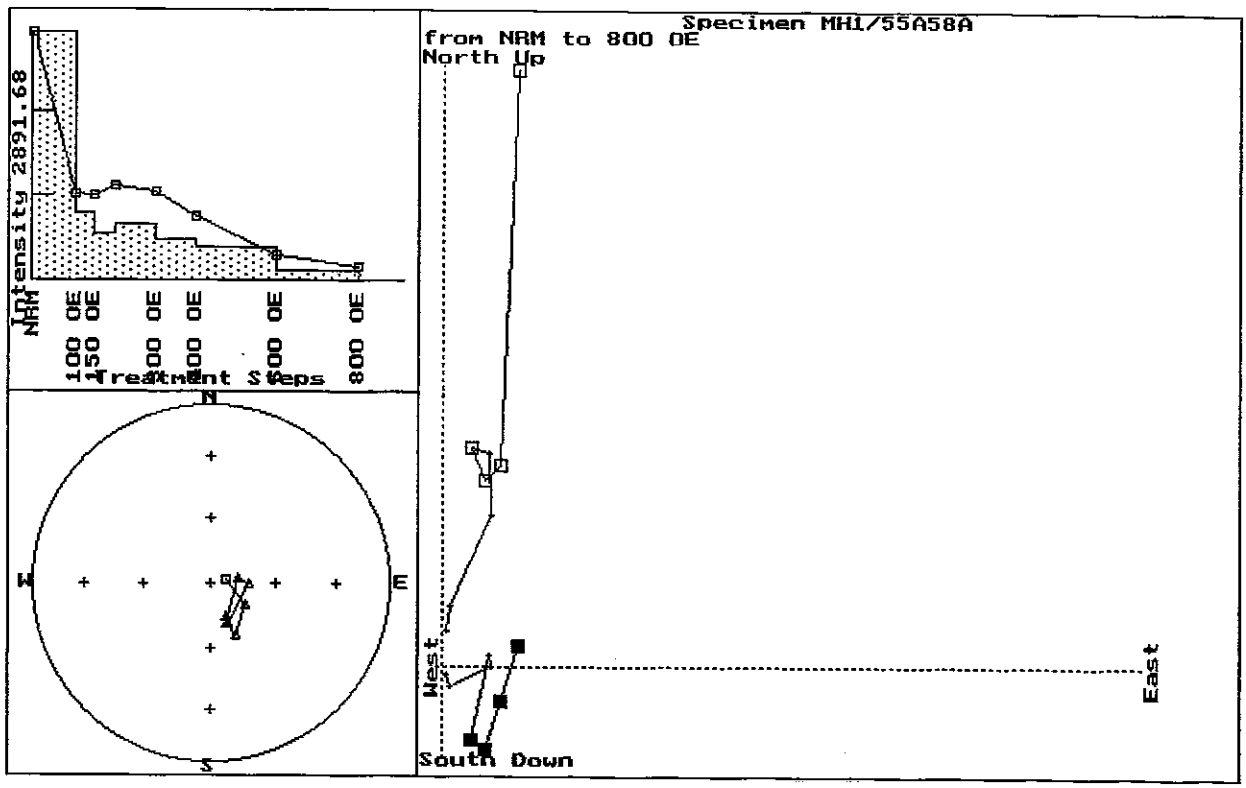
Specimen MH1/55A58A
from NRM to 800 OE
North Up
Intensity 2891.68
NRM
100 OE
150 OE
Treatment Steps
800 OE
N
E
S
W
West
East
South Down

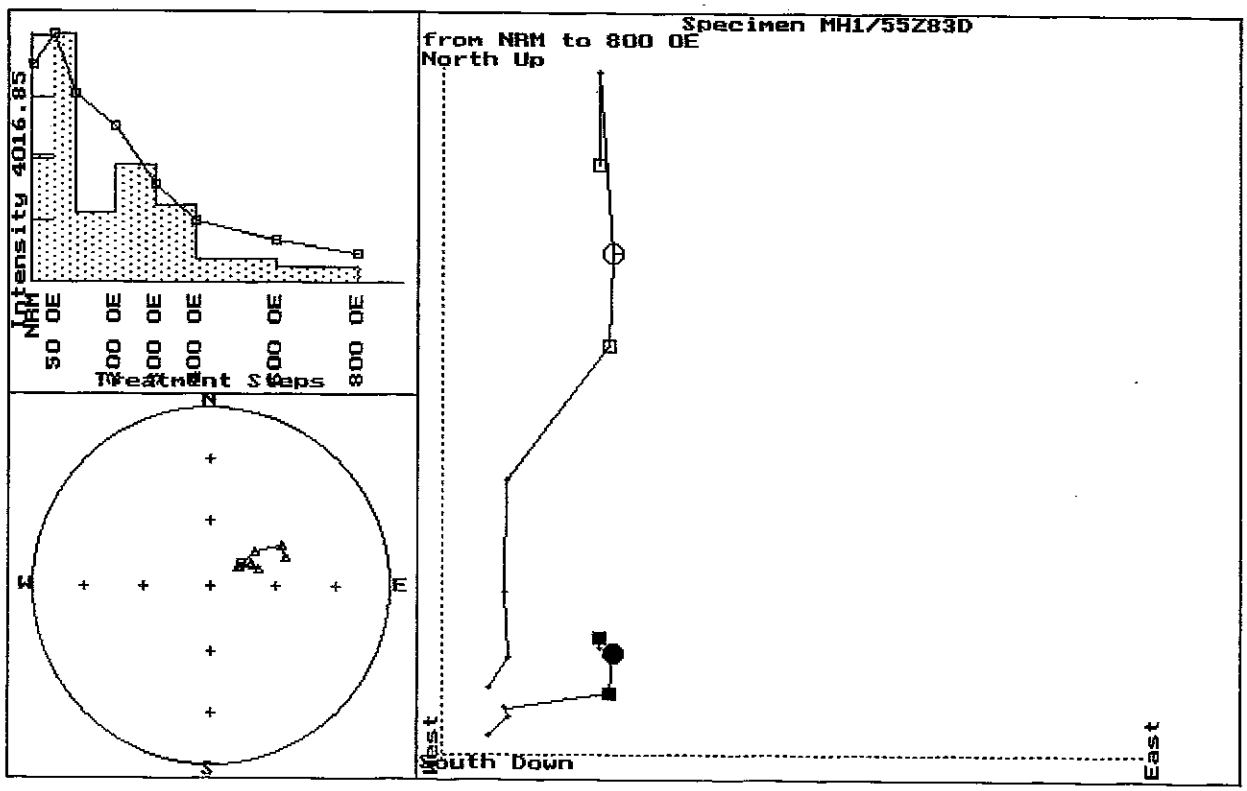
Specimen MH1/55Z83D
from NRM to 800 OE
North Up
Intensity 4016.85
NRM
50 OE
100 OE
Treatment Steps
800 OE
N
E
S
W
West
East
South Down

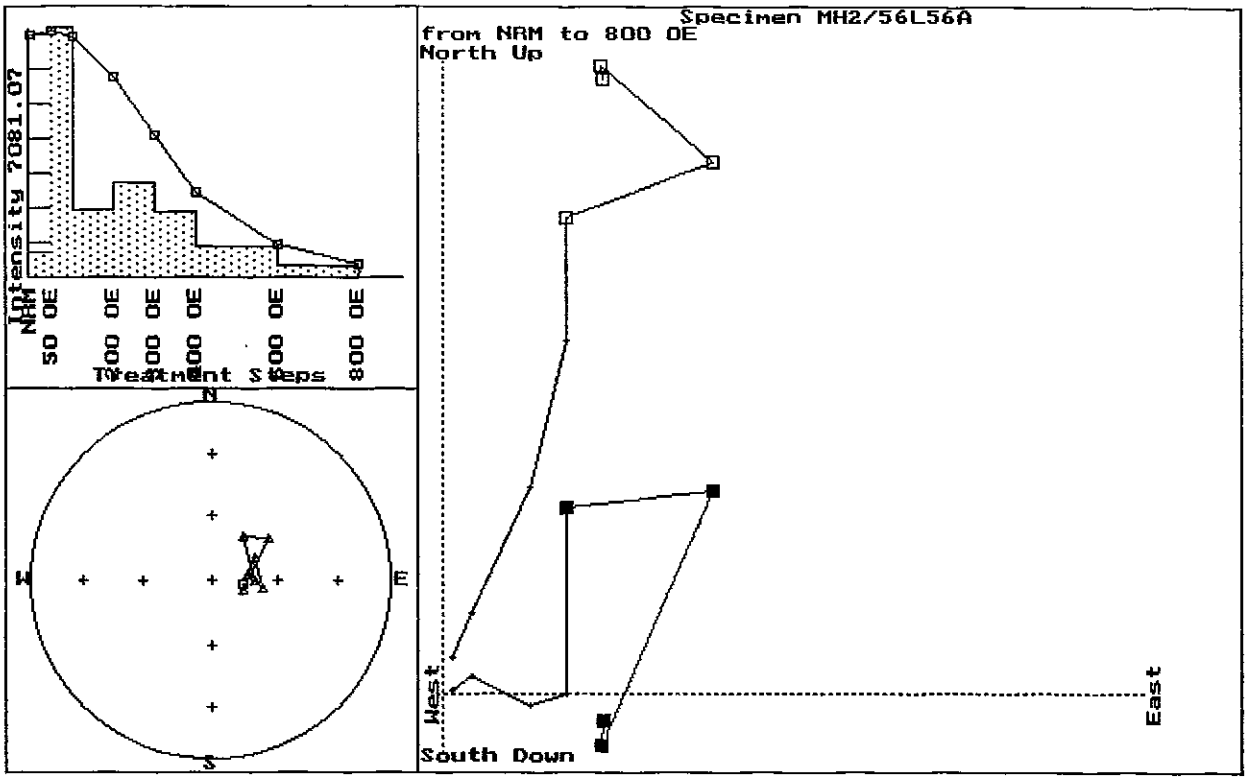
Intensity 7081.07
NRM
50 OE
100 OE
200 OE
300 OE
500 OE
800 OE
Treatment Steps
N
E
S
Specimen MH2/56L56A
from NRM to 800 OE
North Up
West
East
South Down

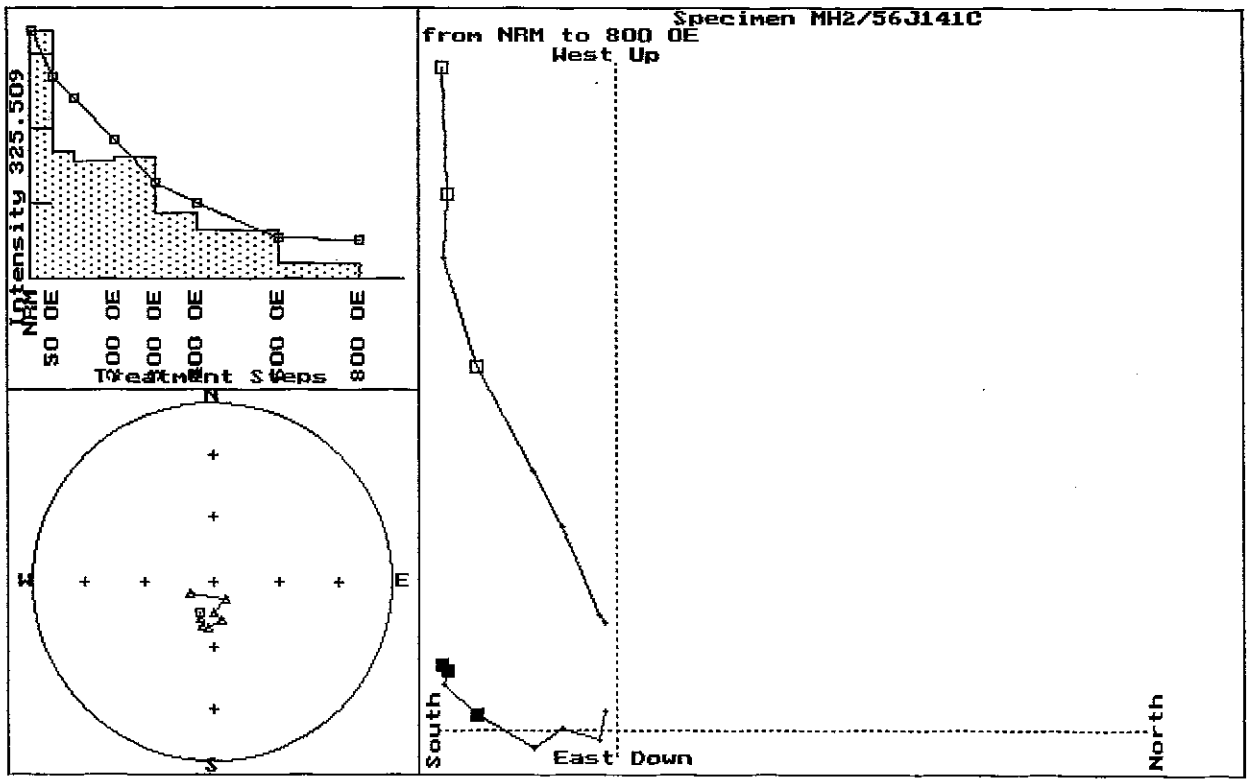
Intensity 325.509
NRM
50 OE
100 OE
200 OE
300 OE
500 OE
800 OE
Treatment Steps
N
E
S
Specimen MH2/56J141C
from NRM to 800 OE
West Up
South
East Down
North

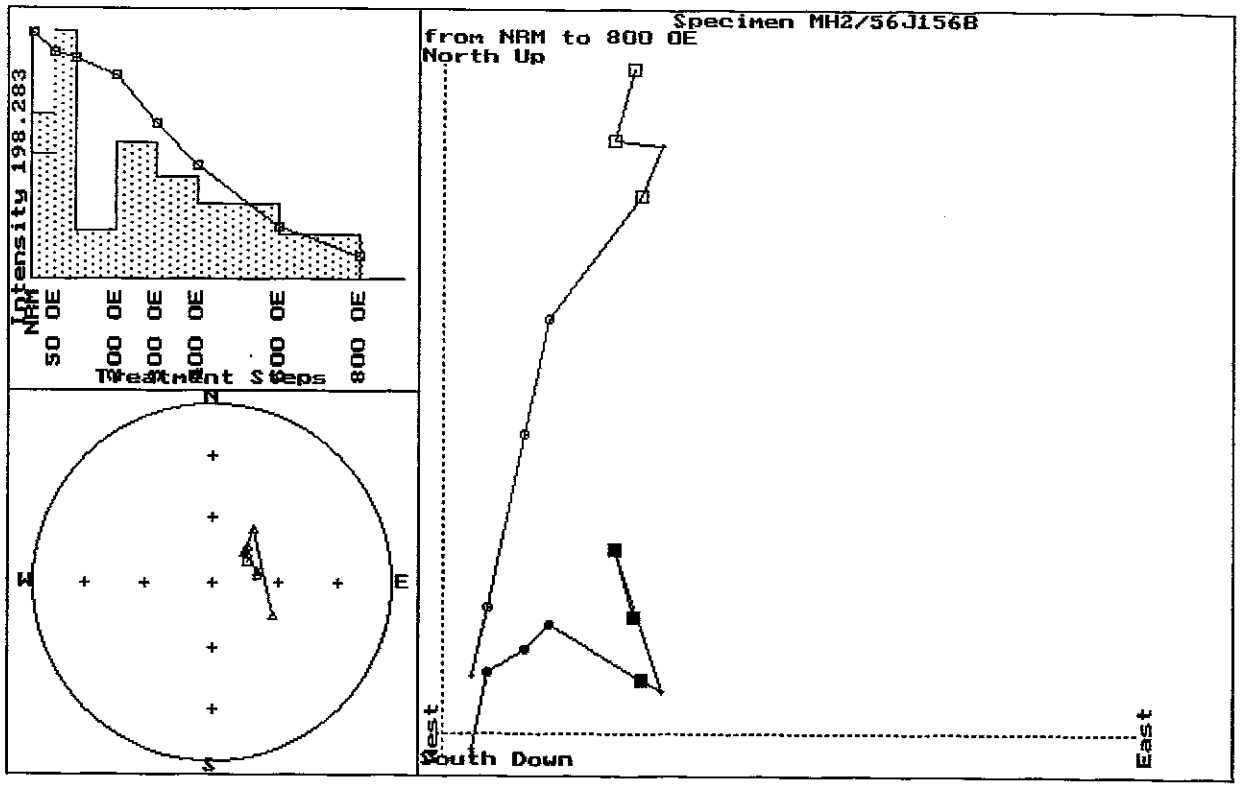
Intensity 198.283
NRM
50 OE
00 OE
00 OE
00 OE
00 OE
800 OE
Treatment Steps
N
E
S
W
Specimen MH2/56J156B
from NRM to 800 OE
North Up
West
East
South Down

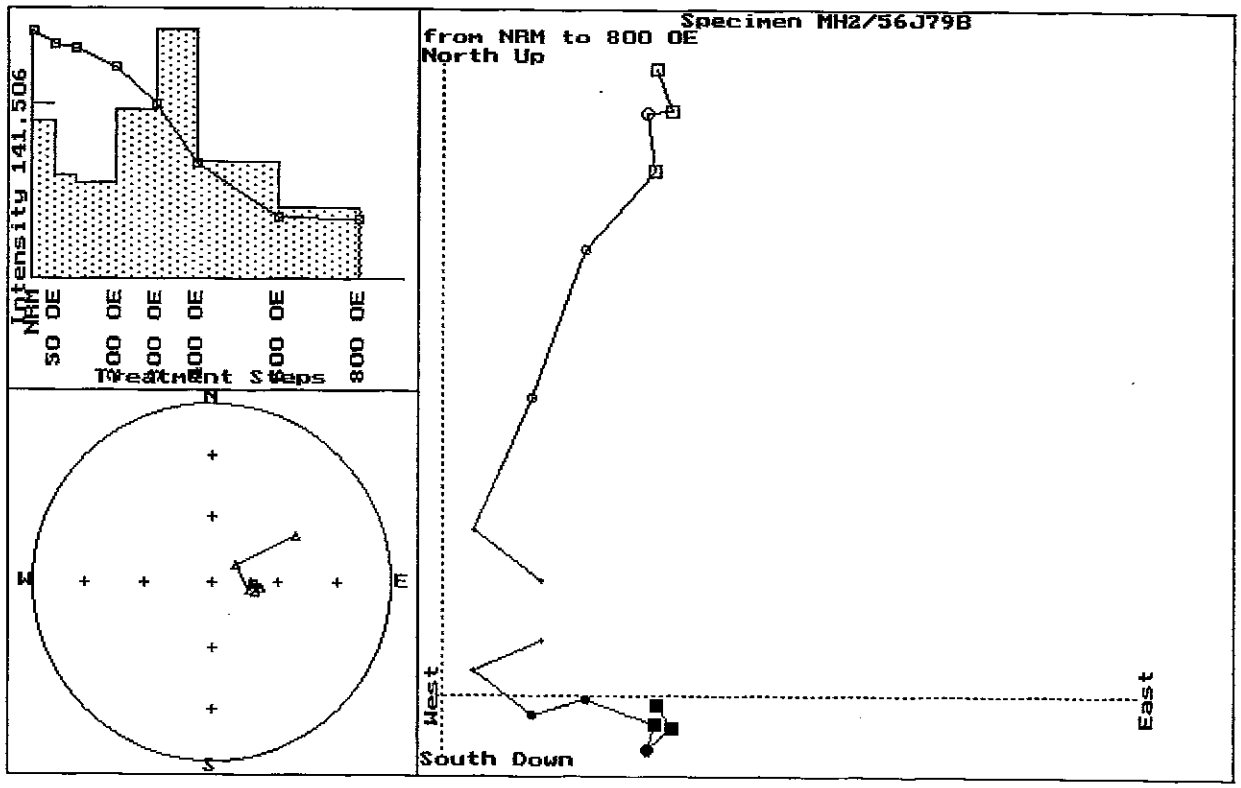
Intensity 141.506
NRM
50 OE
00 OE
00 OE
00 OE
00 OE
800 OE
Treatment Steps
N
E
S
W
Specimen MH2/56J79B
from NRM to 800 OE
North Up
West
East
South Down

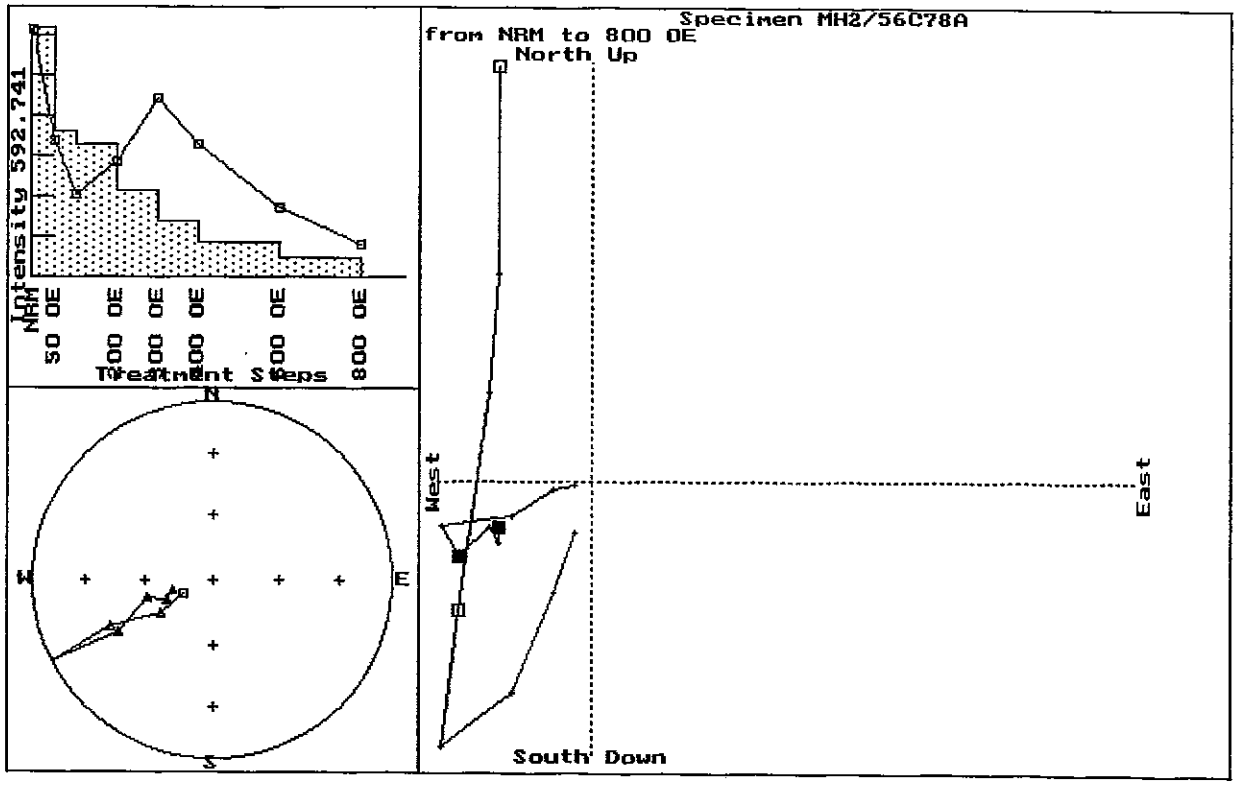
Intensity 592.741
NRM
50 OE
100 OE
200 OE
400 OE
800 OE
Treatment Steps
N
E
S
W
Specimen MH2/56C78A
from NRM to 800 OE
North Up
West
East
South Down

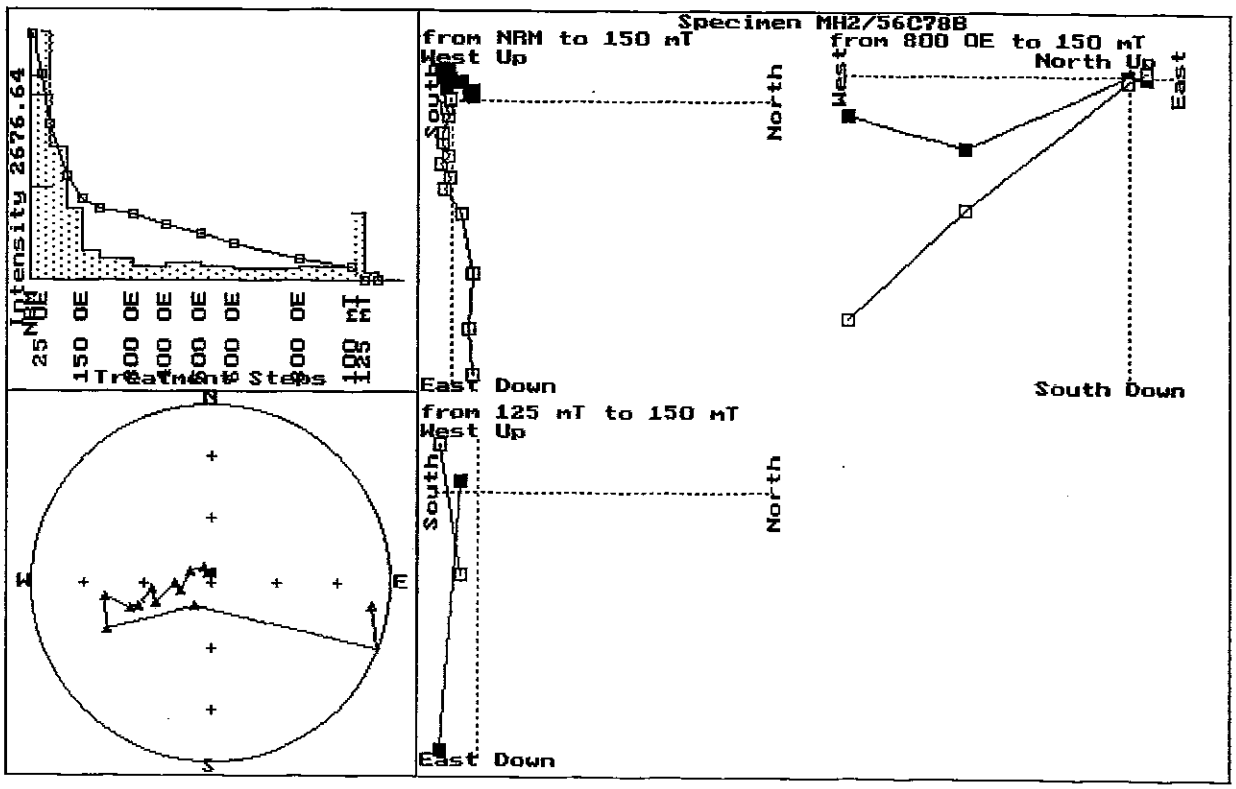
Intensity 2676.64
NRM
25 OE
150 OE
200 OE
400 OE
800 OE
100 mT
125 mT
Treatment Steps
N
E
S
W
Specimen MH2/56C78B
from NRM to 150 mT
West Up
South
North
East Down
from 800 OE to 150 mT
North Up
West
East
South Down
from 125 mT to 150 mT
West Up
South
North
East Down

stockdal.rem NRM

2/56J109

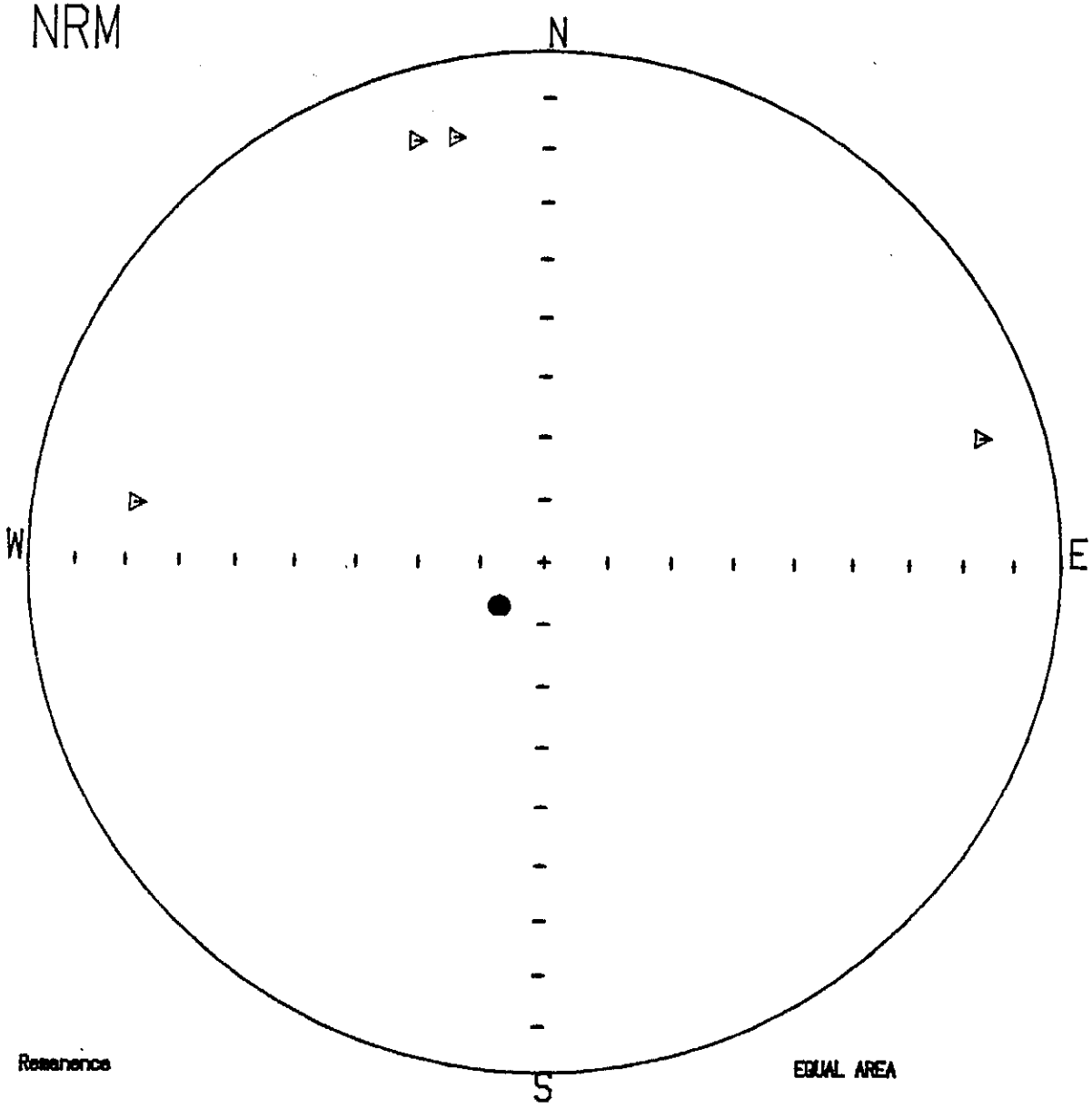

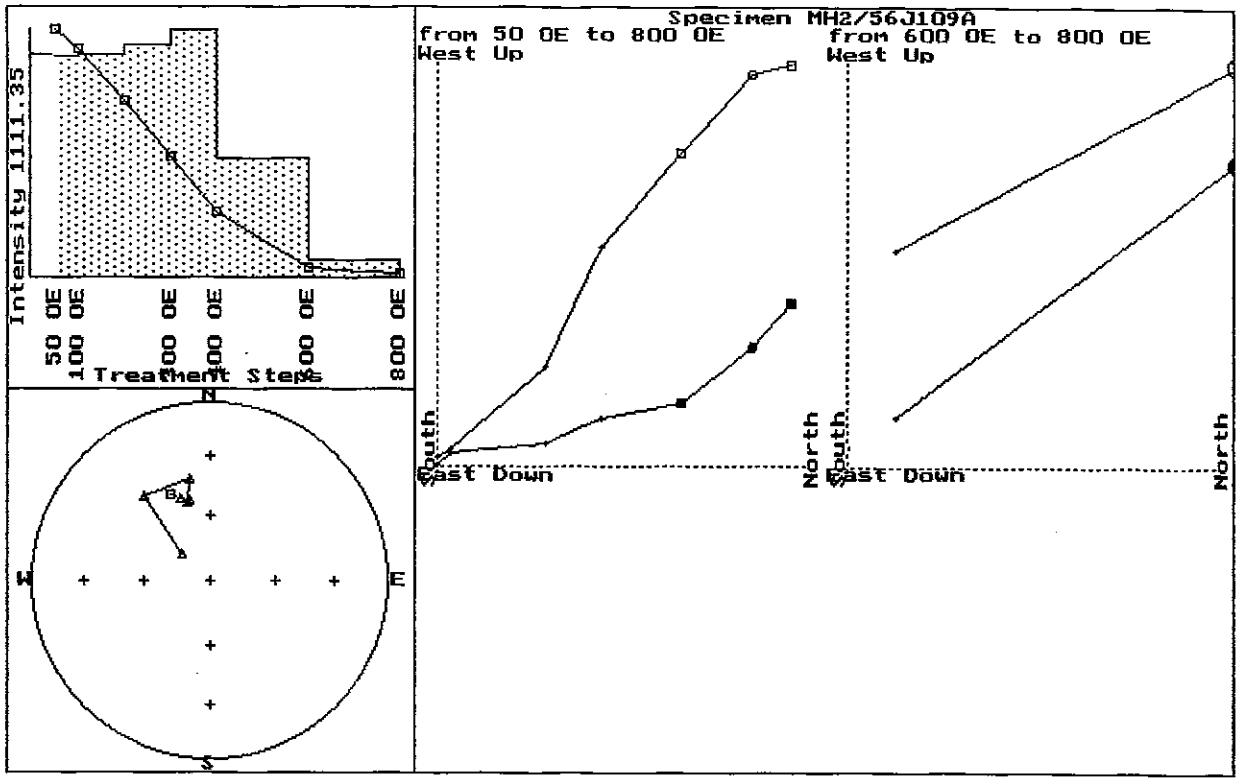
Specimen MH2/56J109A
from 50 OE to 800 OE
West Up
from 600 OE to 800 OE
West Up
Intensity 1111.35
50 OE
100 OE
200 OE
300 OE
400 OE
500 OE
600 OE
800 OE
Treatment Steps
South
East Down
North
South
East Down
North
N
W
E
S

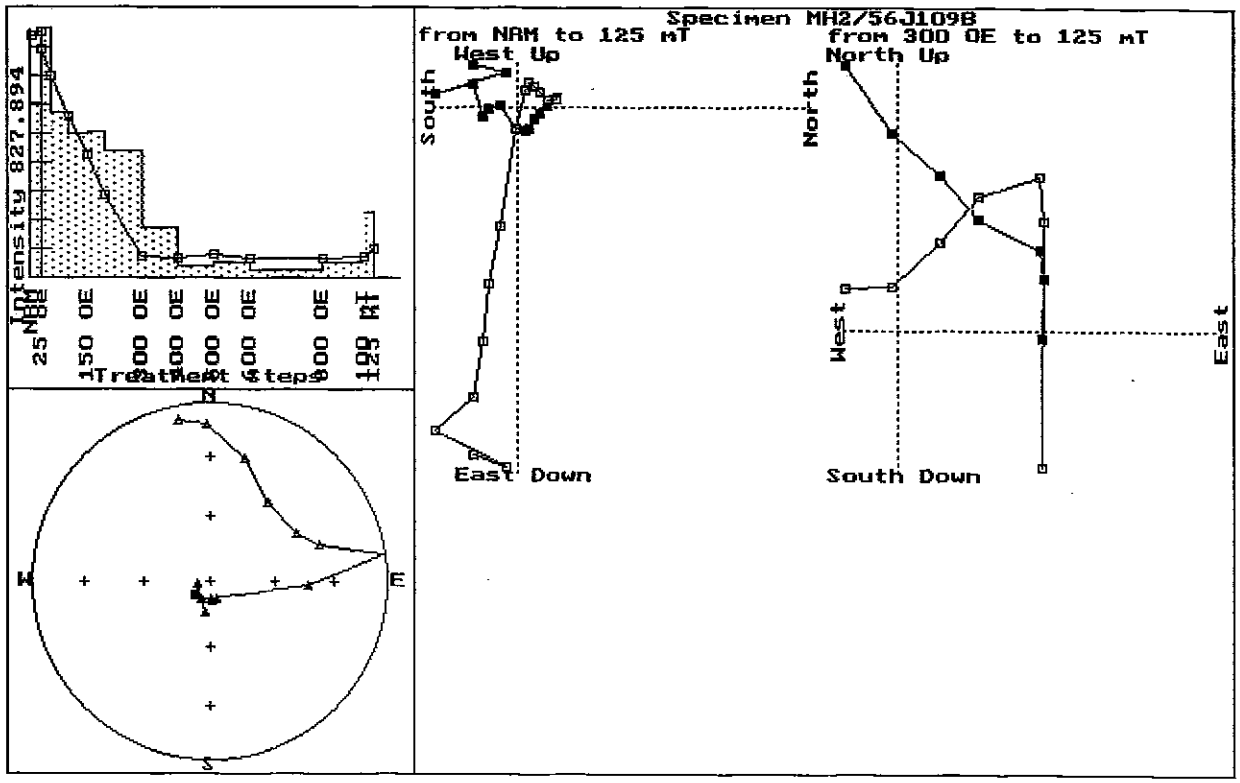
Specimen MH2/56J109B
from NRM to 125 mT
West Up
from 300 OE to 125 mT
North Up
Intensity 827.894
NRM
25 OE
150 OE
200 OE
300 OE
400 OE
500 OE
600 OE
800 OE
125 mT
Treatment Steps
South
East Down
North
West
South Down
East
N
W
E
S

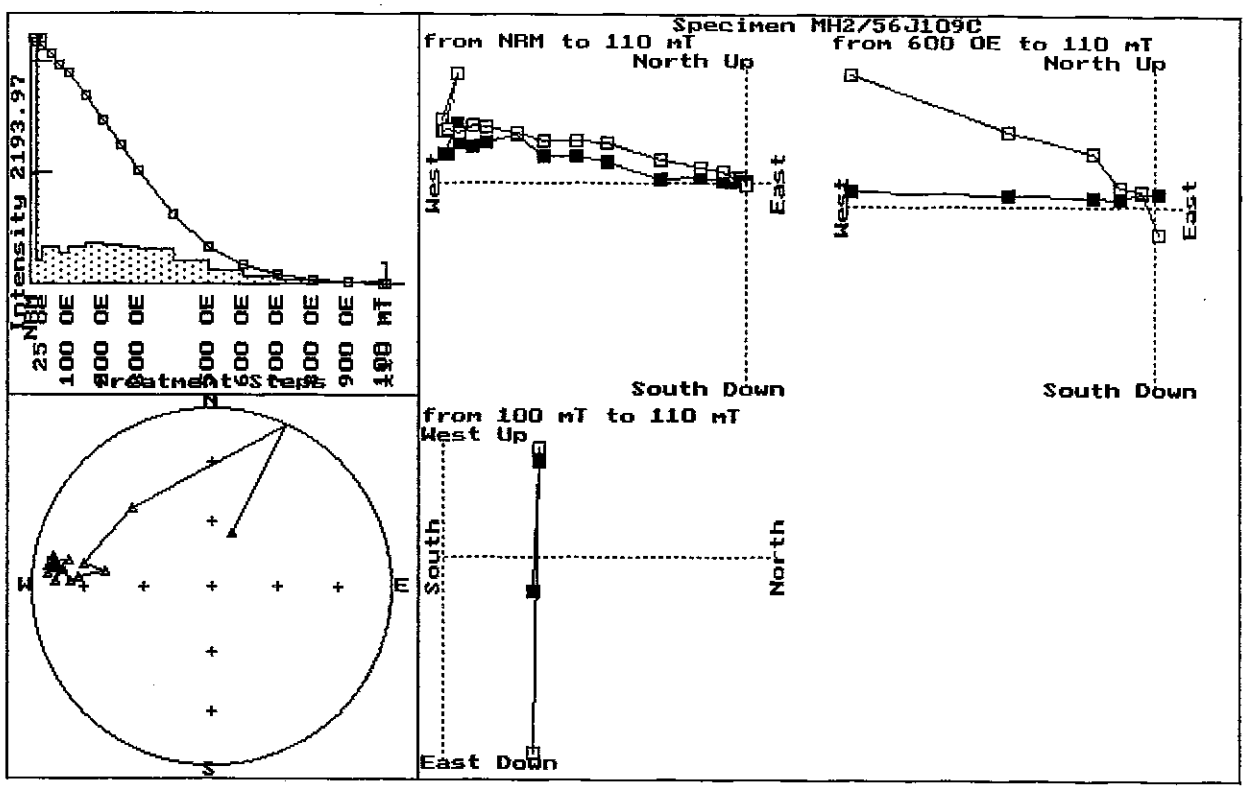
Intensity 2193.97
Treatment Steps
Specimen MH2/56J109C
from NRM to 110 mT
North Up
West
East
South Down
from 600 OE to 110 mT
North Up
West
East
South Down
from 100 mT to 110 mT
West Up
South
North
East Down
N
E
S

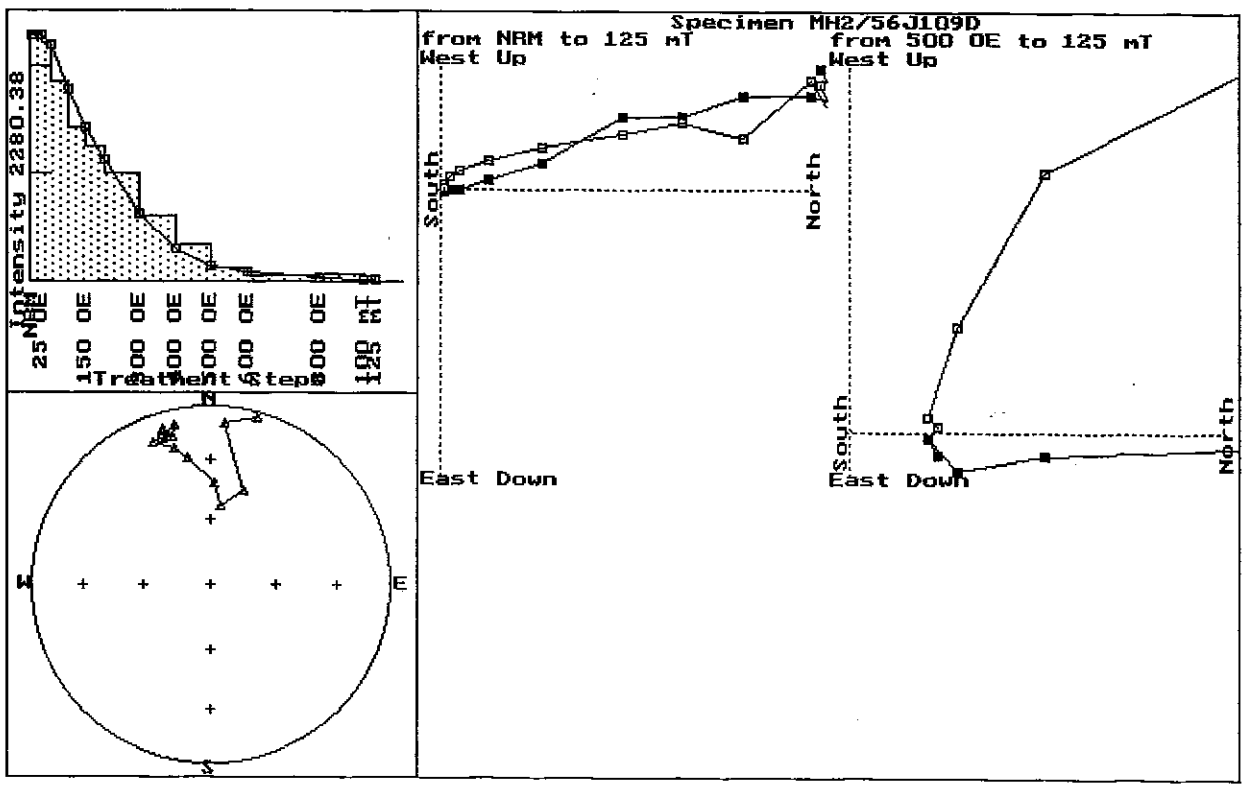
Intensity 2280.38
Treatment Steps
Specimen MH2/56J109D
from NRM to 125 mT
West Up
South
North
East Down
from 500 OE to 125 mT
West Up
South
North
East Down
N
E
S

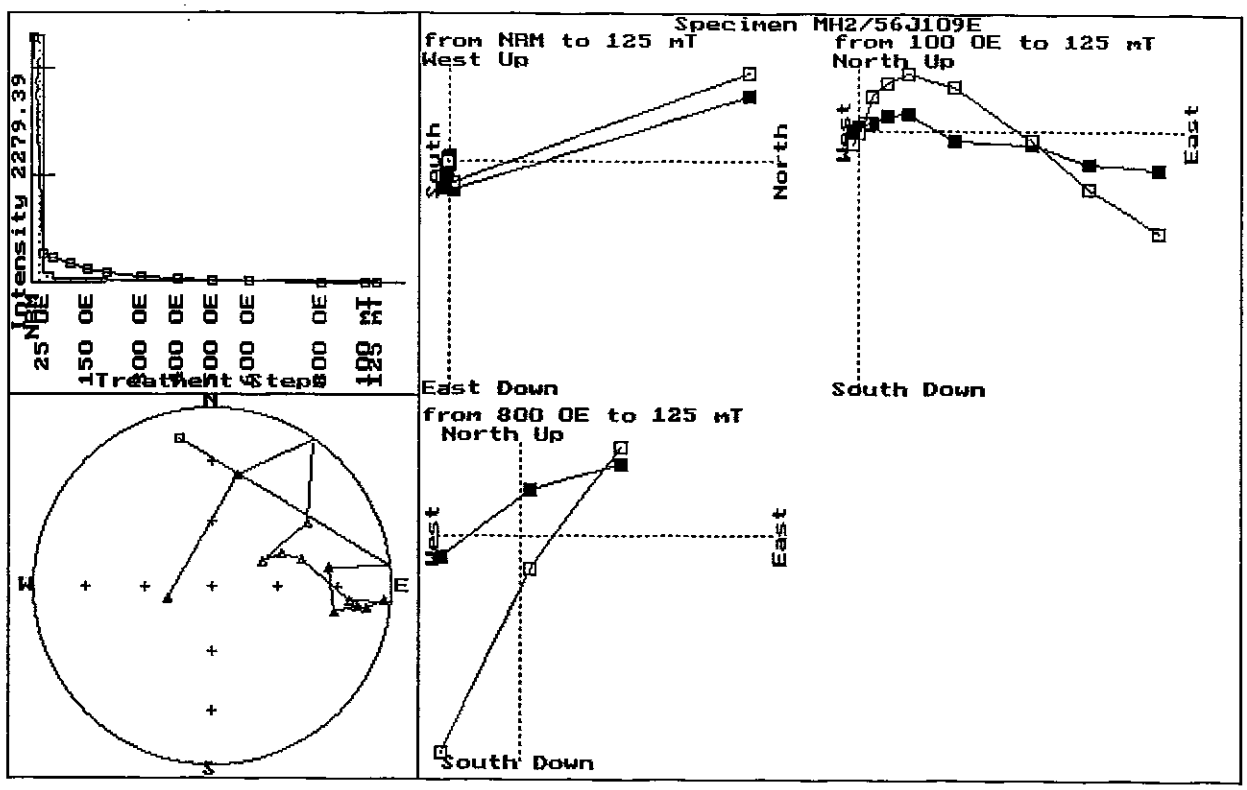
Specimen MH2/56J109E
Intensity 2279.39
Treatment Steps
from NRM to 125 mT
West Up
South
North
East Down
from 100 OE to 125 mT
North Up
West
East
South Down
from 800 OE to 125 mT
North Up
West
East
South Down
N
W
E
S

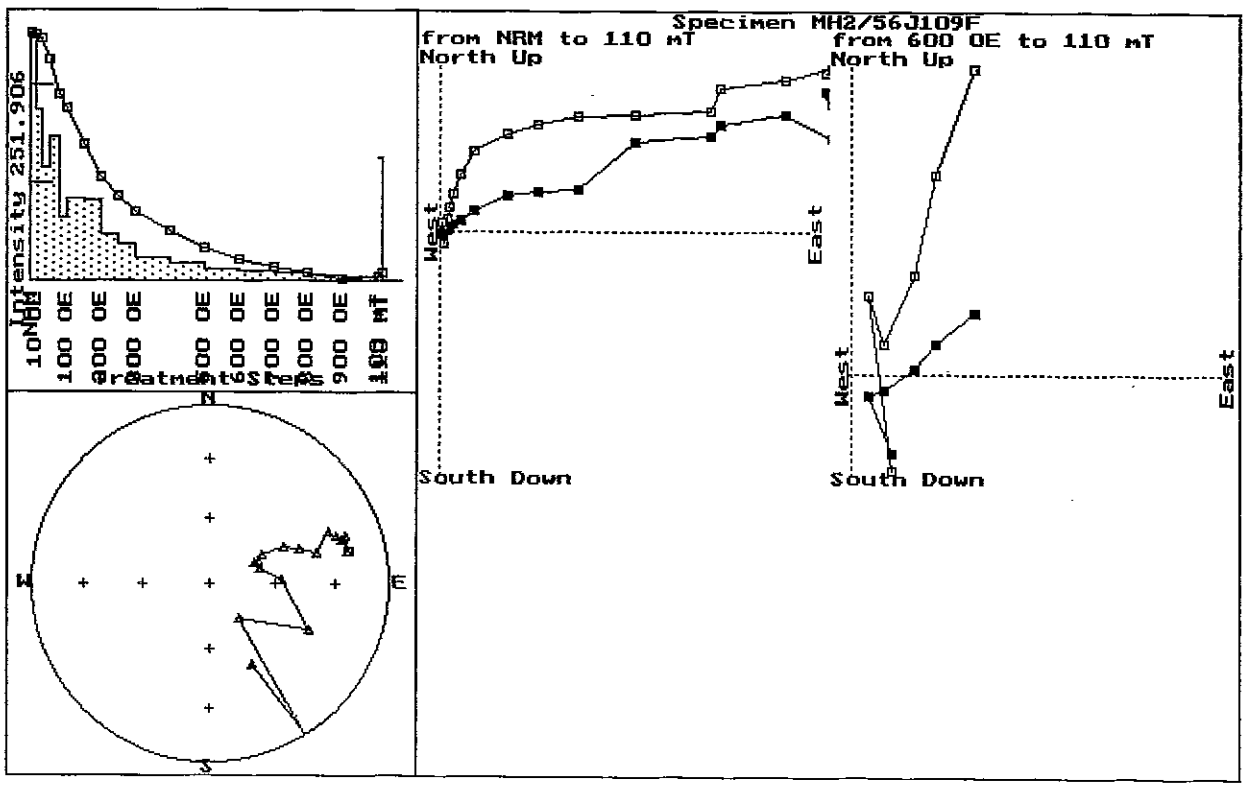
Specimen MH2/56J109F
Intensity 251.906
Treatment Steps
from NRM to 110 mT
North Up
West
East
South Down
from 600 OE to 110 mT
North Up
West
East
South Down
N
W
E
S

Fig.2 Low field thermomagnetic (k-T) curves for kimberlite samples

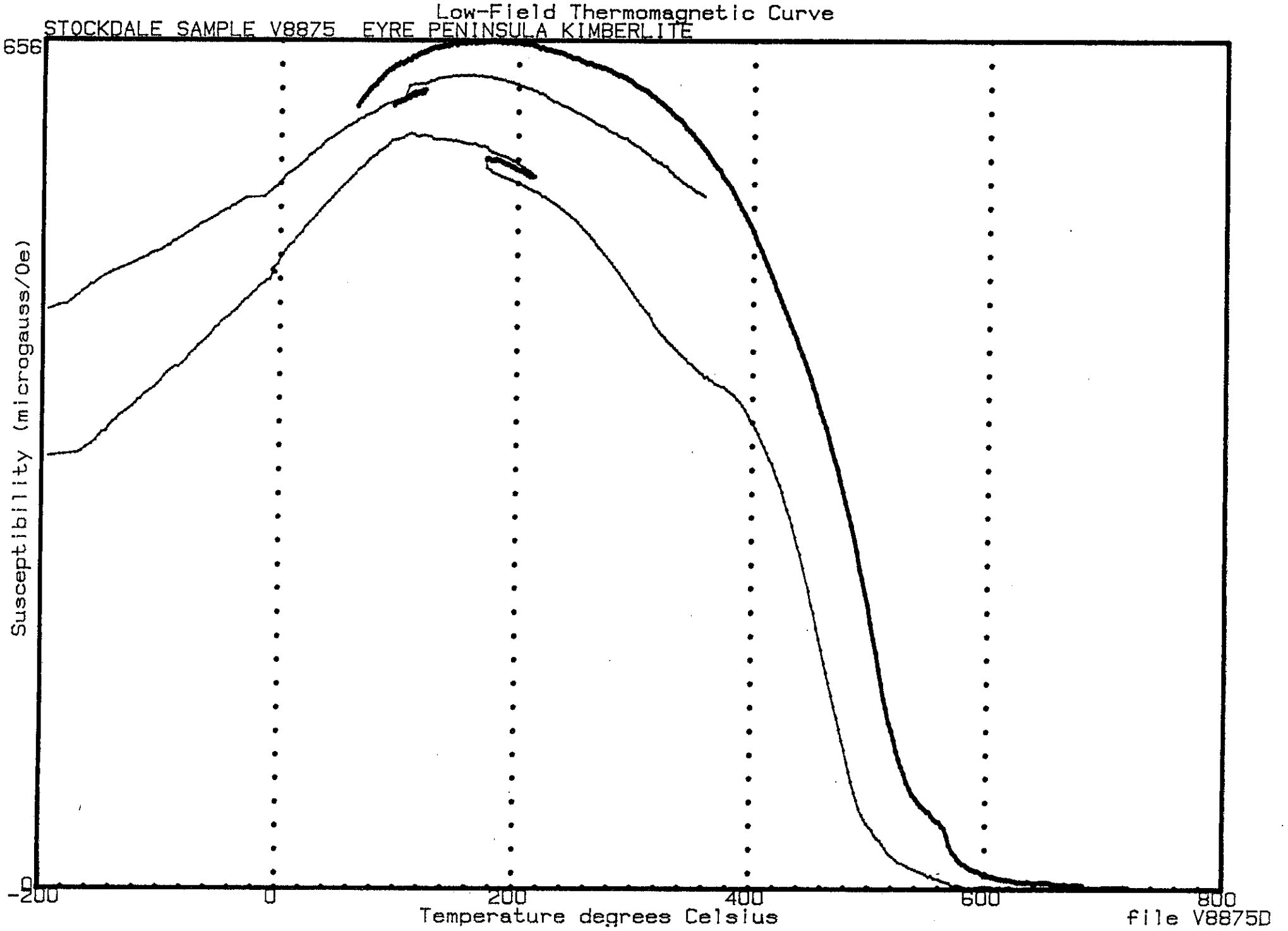
Low-Field Thermomagnetic Curve
STOCKDALE SAMPLE V8875 EYRE PENINSULA KIMBERLITE
656
-0
Susceptibility (microgauss/Oe)
-200
0
200
400
600
800
Temperature degrees Celsius
file V8875D

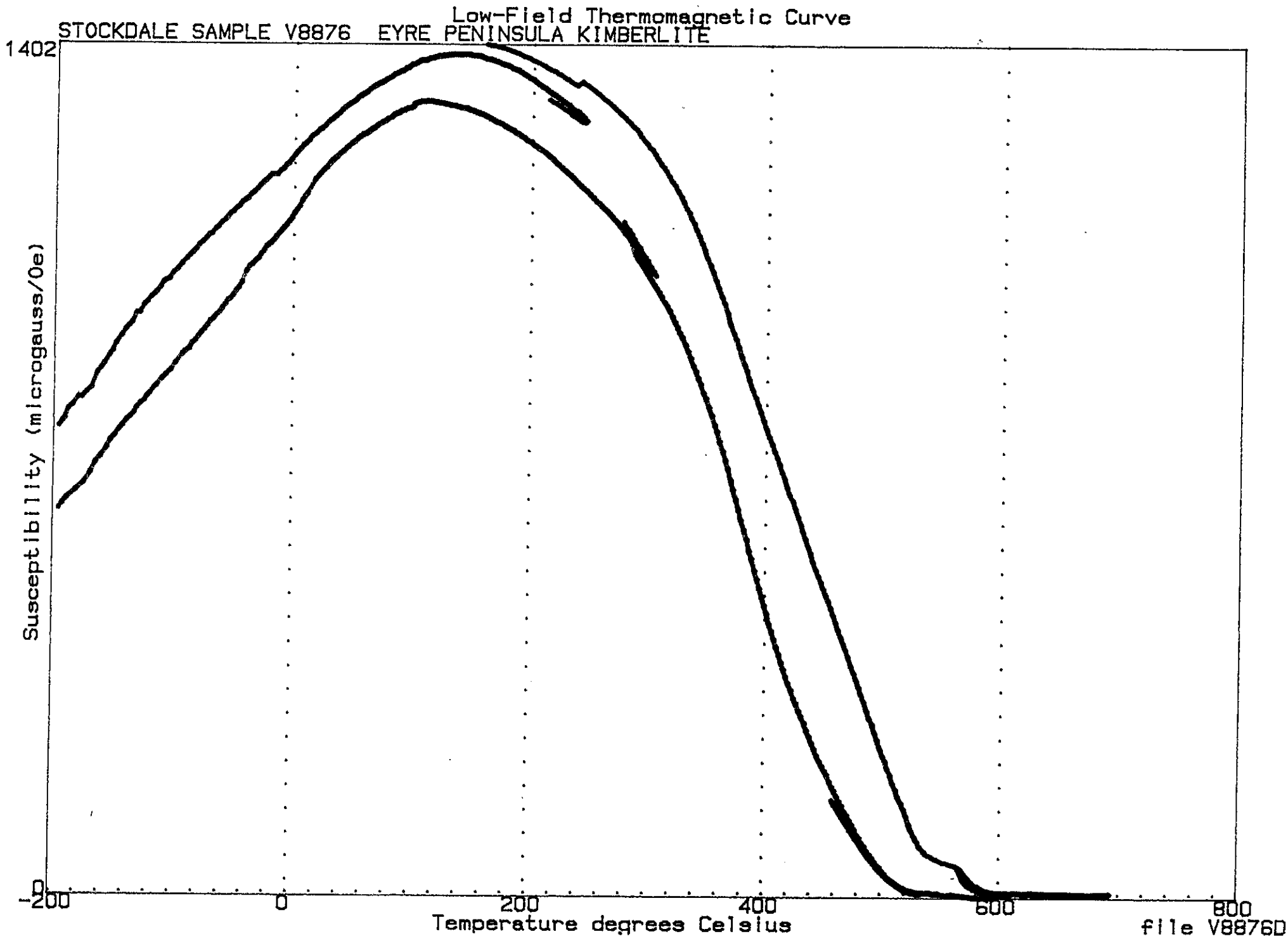
Low-Field Thermomagnetic Curve
STOCKDALE SAMPLE V8876 EYRE PENINSULA KIMBERLITE
1402
0
Susceptibility (microgauss/Oe)
-200
0
200
400
600
800
Temperature degrees Celsius
file V8876D

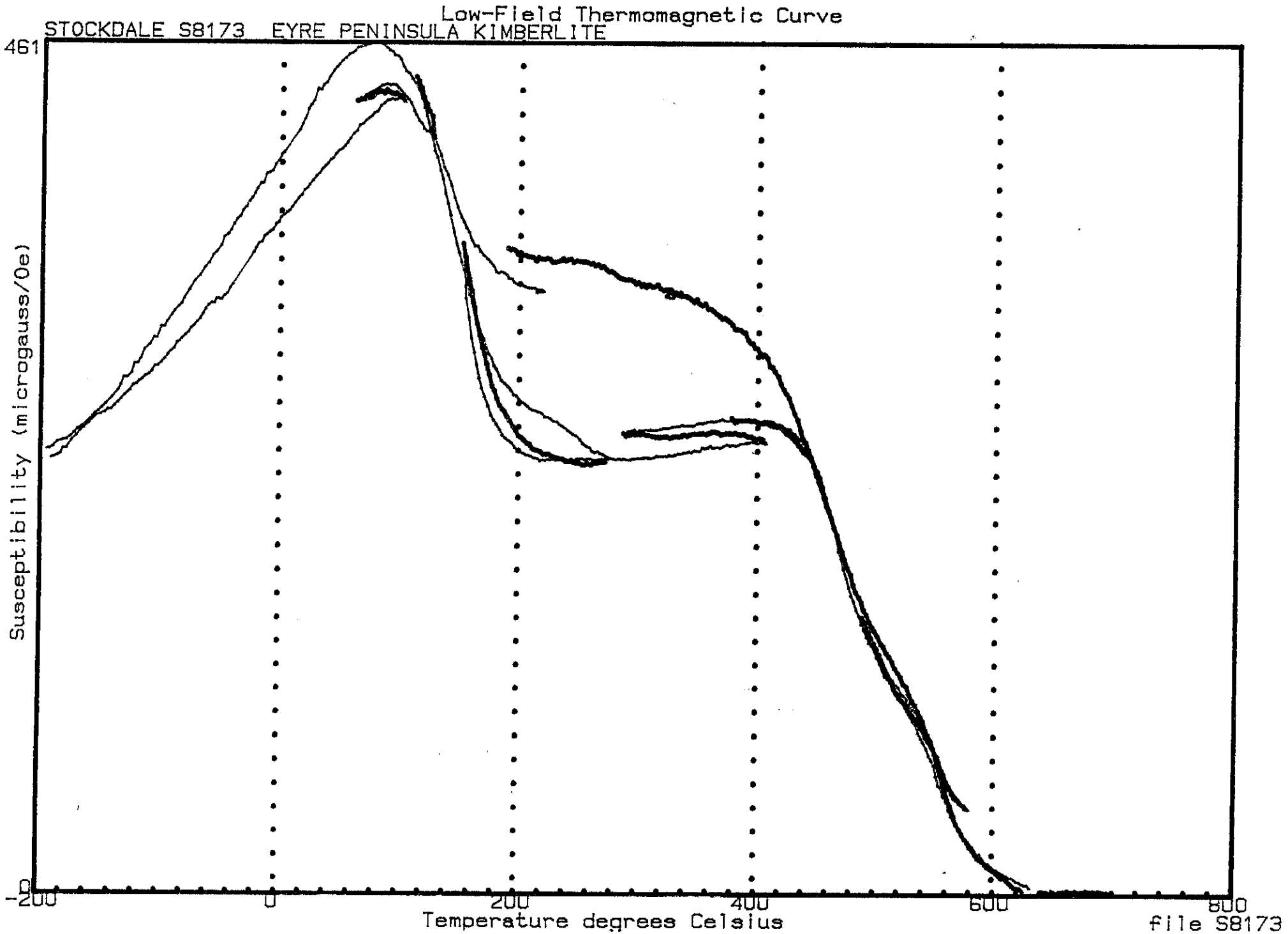
Low-Field Thermomagnetic Curve
STOCKDALE S8173 EYRE PENINSULA KIMBERLITE
461
-0
Susceptibility (microgauss/Oe)
-200
0
200
400
600
800
Temperature degrees Celsius
file S8173

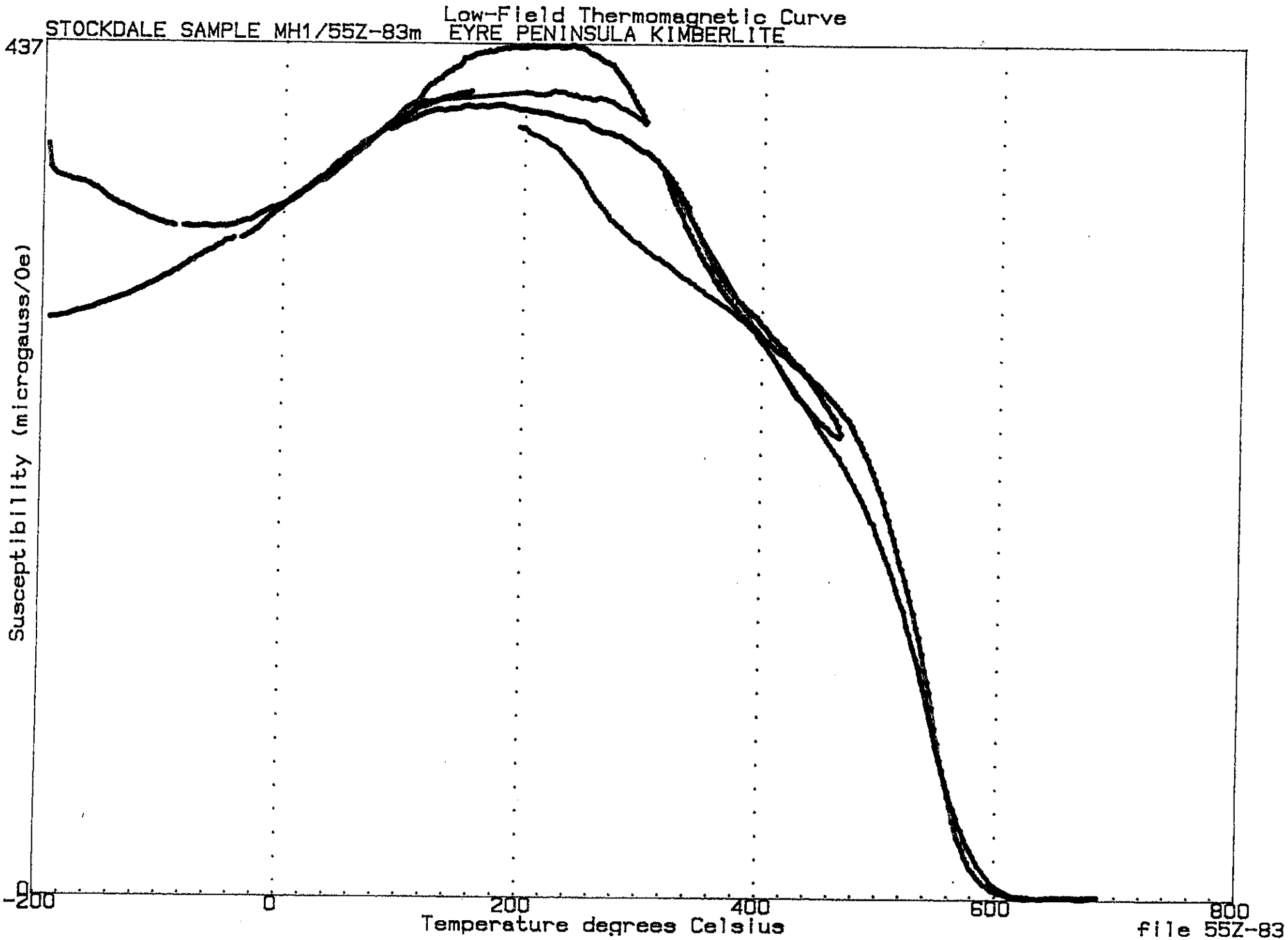
Low-Field Thermomagnetic Curve
STOCKDALE SAMPLE MH1/55Z-83m EYRE PENINSULA KIMBERLITE
437
0
Susceptibility (microgauss/Oe)
-200
0
200
400
600
800
Temperature degrees Celsius
file 55Z-83

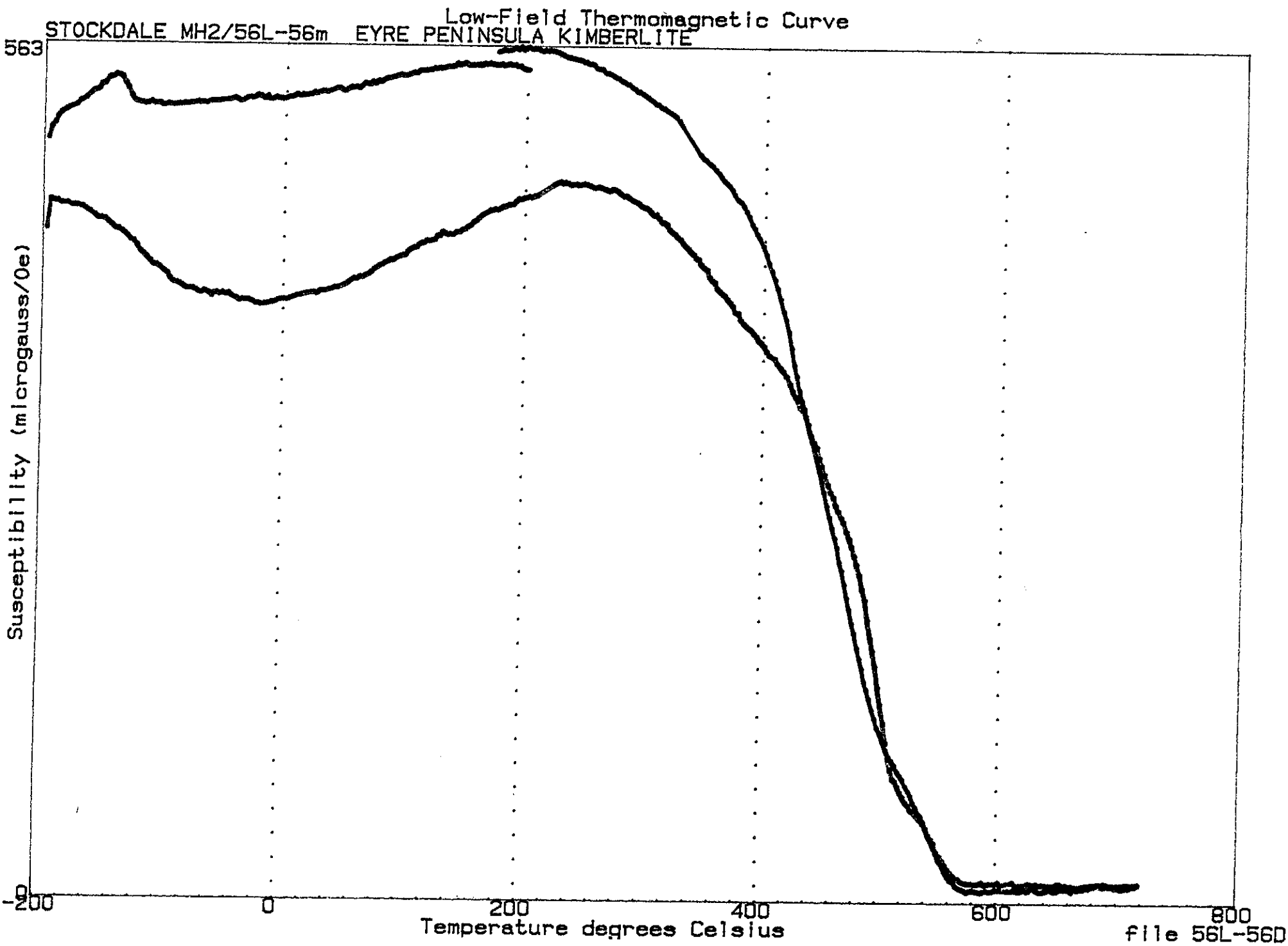
Low-Field Thermomagnetic Curve
STOCKDALE MH2/56L-56m EYRE PENINSULA KIMBERLITE
563
0
Susceptibility (microgauss/Oe)
-200
0
200
400
600
800
Temperature degrees Celsius
file 56L-56D

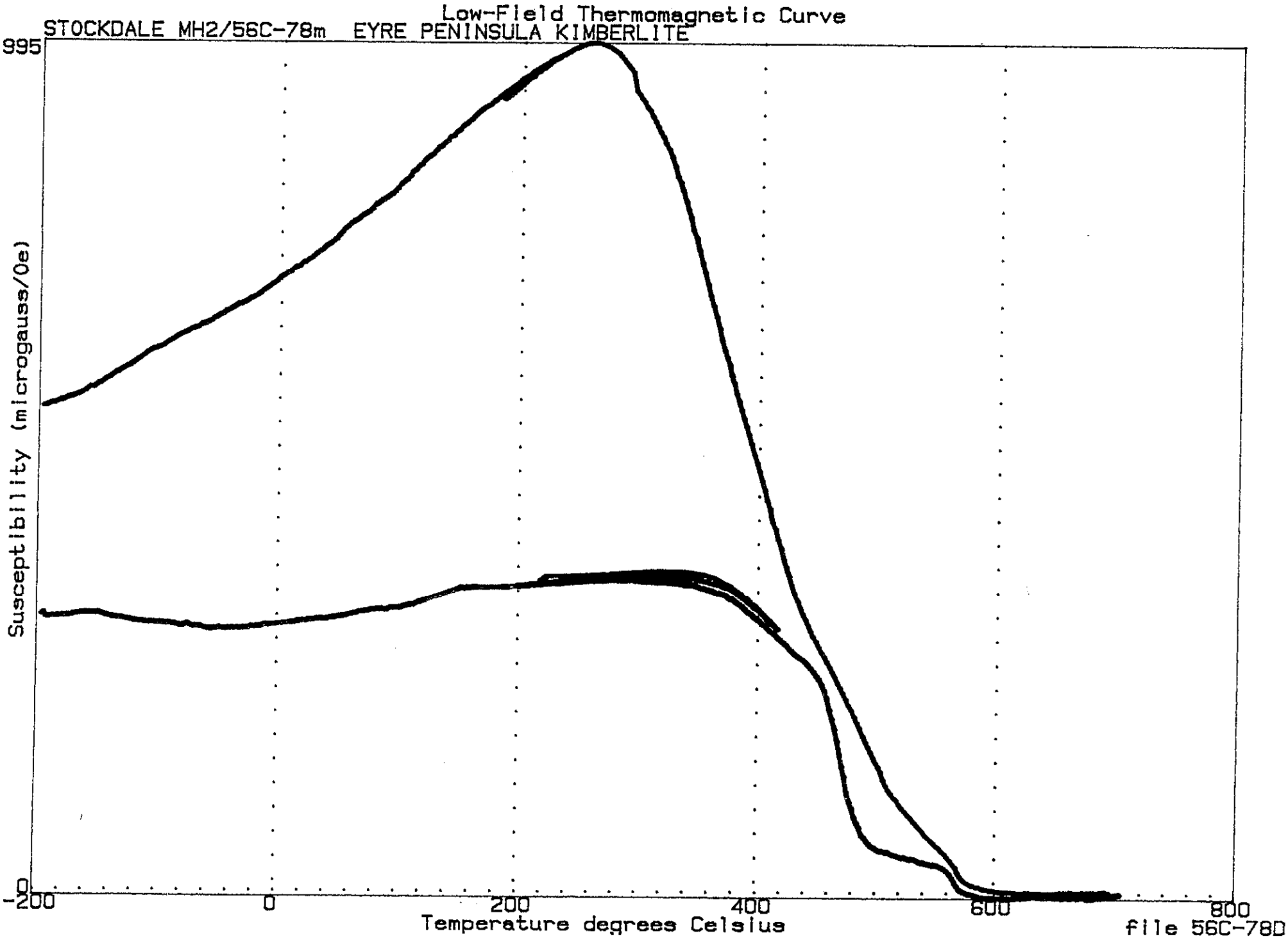
Low-Field Thermomagnetic Curve
STOCKDALE MH2/56C-78m EYRE PENINSULA KIMBERLITE
995
0
Susceptibility (microgauss/Oe)
-200
0
200
400
600
800
Temperature degrees Celsius
file 56C-78D

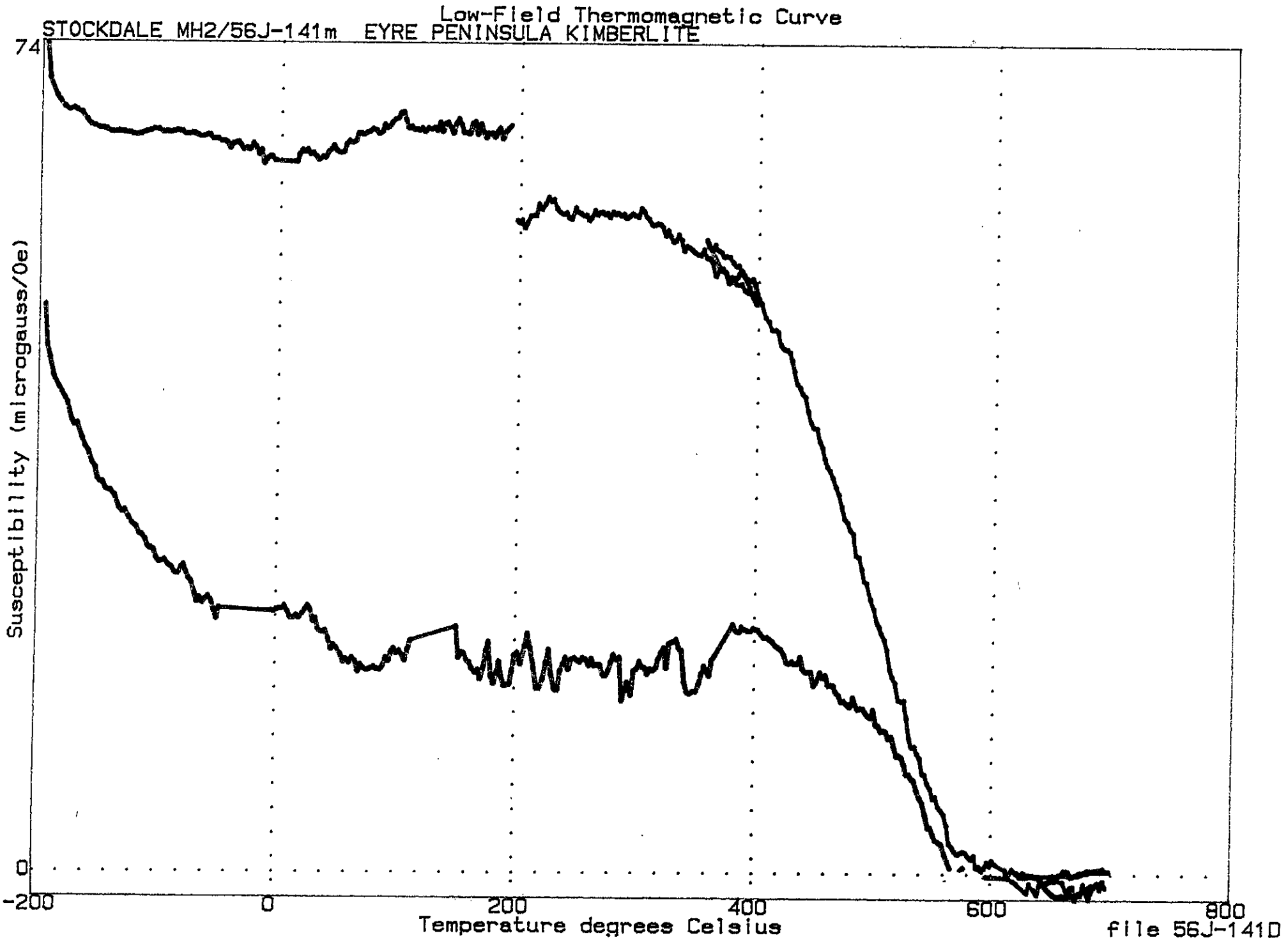
Low-Field Thermomagnetic Curve
STOCKDALE MH2/56J-141m EYRE PENINSULA KIMBERLITE
74
0
-200
0
200
400
600
800
Susceptibility (microgauss/Oe)
Temperature degrees Celsius
file 56J-141D

Fig.3 AF demagnetisation of SIRM of kimberlite samples

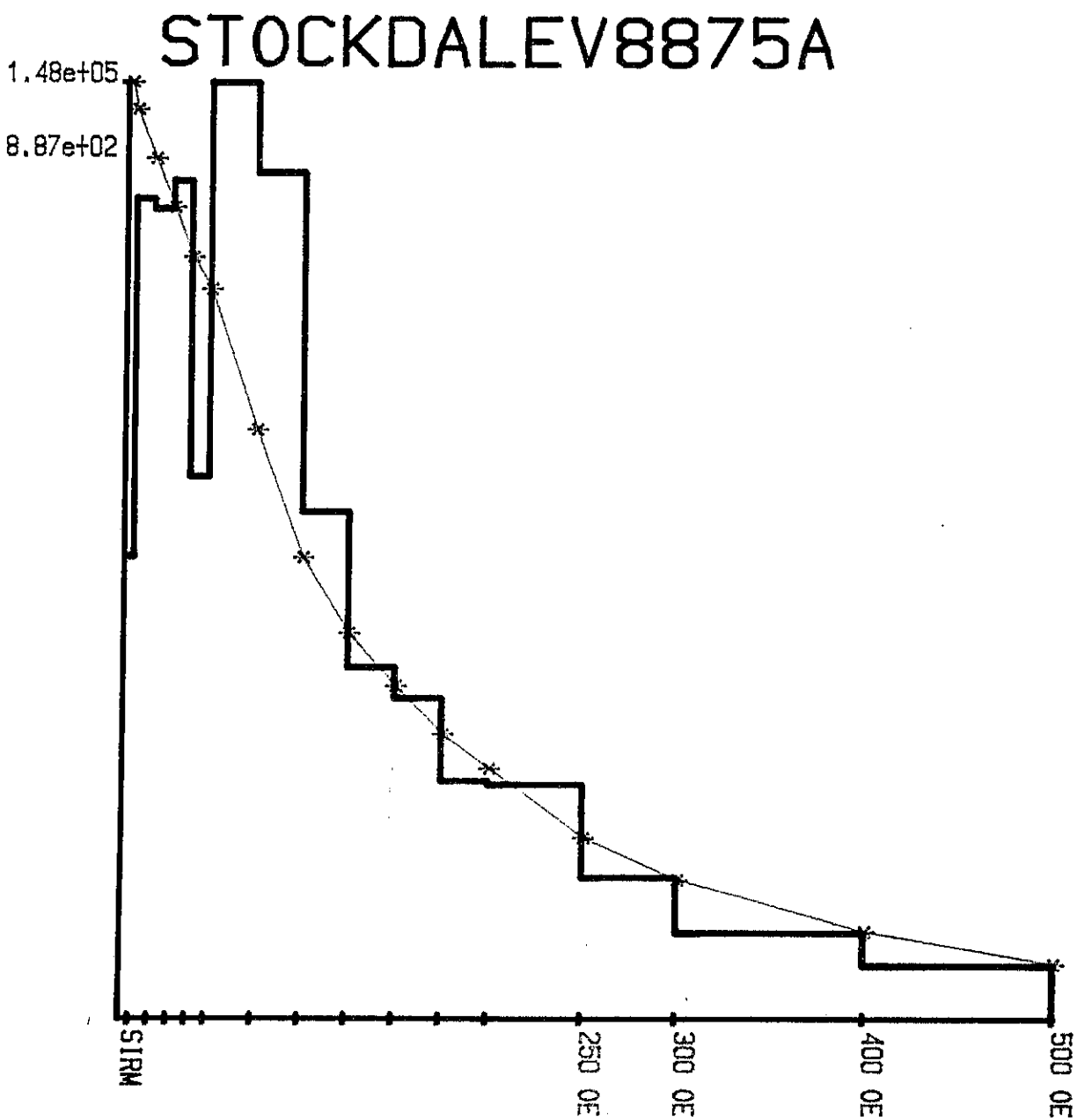
STOCKDALEV8875A
1.48e+05
8.87e+02
STRM
250 OE
300 OE
400 OE
500 OE

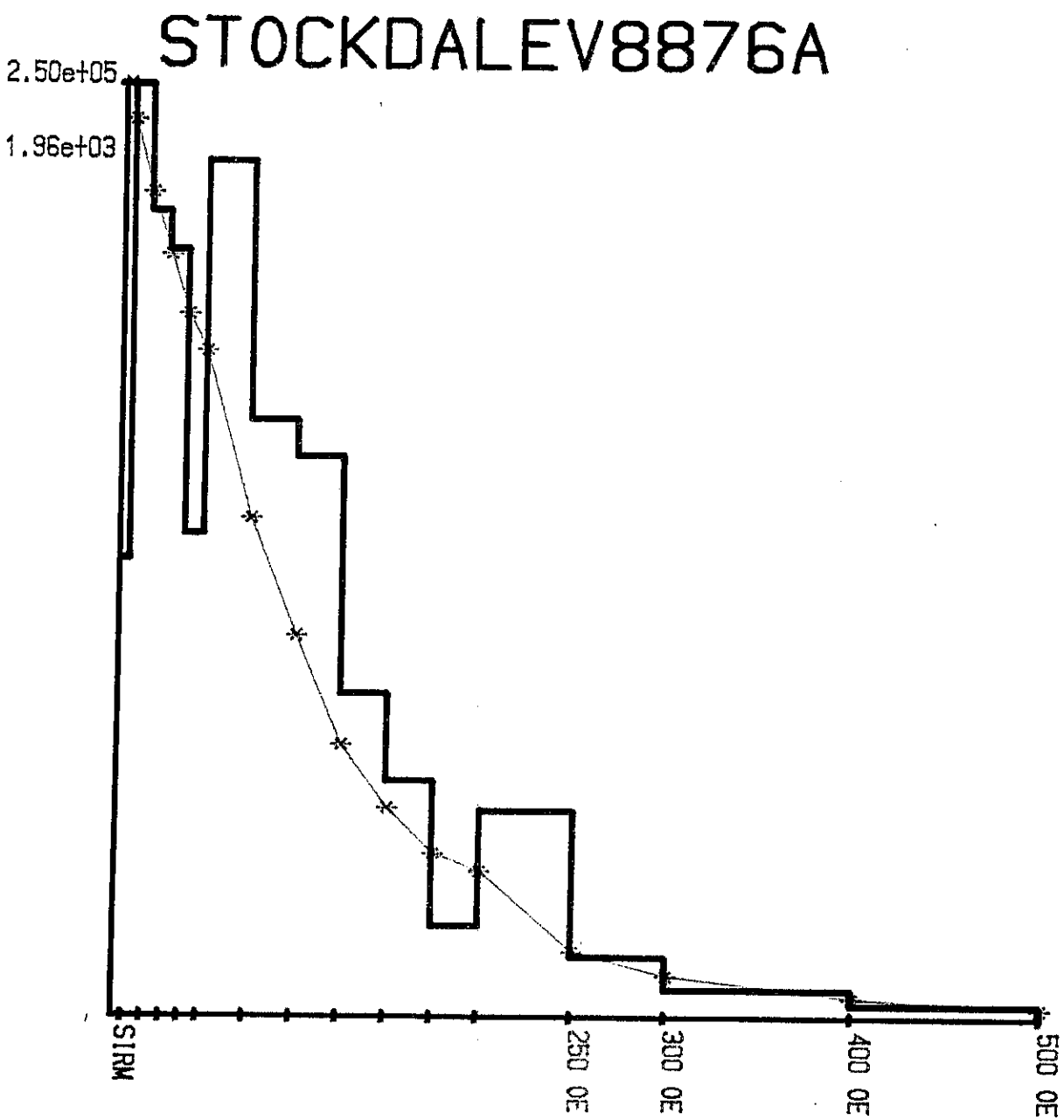
STOCKDALEV8876A
2.50e+05
1.96e+03
SIRM
250 OE
300 OE
400 OE
500 OE

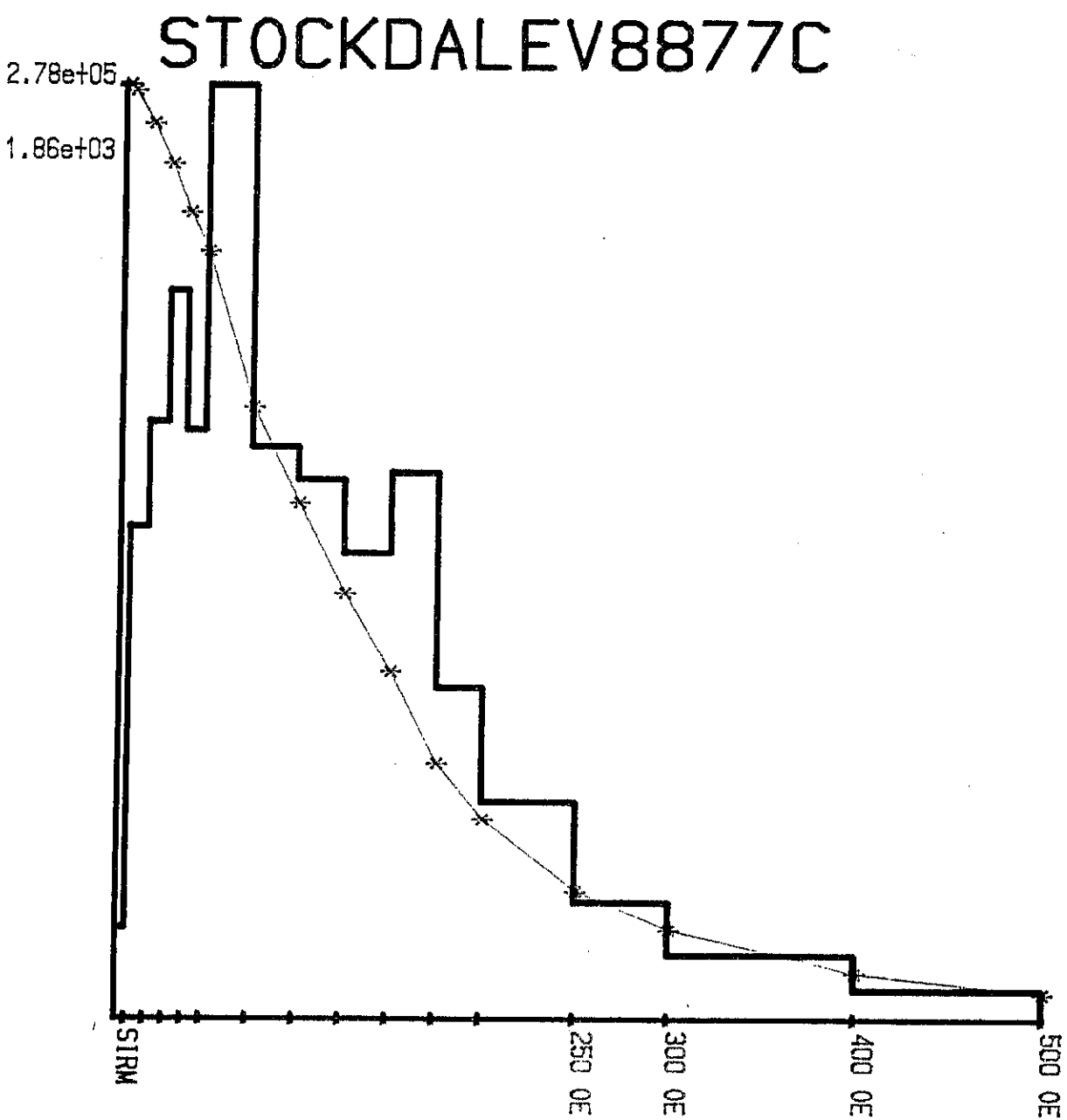
STOCKDALEV8877C
2.78e+05
1.86e+03
SIRM
250 OE
300 OE
400 OE
500 OE

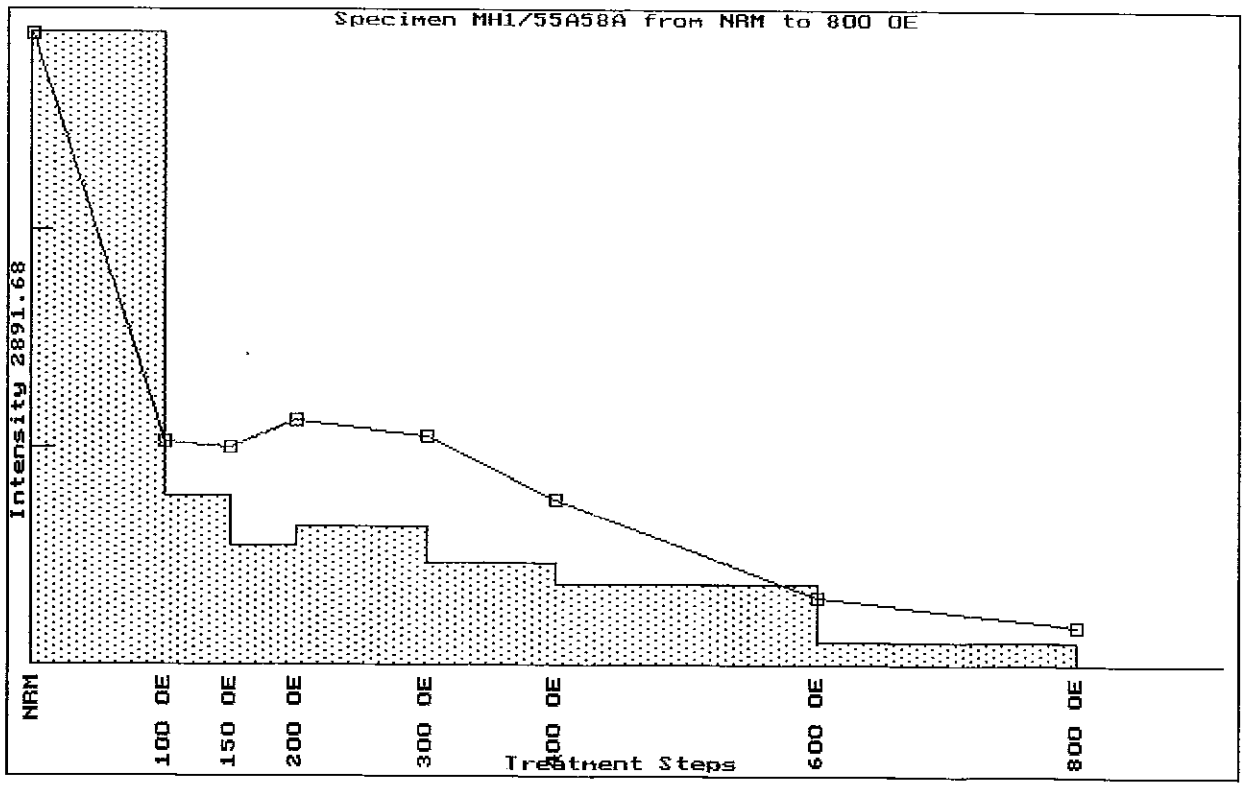
Specimen MH1/55A58A from NRM to 800 OE
Intensity 2891.68
NRM
100 OE
150 OE
200 OE
300 OE
600 OE
800 OE
Treatment Steps

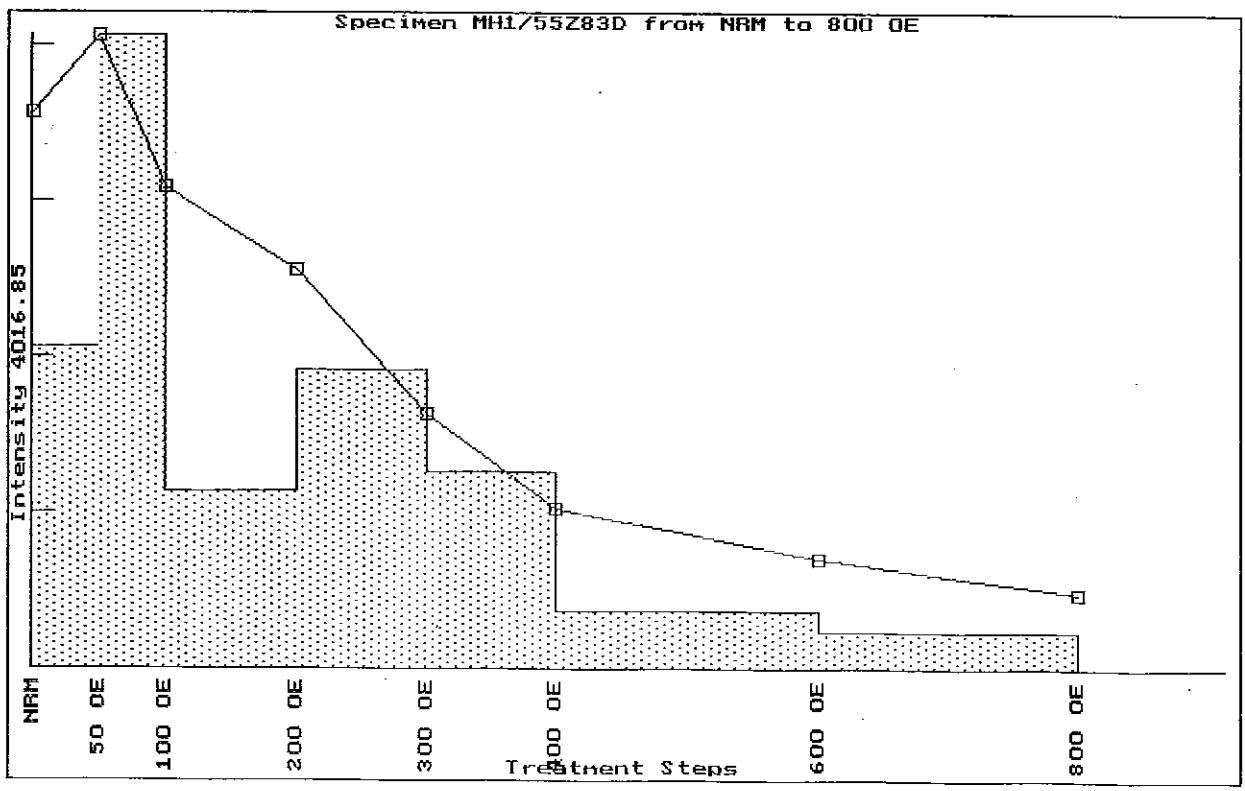
Specimen MH1/55Z83D from NRM to 800 OE
Intensity 4016.85
NRM
50 OE
100 OE
200 OE
300 OE
600 OE
800 OE
Treatment Steps

Fig.4 Thermal demagnetisation of SIRM or three-component remanence carried by kimberlite samples
(z-component = coercivity greater than 1000 Oe
x-component = coercivity between 200 and 1000 Oe
y-component = coercivity less than 200 Oe)

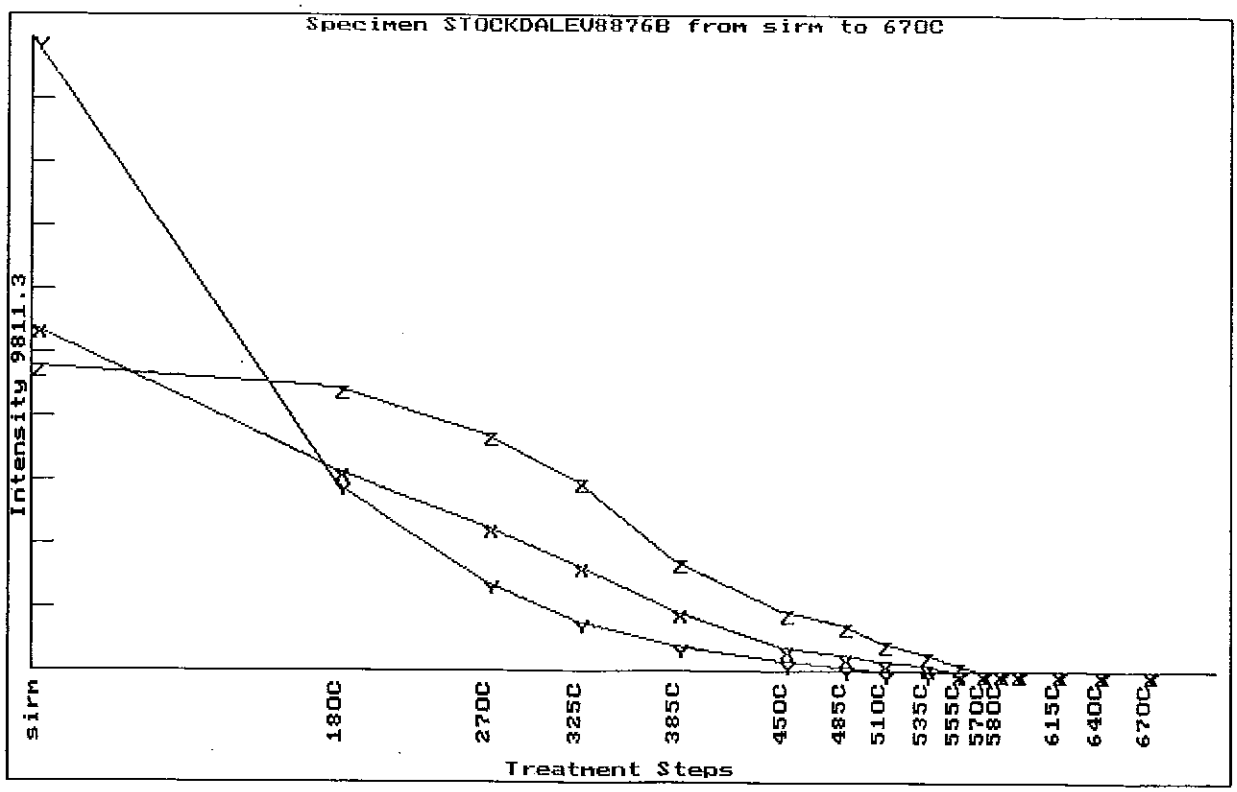
Specimen STOCKDALEV8876B from sirm to 670C
Intensity 9811.3
sirm
180C
270C
325C
385C
450C
485C
510C
535C
555C
570C
580C
615C
640C
670C
Treatment Steps

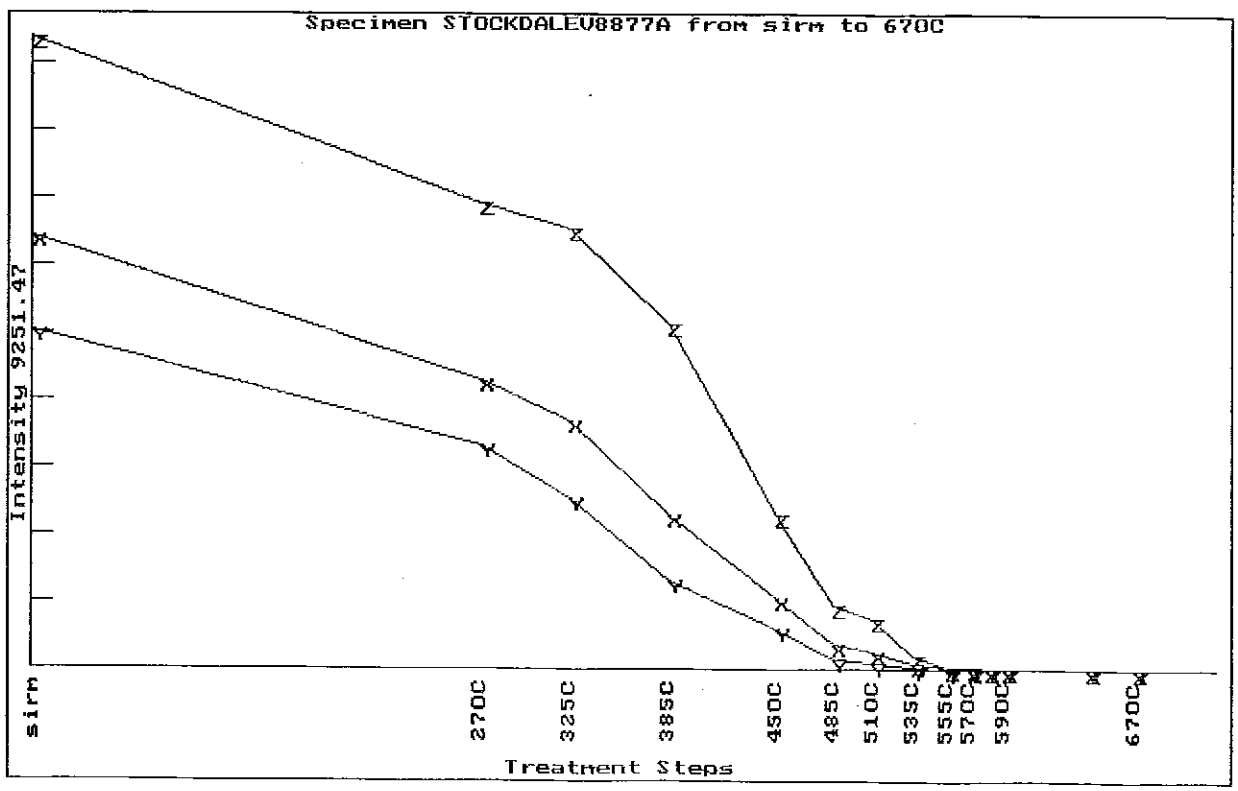
Specimen STOCKDALEV8877A from sirm to 670C
Intensity 9251.47
sirm
270C
325C
385C
450C
485C
510C
535C
555C
570C
590C
670C
Treatment Steps

Specimen STOCKDALES8173D from sirm to 670C

Intensity 8759.34

sirm

180C

270C

325C

385C

450C

485C

510C

535C

555C

570C

580C

615C

640C

670C

Treatment Steps

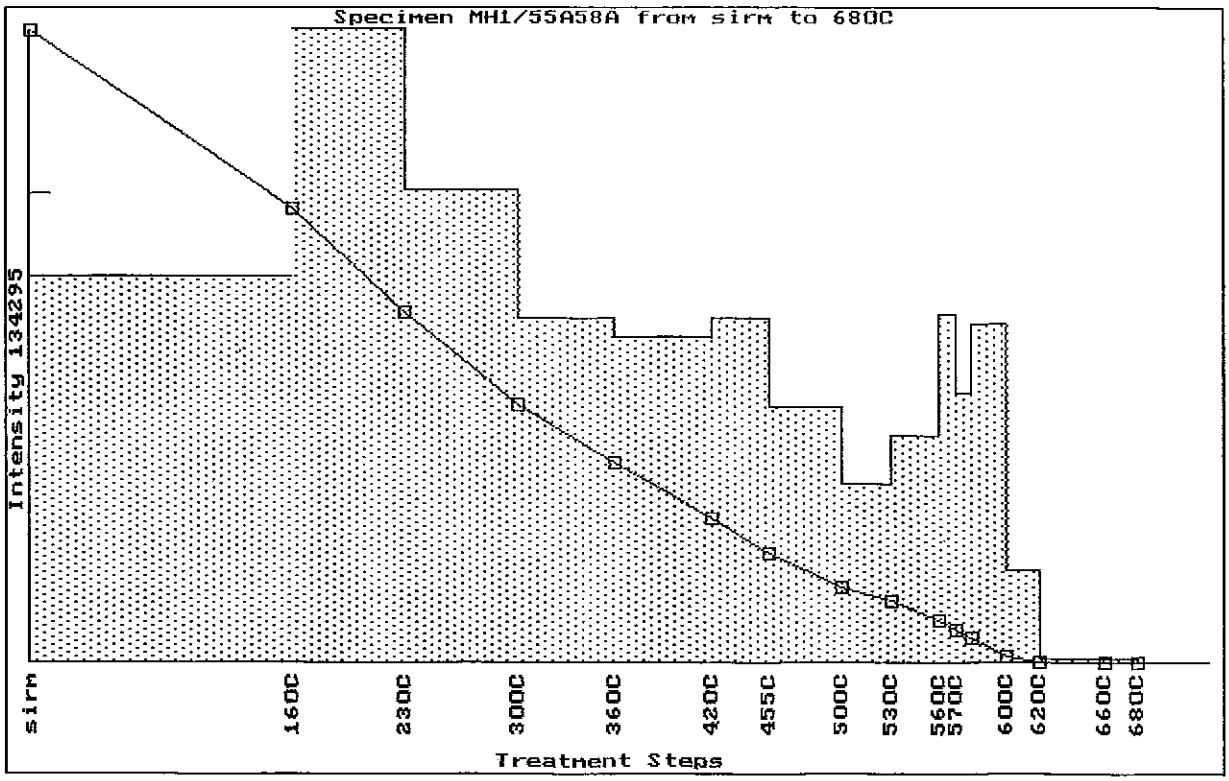
Specimen MH1/55A58A from sirm to 680C
Intensity 134295
sirm
160C
230C
300C
360C
420C
455C
500C
530C
560C
570C
600C
620C
660C
680C
Treatment Steps

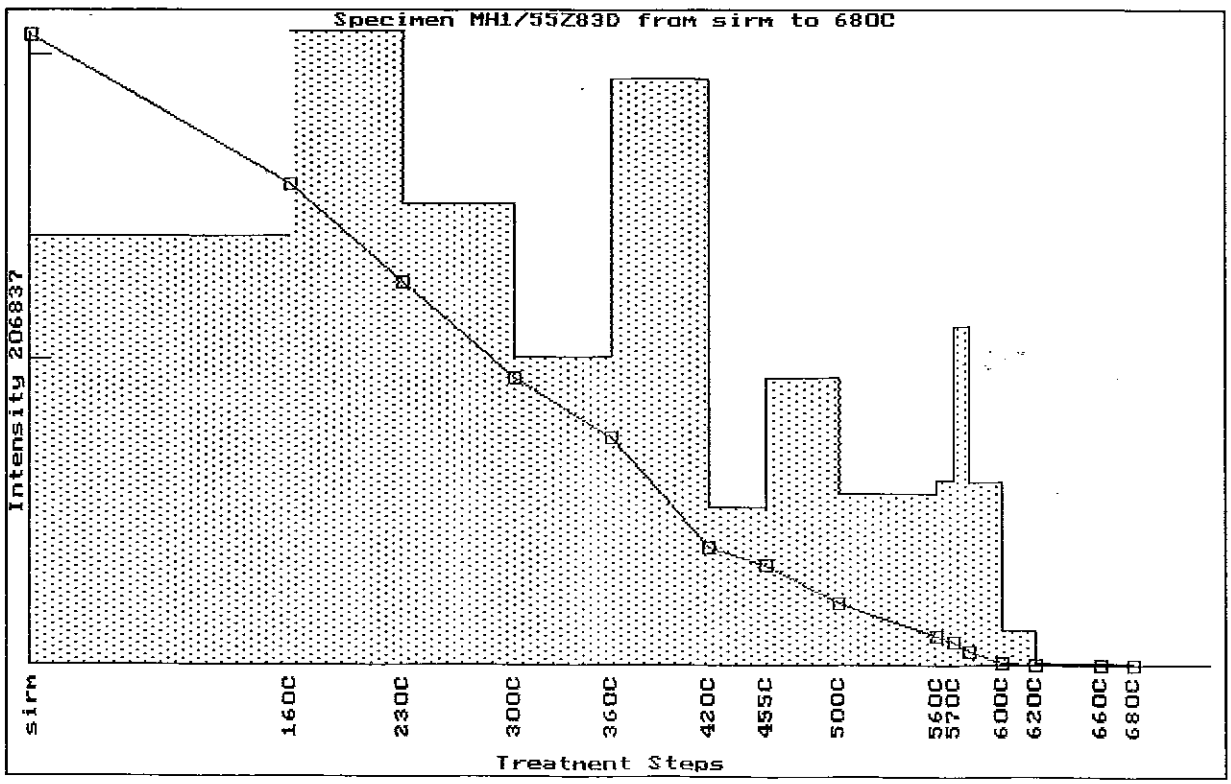
Specimen MH1/55Z83D from sirm to 680C
Intensity 206837
sirm
160C
230C
300C
360C
420C
455C
500C
560C
570C
600C
620C
660C
680C
Treatment Steps

Fig.5 Low field thermomagnetic (k-T) curves for lamproite samples

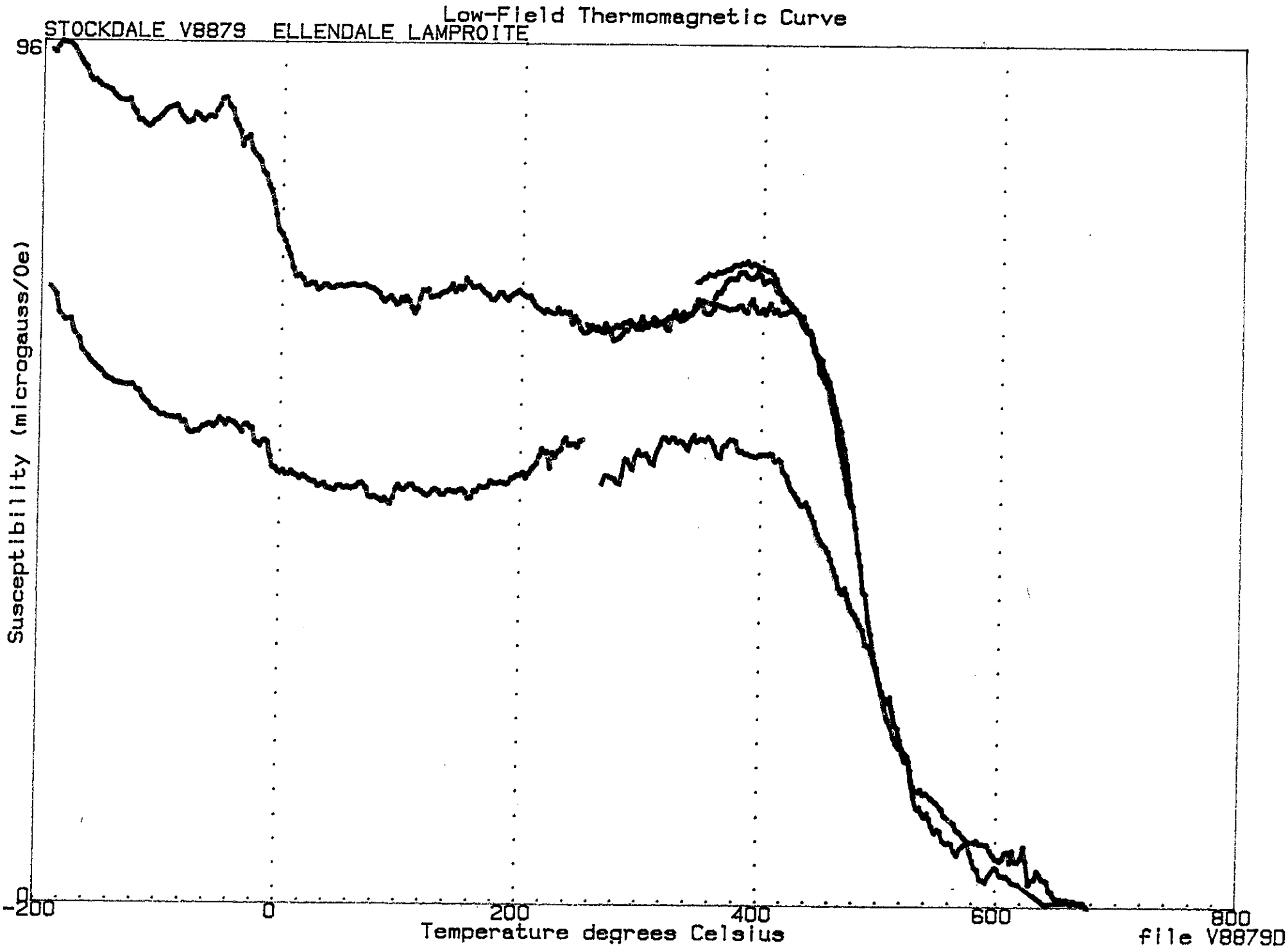
Low-Field Thermomagnetic Curve
STOCKDALE V8879 ELLENDALE LAMPROITE
96
0
Susceptibility (microgauss/Oe)
-200
0
200
400
600
800
Temperature degrees Celsius
file V8879D

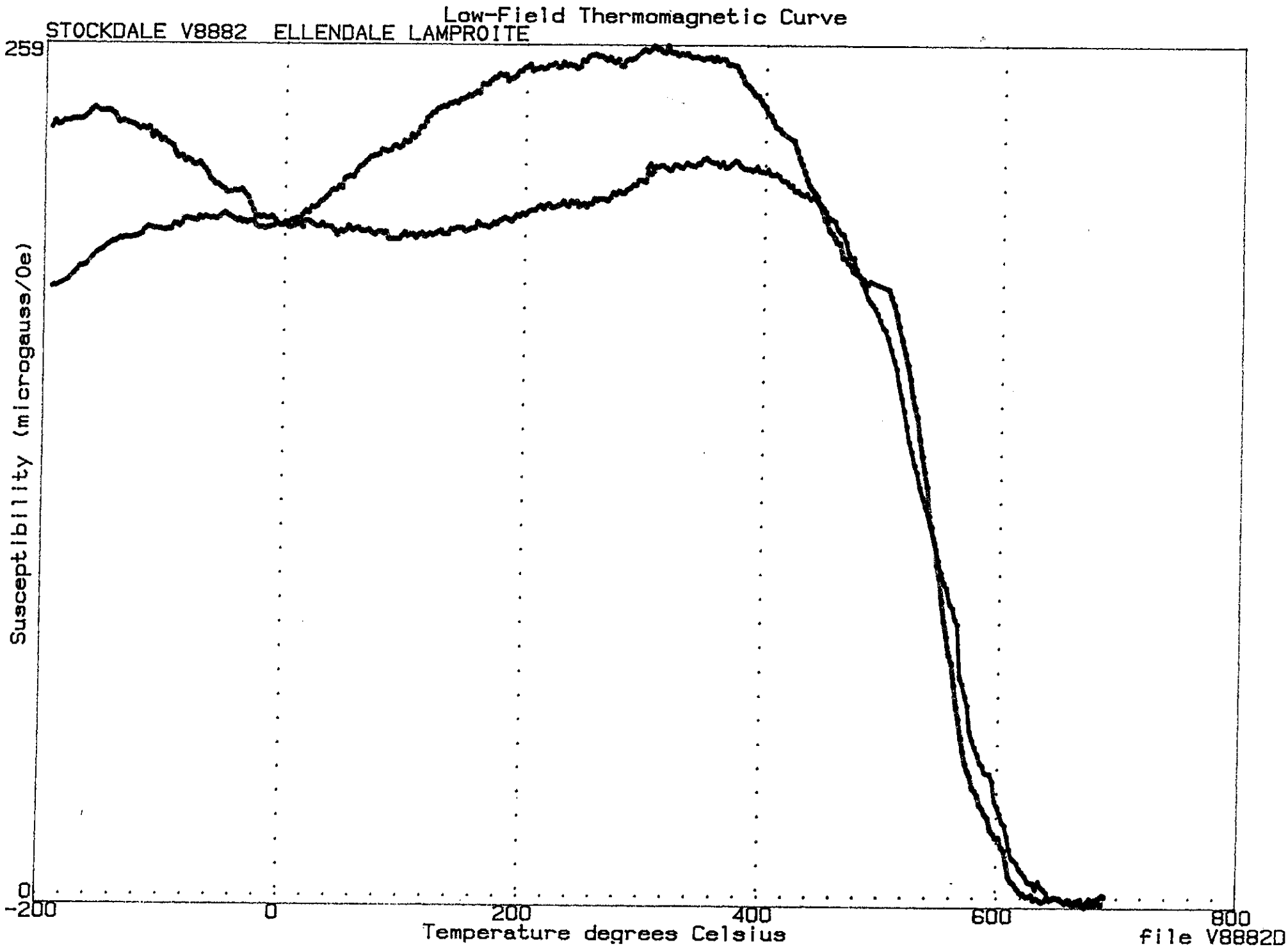
Low-Field Thermomagnetic Curve
STOCKDALE V8882 ELLENDALE LAMPROITE
259
0
Susceptibility (microgauss/Oe)
-200
0
200
400
600
800
Temperature degrees Celsius
file V8882D

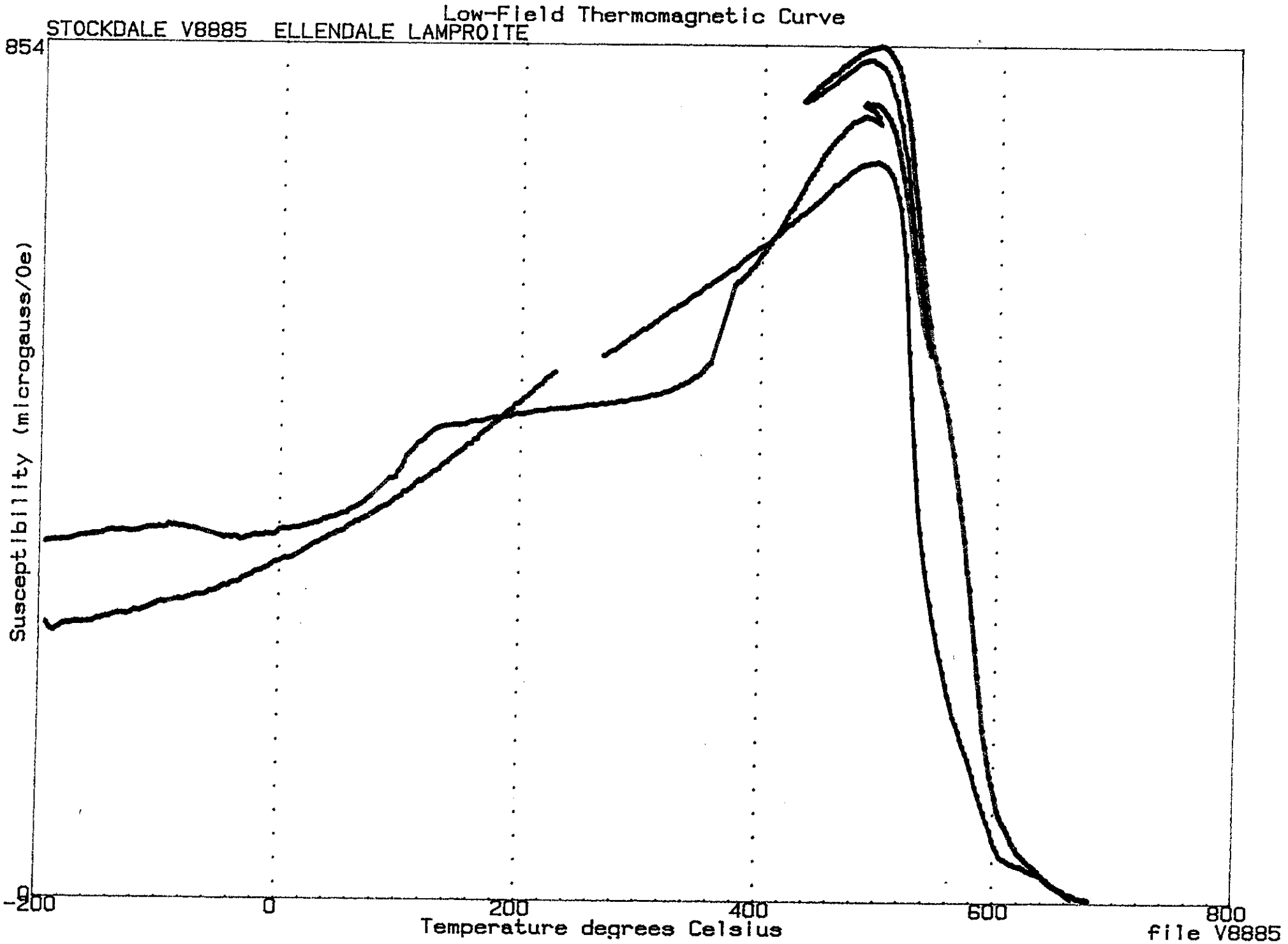
Low-Field Thermomagnetic Curve
STOCKDALE V8885 ELLENDALE LAMPROITE
854
-9
Susceptibility (microgauss/Oe)
-200
0
200
400
600
800
Temperature degrees Celsius
file V8885

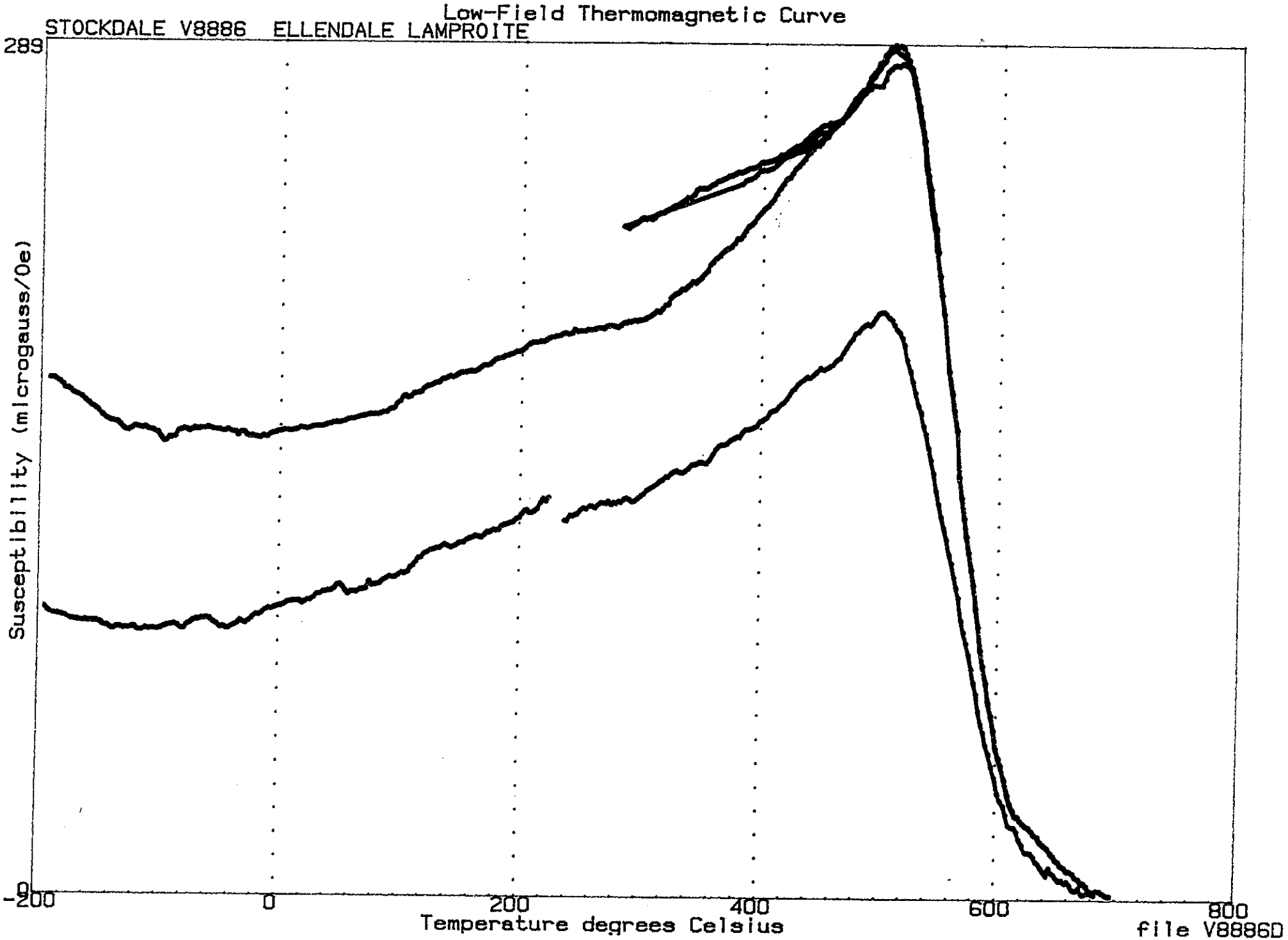
Low-Field Thermomagnetic Curve
STOCKDALE V8886 ELLENDALE LAMPROITE
289
-9
Susceptibility (microgauss/Oe)
-200
0
200
400
600
800
Temperature degrees Celsius
file V8886D

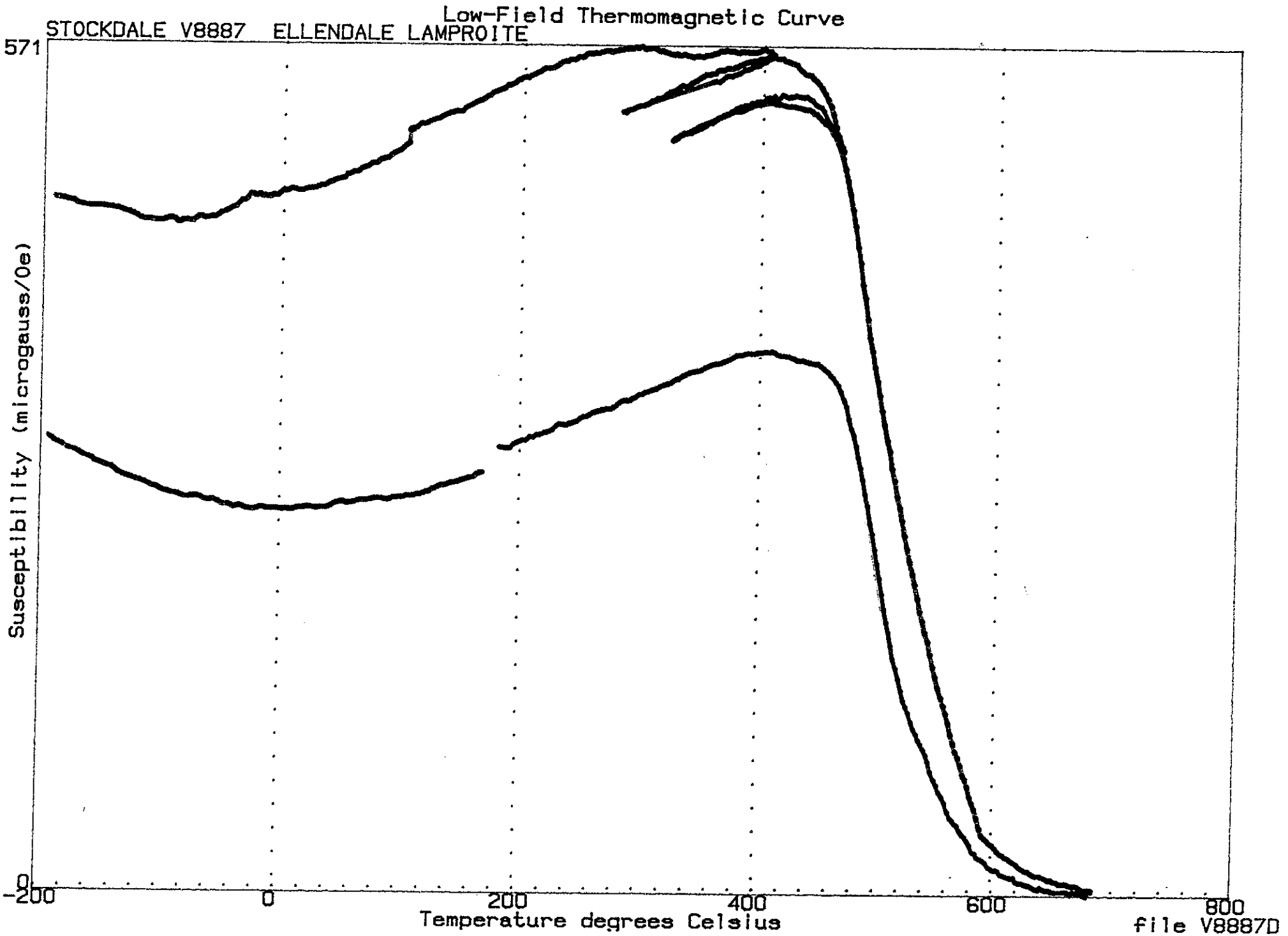
Low-Field Thermomagnetic Curve
STOCKDALE V8887 ELLENDALE LAMPROITE
571
0
Susceptibility (microgauss/Oe)
-200
0
200
400
600
800
Temperature degrees Celsius
file V8887D

Fig.6 AF demagnetisation of SIRM of lamproite samples

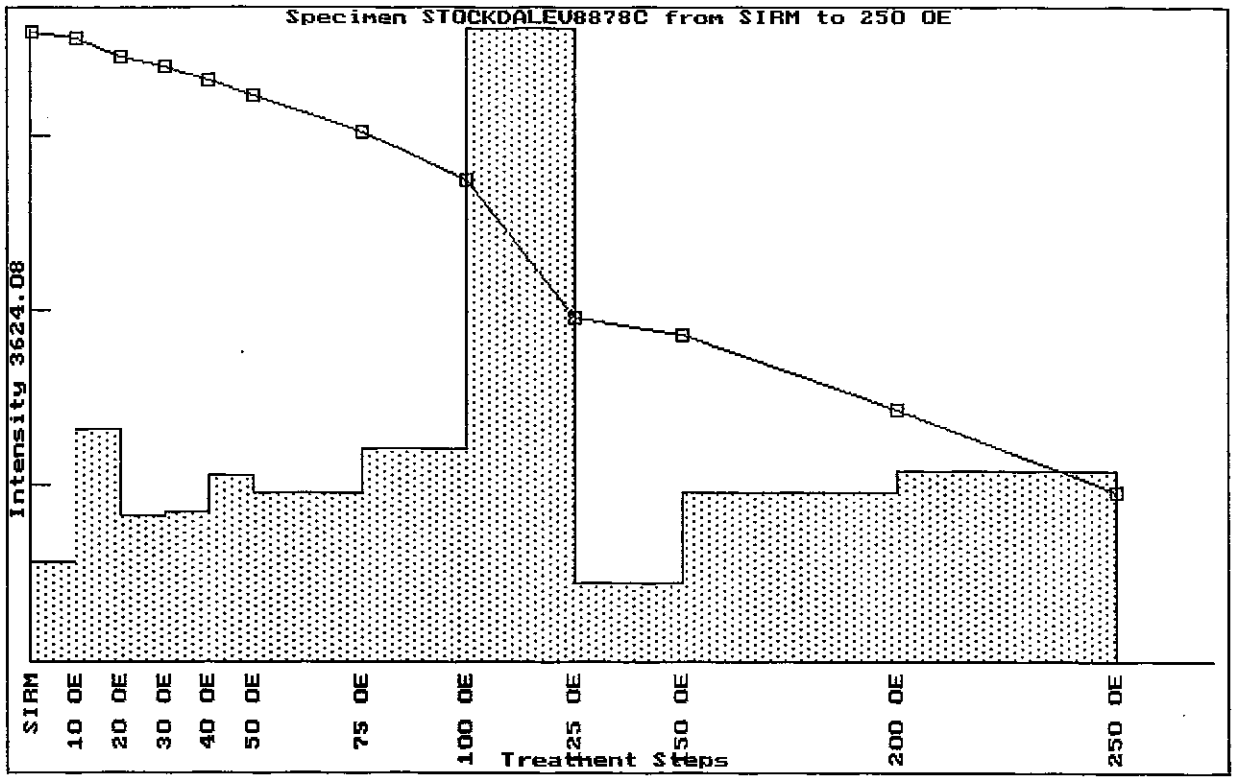
Specimen STOCKDALEU8878C from SIRM to 250 OE
Intensity 3624.08
SIRM
10 OE
20 OE
30 OE
40 OE
50 OE
75 OE
100 OE
125 OE
150 OE
200 OE
250 OE
Treatment Steps

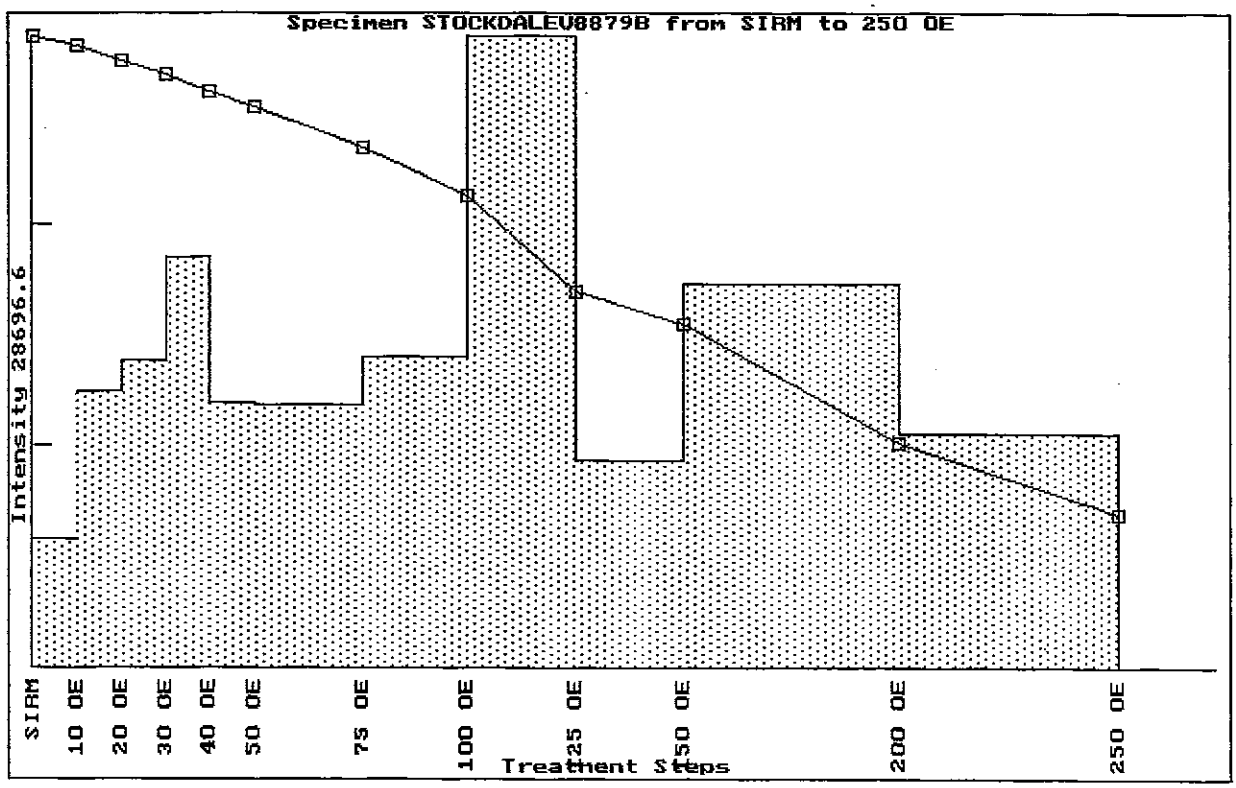
Specimen STOCKDALEU8879B from SIRM to 250 OE
Intensity 28696.6
SIRM
10 OE
20 OE
30 OE
40 OE
50 OE
75 OE
100 OE
125 OE
150 OE
200 OE
250 OE
Treatment Steps

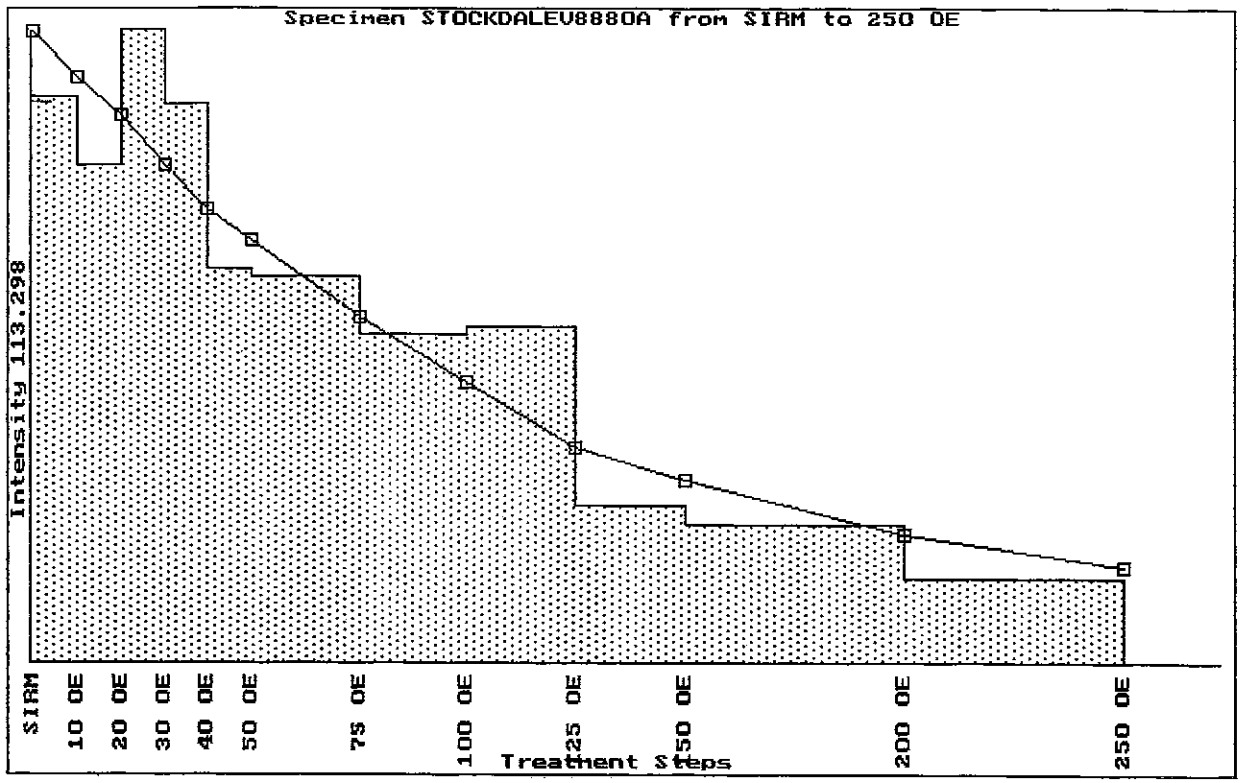
Specimen STOCKDALEV8880A from SIRM to 250 OE
Intensity 113.298
SIRM
10 OE
20 OE
30 OE
40 OE
50 OE
75 OE
100 OE
125 OE
150 OE
200 OE
250 OE
Treatment Steps

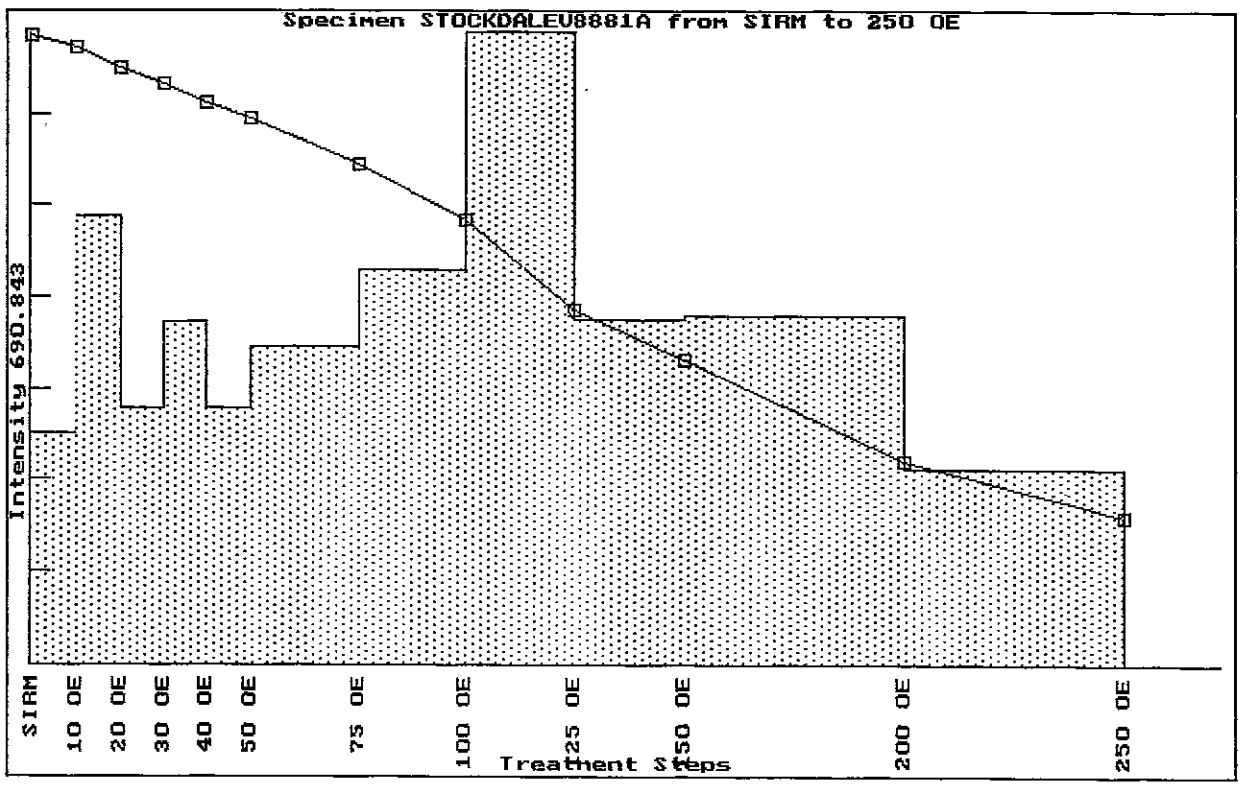
Specimen STOCKDALEV8881A from SIRM to 250 OE
Intensity 690.843
SIRM
10 OE
20 OE
30 OE
40 OE
50 OE
75 OE
100 OE
125 OE
150 OE
200 OE
250 OE
Treatment Steps

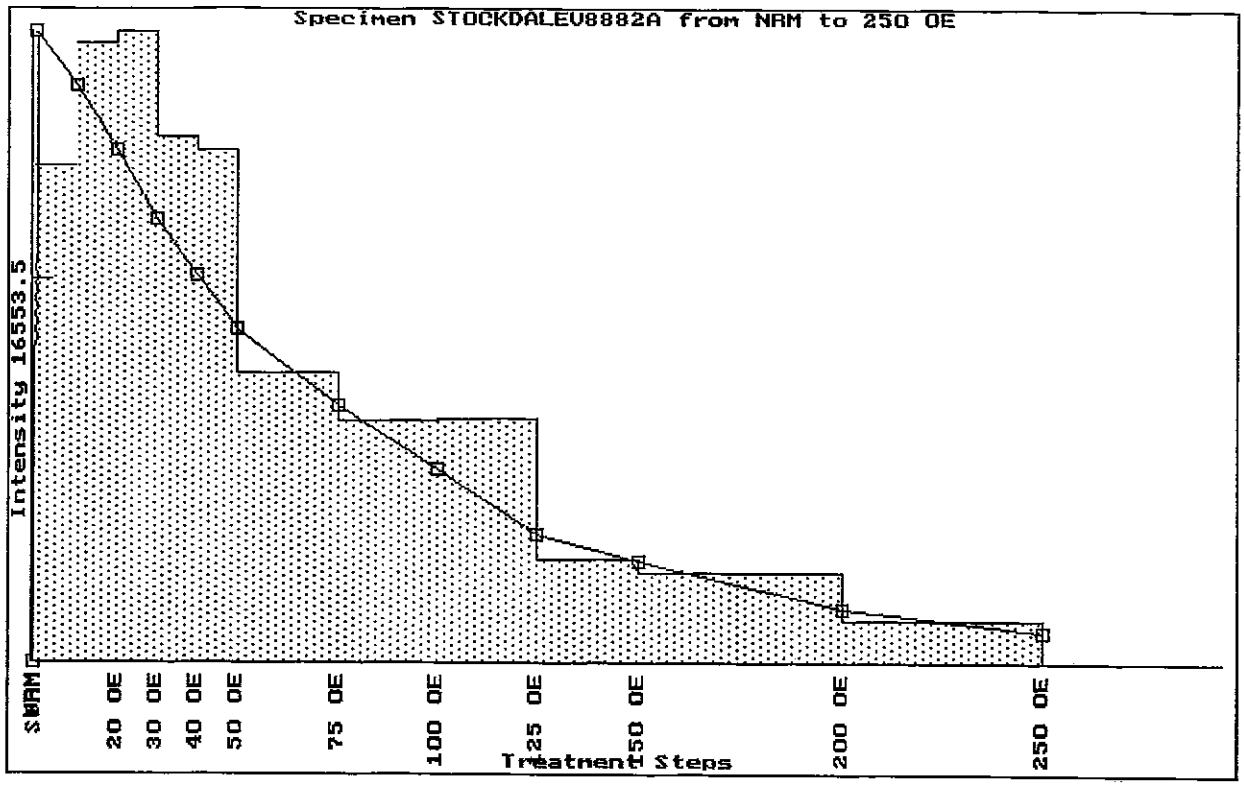
Specimen STOCKDALEV8882A from NRM to 250 OE
Intensity 16553.5
NRM
20 OE
30 OE
40 OE
50 OE
75 OE
100 OE
125 OE
150 OE
200 OE
250 OE
Treatment Steps

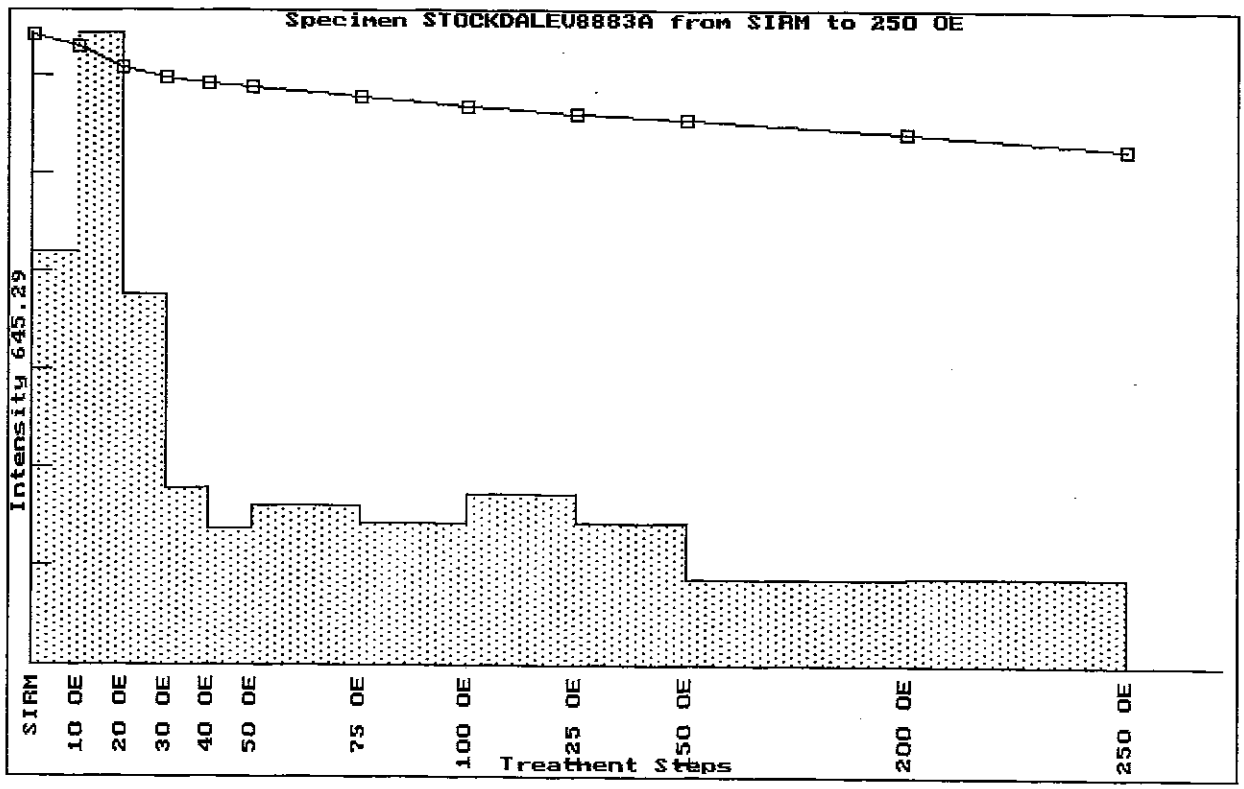
Specimen STOCKDALEV8883A from SIRM to 250 OE
Intensity 645.29
SIRM
10 OE
20 OE
30 OE
40 OE
50 OE
75 OE
100 OE
125 OE
150 OE
200 OE
250 OE
Treatment Steps

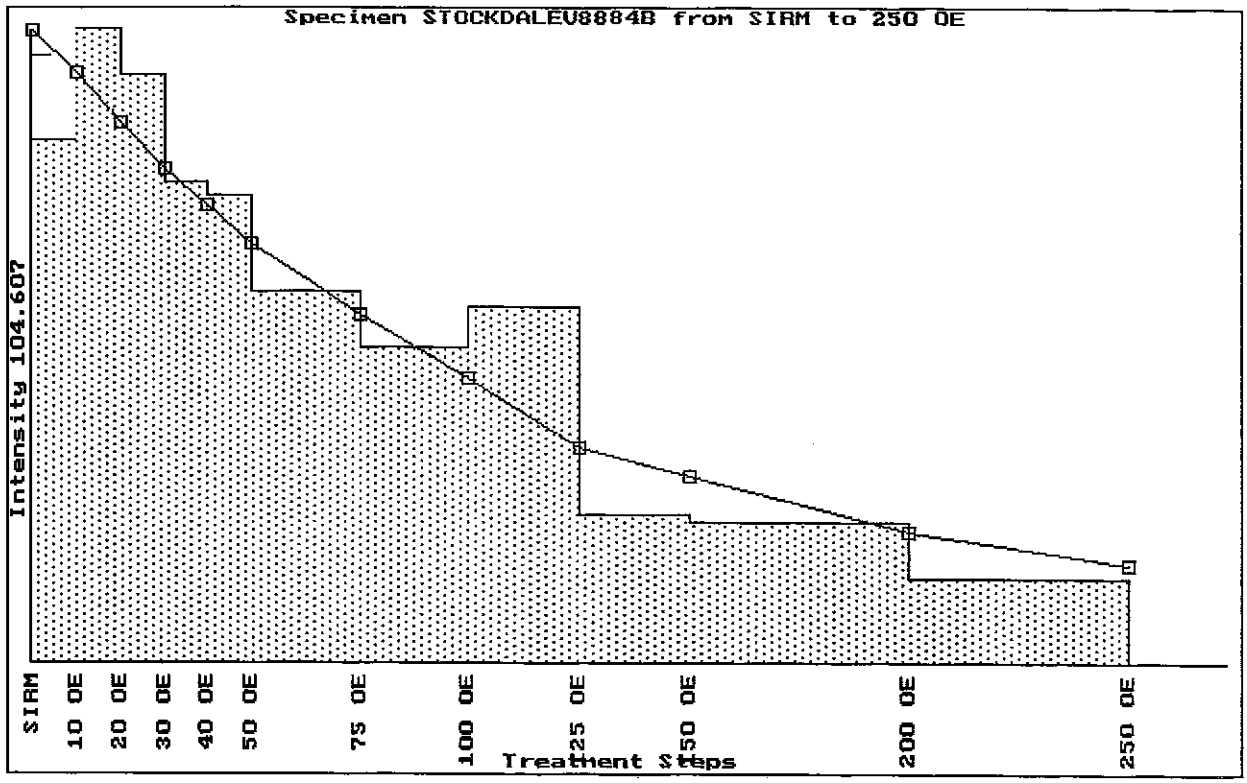
Specimen STOCKDALEV8884B from SIRM to 250 OE
Intensity 104.607
SIRM
10 OE
20 OE
30 OE
40 OE
50 OE
75 OE
100 OE
125 OE
150 OE
200 OE
250 OE
Treatment Steps

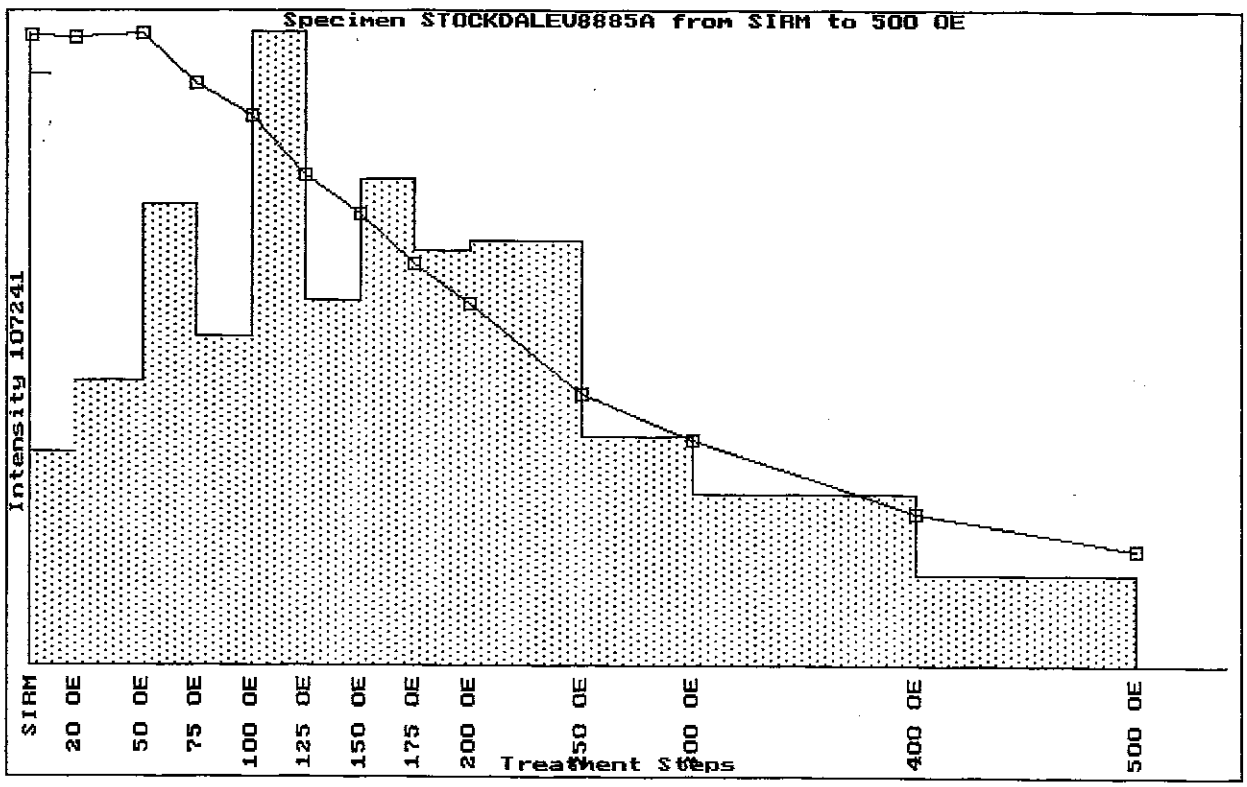
Specimen STOCKDALEV8885A from SIRM to 500 OE
Intensity 107241
SIRM
20 OE
50 OE
75 OE
100 OE
125 OE
150 OE
175 OE
200 OE
250 OE
300 OE
400 OE
500 OE
Treatment Steps

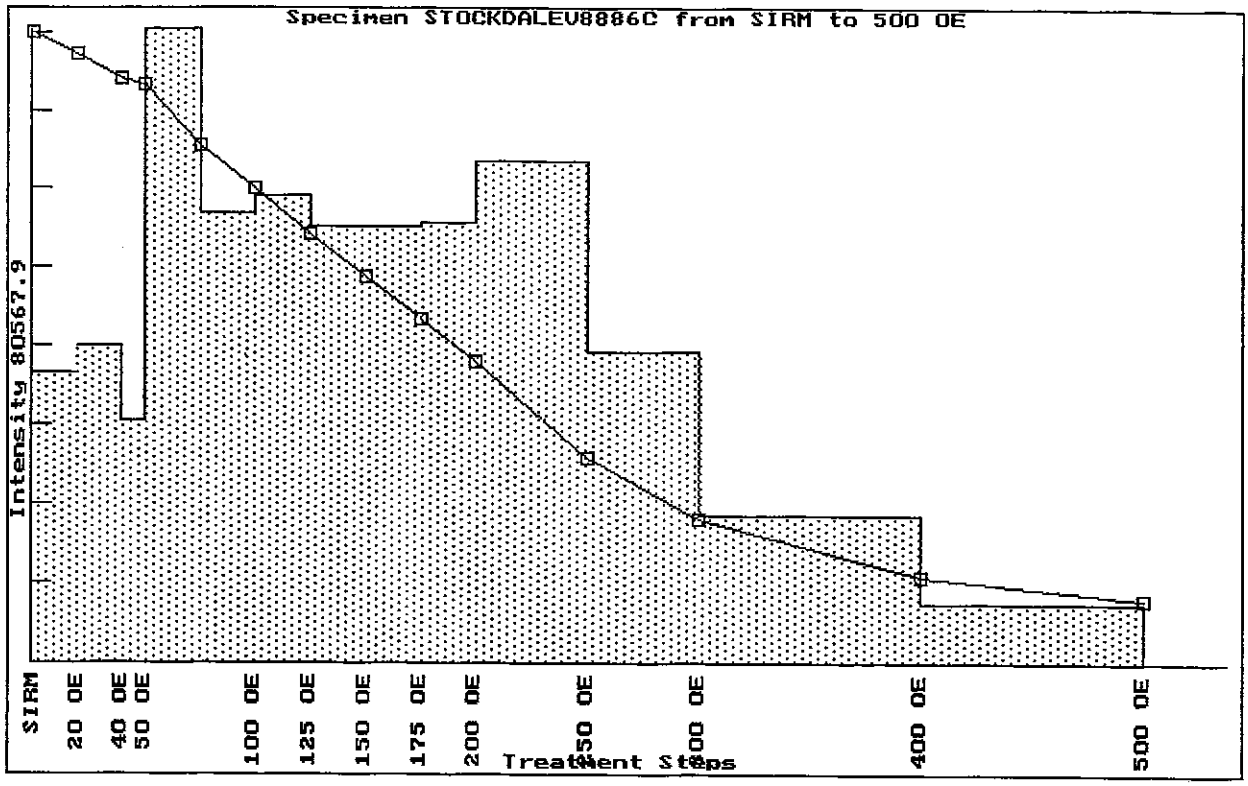
Specimen STOCKDALEV8886C from SIRM to 500 OE
Intensity 80567.9
SIRM
20 OE
40 OE
50 OE
100 OE
125 OE
150 OE
175 OE
200 OE
400 OE
500 OE
Treatment Steps

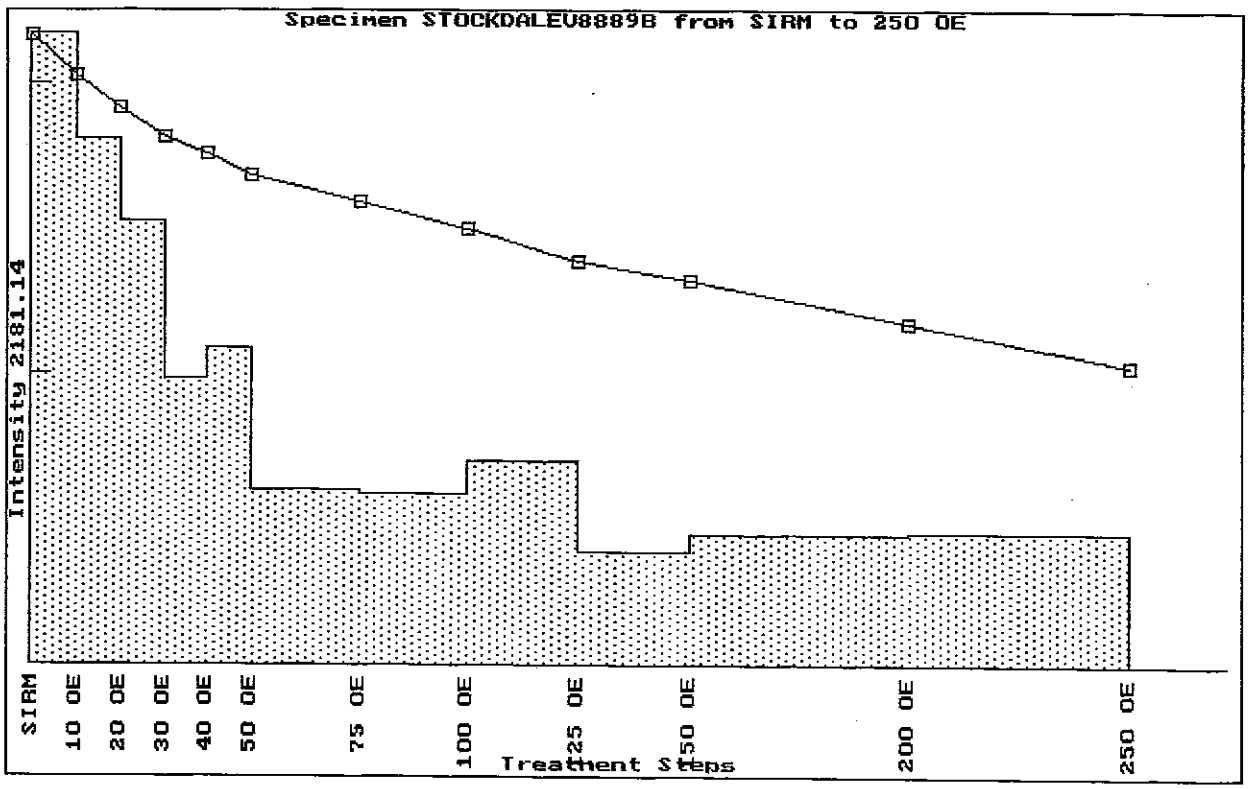
Specimen STOCKDALEV8889B from SIRM to 250 OE
Intensity 2181.14
SIRM
10 OE
20 OE
30 OE
40 OE
50 OE
75 OE
100 OE
200 OE
250 OE
Treatment Steps

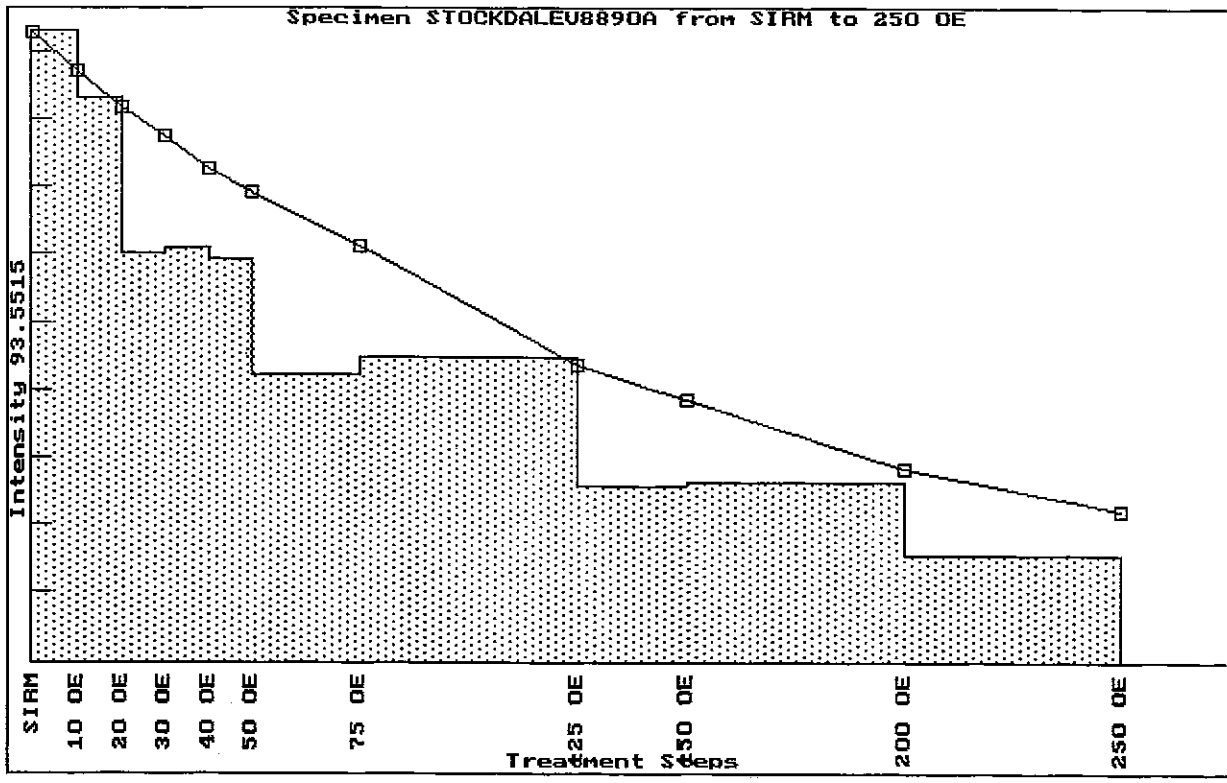
Specimen STOCKDALEU8890A from SIRM to 250 OE
Intensity 93.5515
SIRM
10 OE
20 OE
30 OE
40 OE
50 OE
75 OE
125 OE
150 OE
200 OE
250 OE
Treatment Steps

Fig.7 Thermal demagnetisation of three-component remanence carried by lamproite samples (z-component = coercivity greater than 1000 Oe; x-component = coercivity between 200 and 1000 Oe; y-component = coercivity less than 200 Oe)

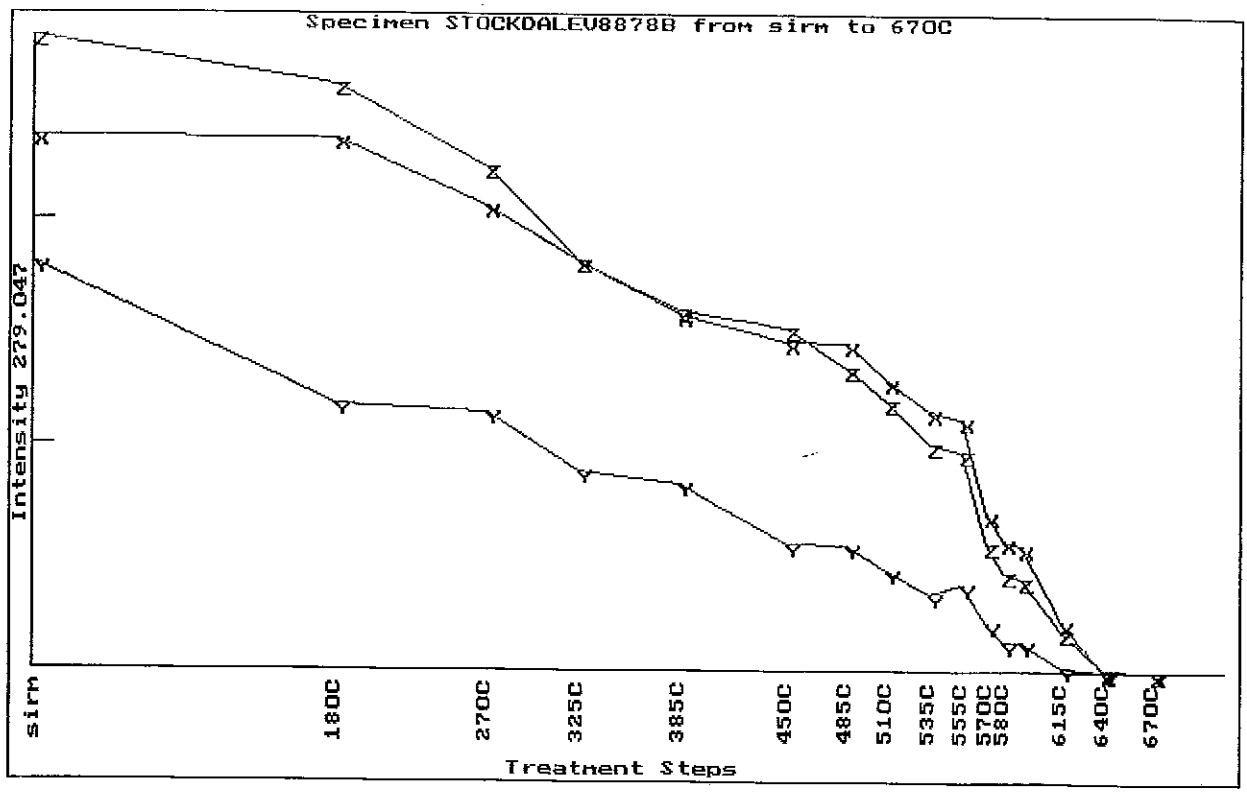
Specimen STOCKDALEV8878B from sirm to 670C
Intensity 279.047
sirm
180C
270C
325C
385C
450C
485C
510C
535C
555C
570C
580C
615C
640C
670C
Treatment Steps

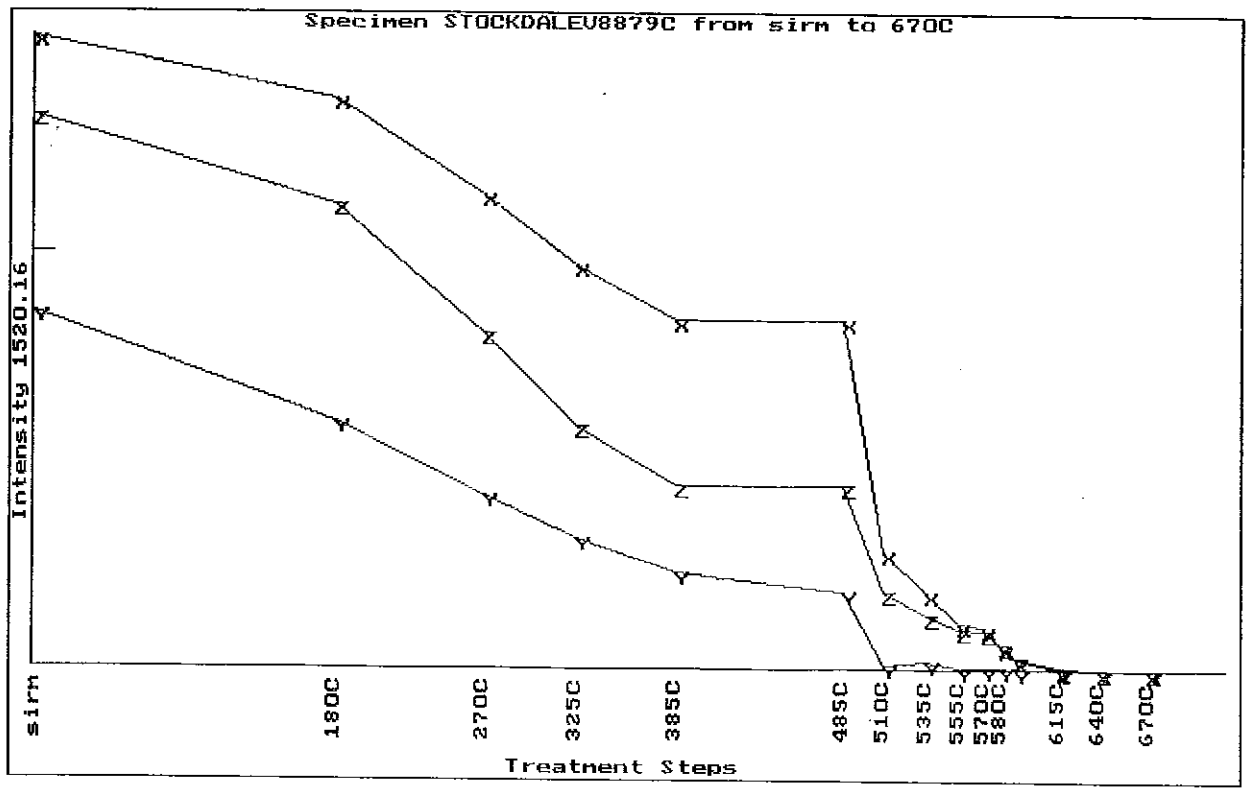
Specimen STOCKDALEV8879C from sirm to 670C
Intensity 1520.16
sirm
180C
270C
325C
385C
485C
510C
535C
555C
570C
580C
615C
640C
670C
Treatment Steps

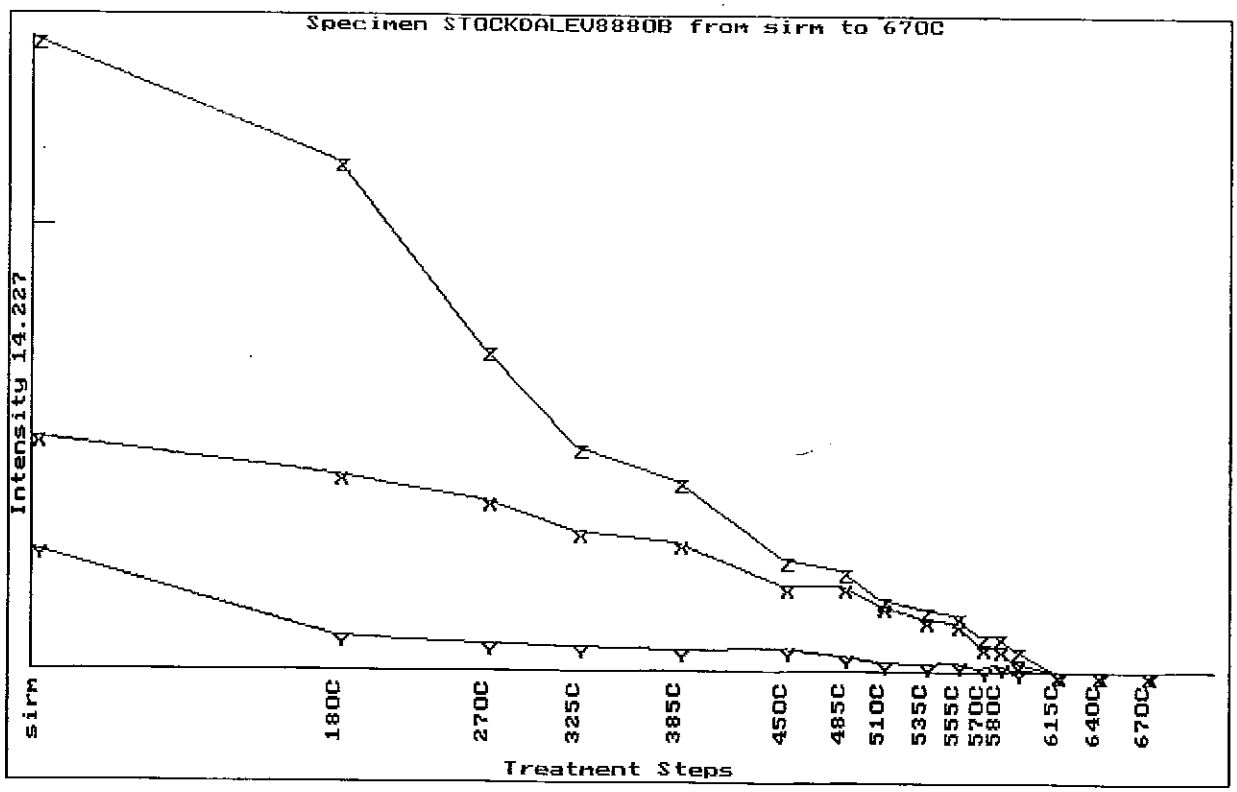
Specimen STOCKDALEV8880B from sirm to 670C
Intensity 14.227
sirm
180C
270C
325C
385C
450C
485C
510C
535C
555C
570C
580C
615C
640C
670C
Treatment Steps

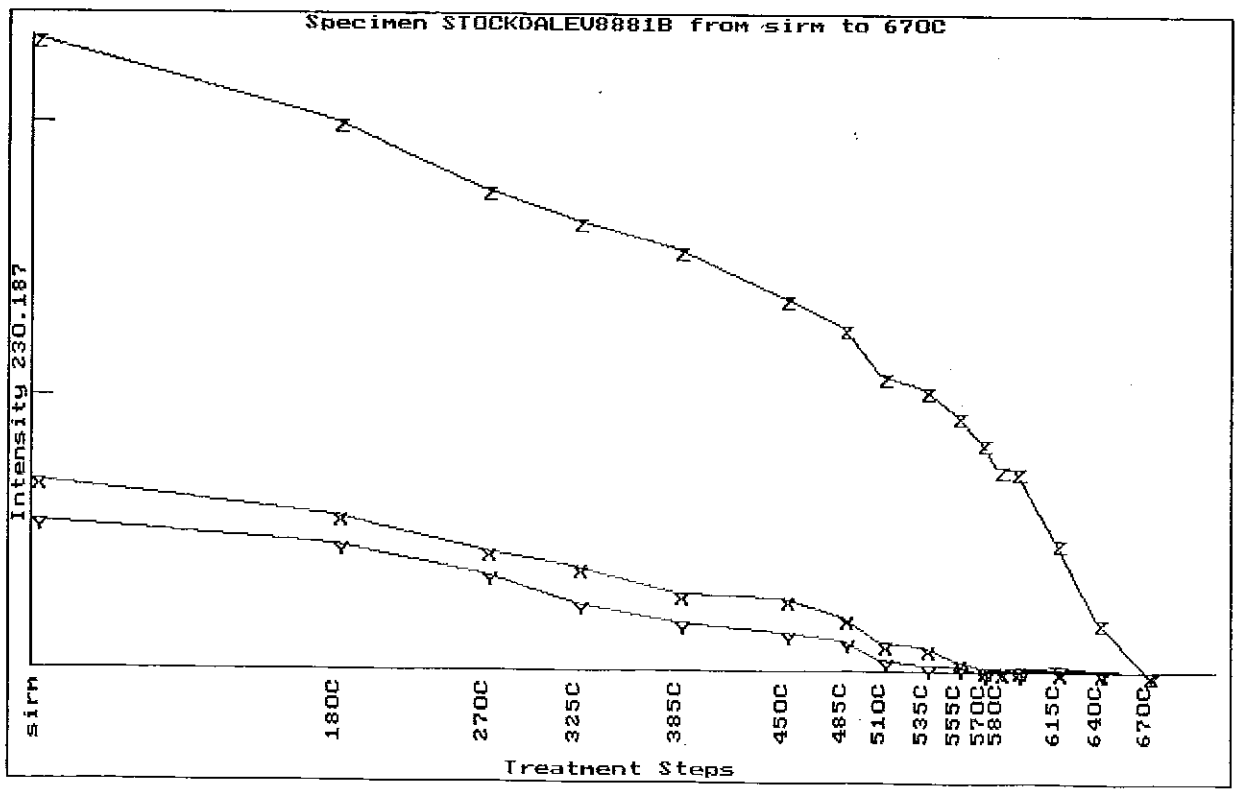
Specimen STOCKDALEV8881B from sirm to 670C
Intensity 230.187
sirm
180C
270C
325C
385C
450C
485C
510C
535C
555C
570C
580C
615C
640C
670C
Treatment Steps

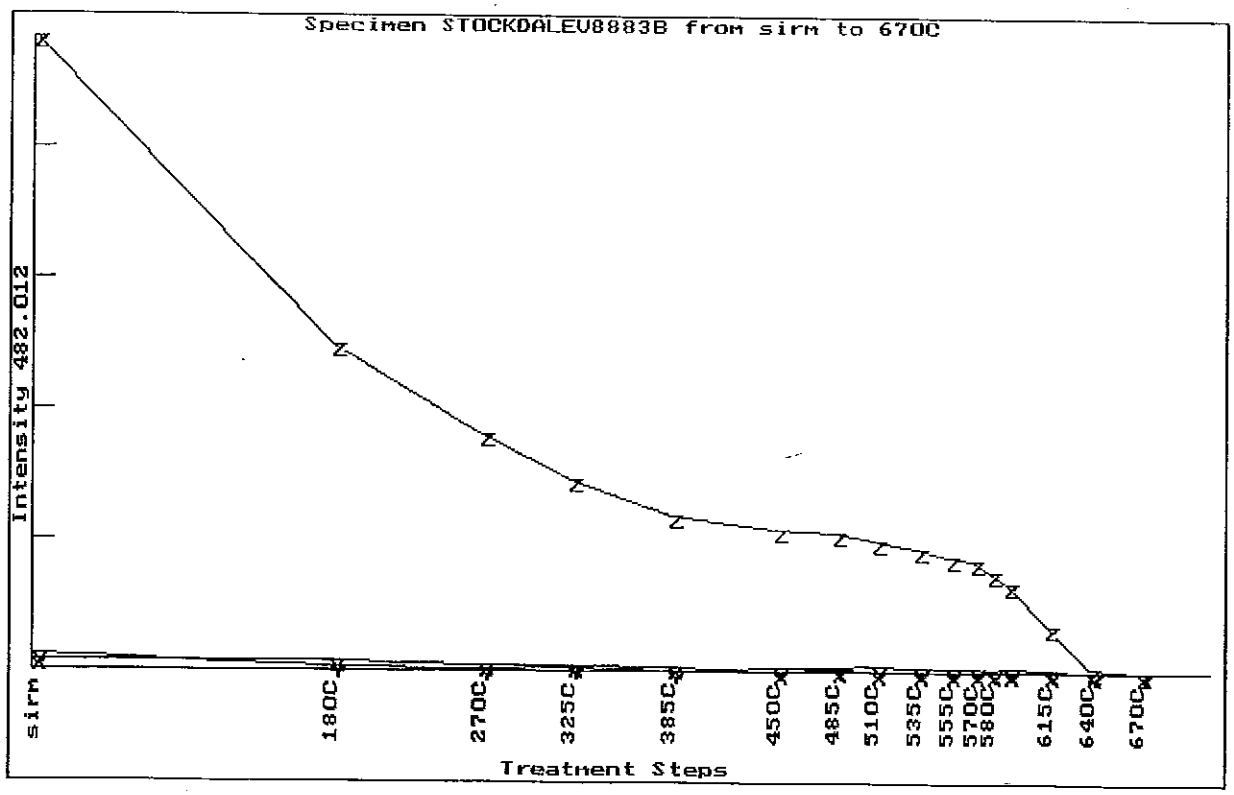
Specimen STOCKDALEU8883B from sirm to 670C
Intensity 482.012
sirm
180C
270C
325C
385C
450C
485C
510C
535C
555C
570C
580C
615C
640C
670C
Treatment Steps

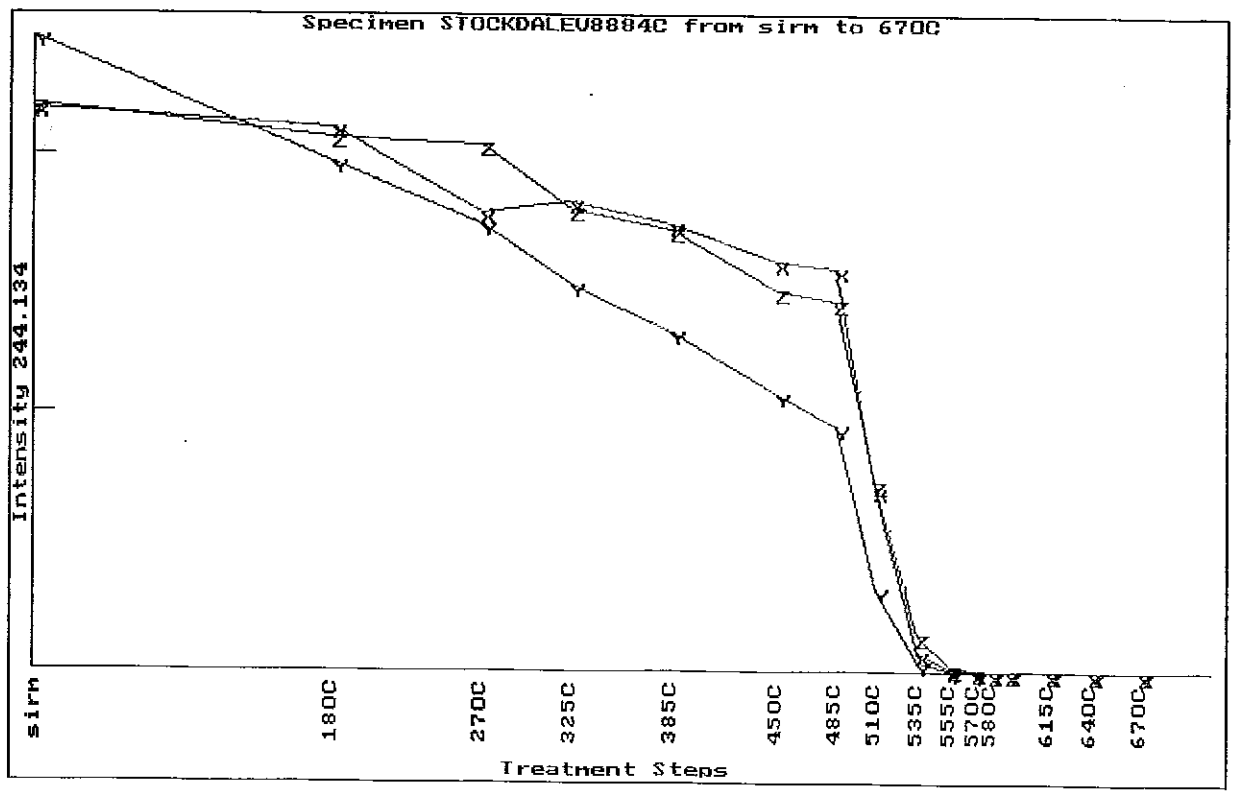
Specimen STOCKDALEU8884C from sirm to 670C
Intensity 244.134
sirm
180C
270C
325C
385C
450C
485C
510C
535C
555C
570C
580C
615C
640C
670C
Treatment Steps

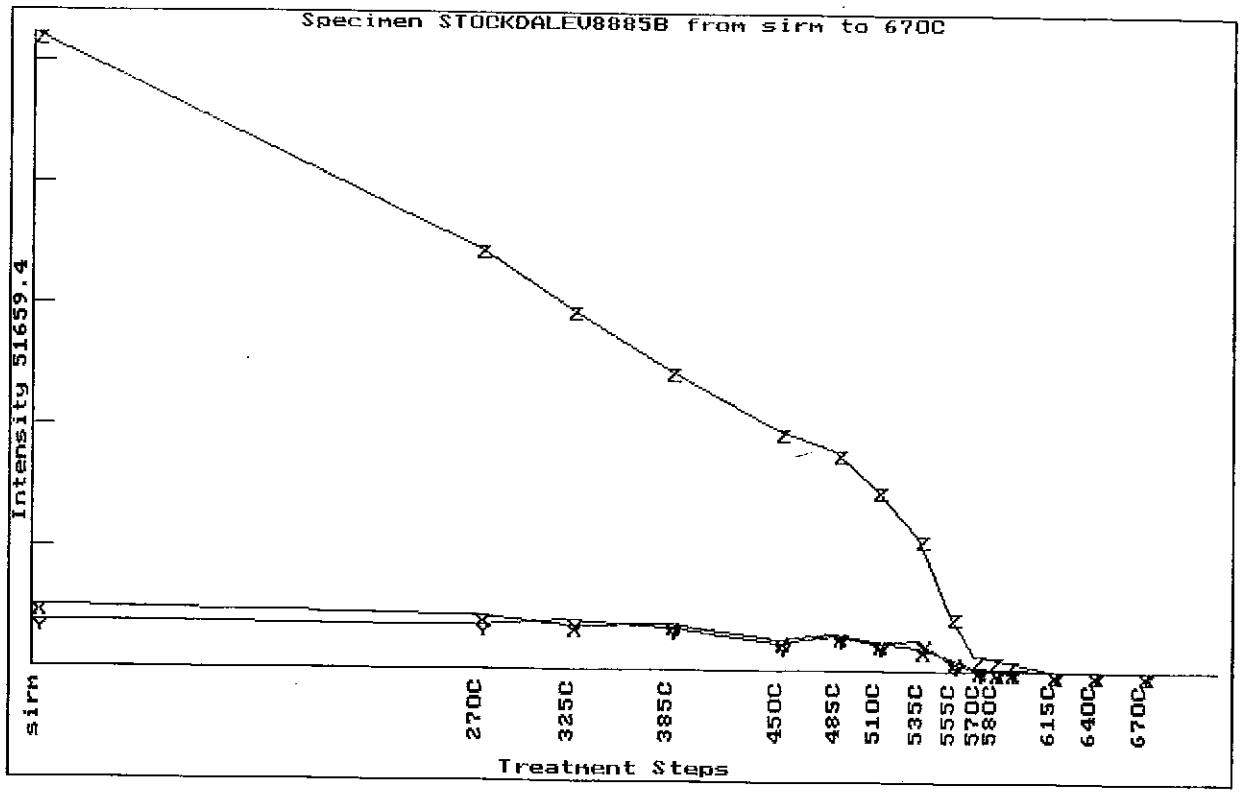
Specimen STOCKDALEV8885B from sirm to 670C
Intensity 51659.4
sirm
270C
325C
385C
450C
485C
510C
535C
555C
570C
580C
615C
640C
670C
Treatment Steps

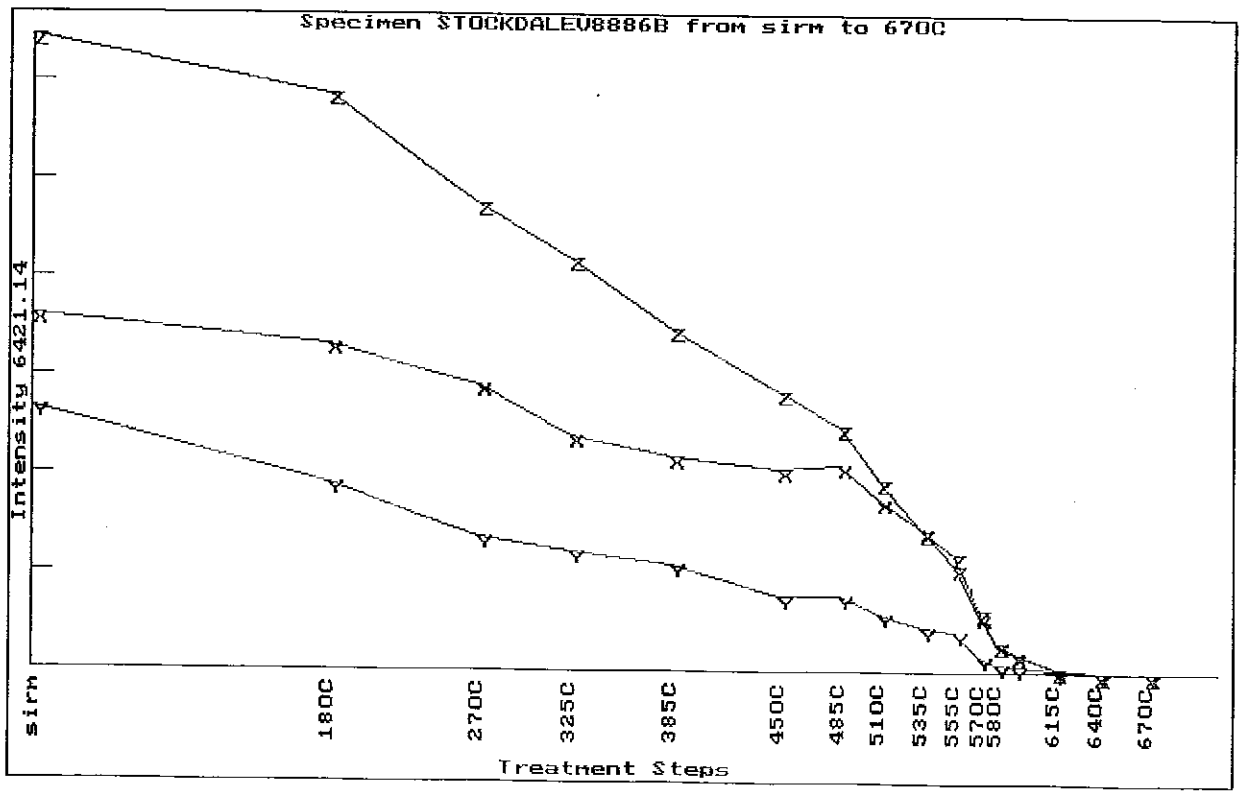
Specimen STOCKDALEV8886B from sirm to 670C
Intensity 6421.14
sirm
180C
270C
325C
385C
450C
485C
510C
535C
555C
570C
580C
615C
640C
670C
Treatment Steps

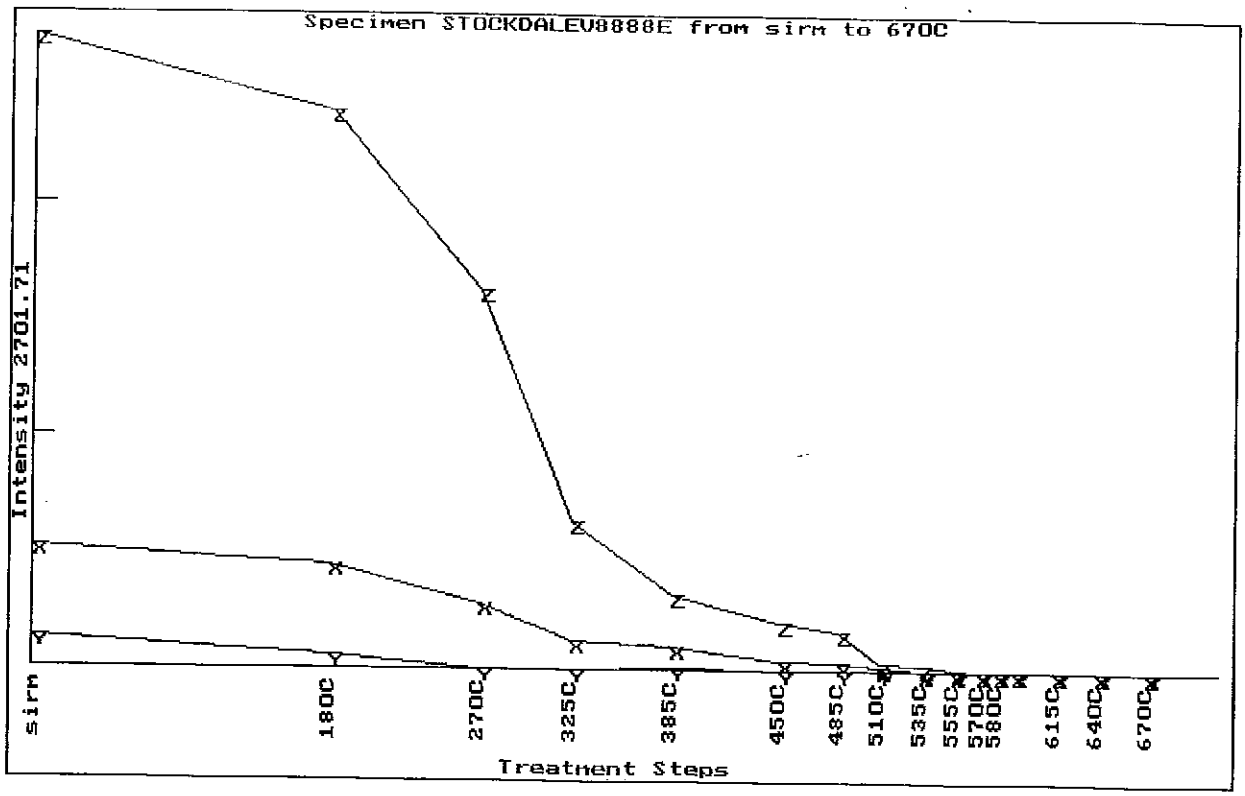
Specimen STOCKDALEV8888E from sirm to 670C
Intensity 2701.71
sirm
180C
270C
325C
385C
450C
485C
510C
535C
555C
570C
580C
615C
640C
670C
Treatment Steps

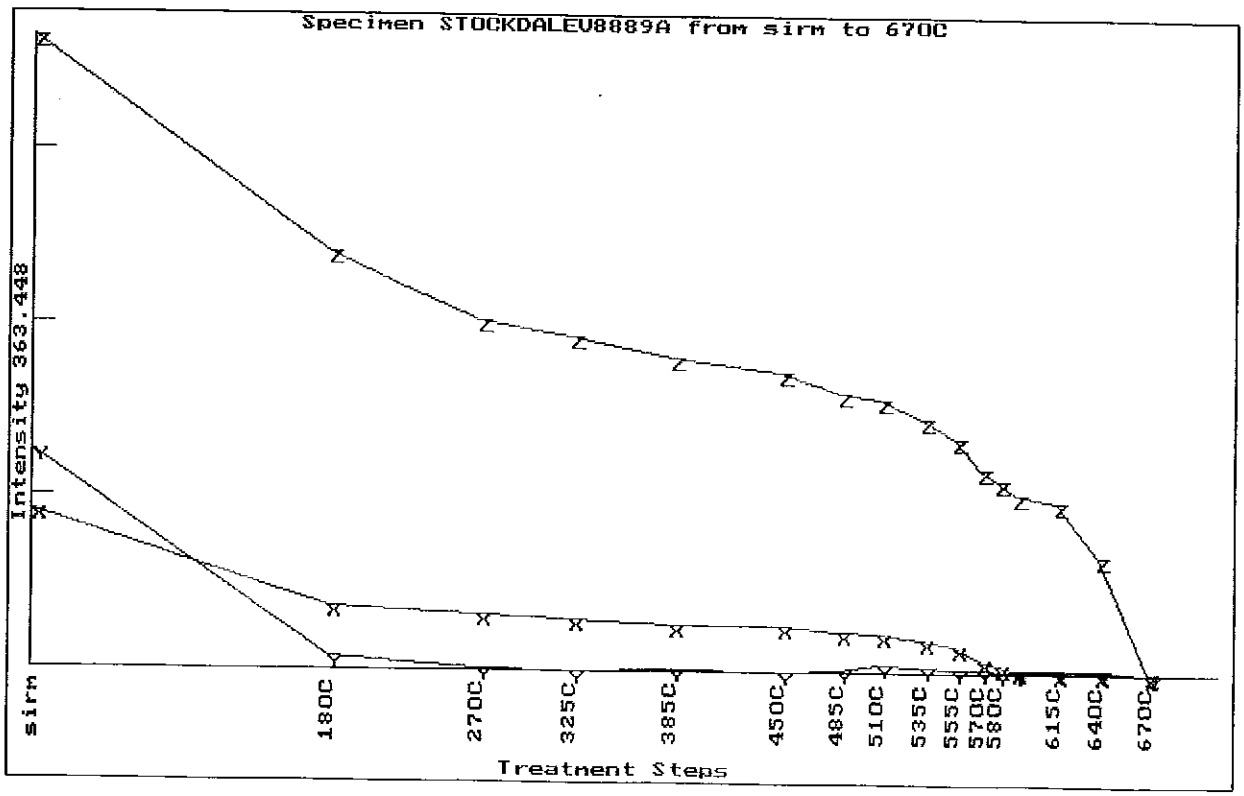
Specimen STOCKDALEV8889A from sirm to 670C
Intensity 363.448
sirm
180C
270C
325C
385C
450C
485C
510C
535C
555C
570C
580C
615C
640C
670C
Treatment Steps

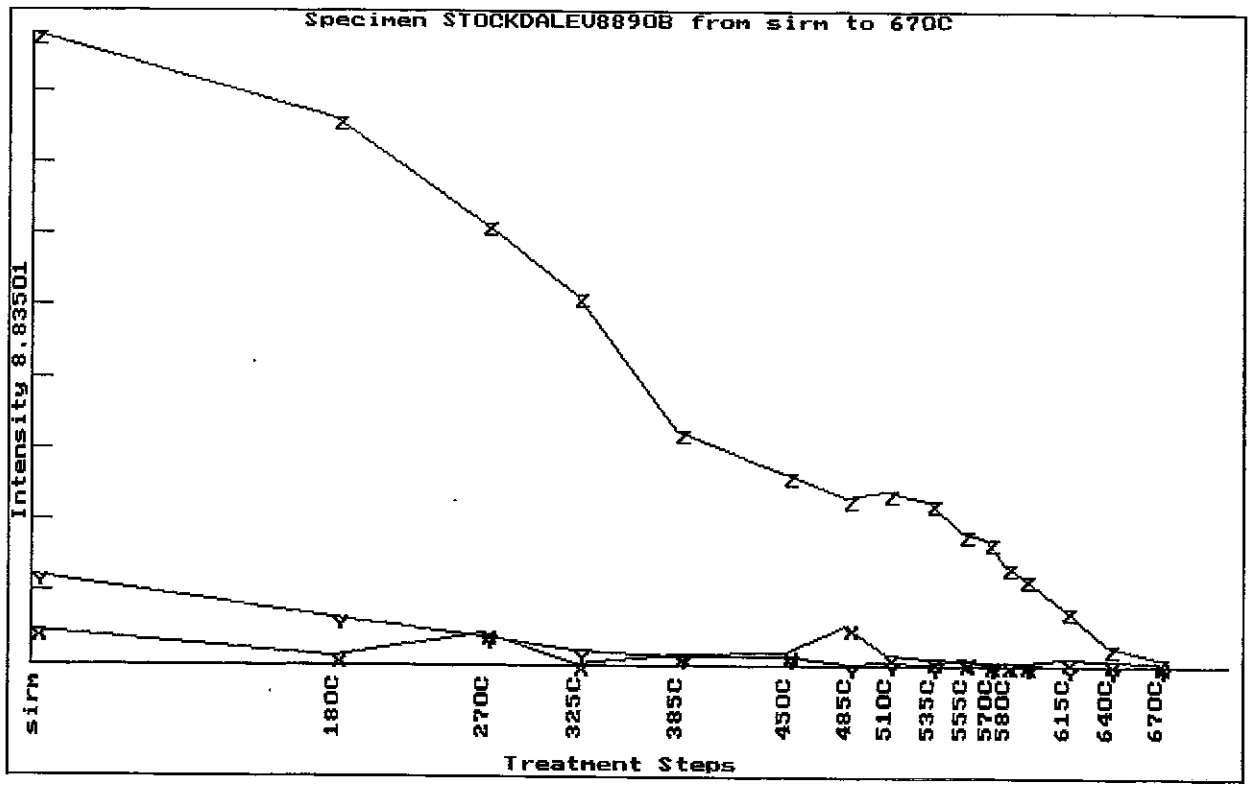
Specimen STOCKDALEV8890B from sirm to 670C
Intensity 8.83501
sirm
180C
270C
325C
385C
450C
485C
510C
535C
555C
570C
580C
615C
640C
670C
Treatment Steps